1. Introduction

1.1 The scope of the thesis

Water is becoming a more and more expensive and scare resource over the whole world today. As the population growing and the regional economy booming, not only is the direct fresh water consumption, like the water for drinking, washing, sewerage, dramatically increasing, but also the indirect water uses are becoming more essential than the past. A typical example of indirect water use is the irrigation water which insures the growth of crops. Further, it guarantees all people's basic needs and the development of economies. Facing to the conflict between the total amount of water and the water consumption, proper water management is necessary to solve the problem. Hence, as to irrigation, more accurate and flexible irrigation systems are required. Here accurate means that the actual water supply matches the desired supply, and flexible requires that the water delivery meets the changing water requirements of the users (J. Schuurmans et al. 1999).

In order to fulfill the two functions of an irrigation canal, all the infrastructures, like check and lateral gates or weirs, pumps and power stations, should be manipulated properly to transports large amount of water. And the efficiency becomes a key factor for the irrigation system. In practice, a considerable amount of water is wasted due to the inaccurate manual operation or the lack of control. Therefore, it is useful to apply automatic control to those check or lateral structures to control the water level or flow and efficiently distribute the incoming water, finally, minimize the water losses. Several control methods can be applied to the canal, like classic Feedback Control, Feedforward Control and more advanced Model Predictive Control (MPC). They have different applications to different systems depending on the actual situations.

Based on the increasing requirements on the performance of irrigation canals, the control methods should also show the best possible performance. Therefore, the selection of control methods would be the first step, considering the given canal characteristics and the effort of realizing the control action. Classic feedback and feedforward control have been developed for a long time and they are being applied widely all over the world. They can perform very well in practice if the irrigation system is not complex. Otherwise, more advanced control technique is need like MPC used in this research. MPC can deal with the issues in a systematic way that it uses all the measurements and predictions in an optimization to calculate the control actions.

1.2 Problem statement

Recently, some implementations of Model Predictive Control on the actual irrigation canals have been conducted. They are mostly based on the simplified Integrator Delay (ID) model which only takes the delay time and the surface area into account. Because of the drawbacks of less canal dynamics in this model, for example, resonance waves are not considered, it is a worthy trying to build up another complex one that consists of more properties. But the comparison of models is necessary for a proper implementation. Considering the simulation time for application, the ID model of a whole canal with several pools has already been a big

system in matrices formulation and the calculation time tends to be large. Therefore, the verification of applicability of more complex model would be another important factor in the research. The Integrator Delay model is always a worthy application to generate cases on different canals in order for the future comparison or verification.

In this research, MPC is applied on the Central Main Canal, which is the main irrigation water supply canal in Eloy district, Arizona. It is long, flat, and contains 7 pools separated by 8 gates. The head gate takes water from the Central Arizona Project (CAP) and can only be changed twice a day (thought to be no control), while the last gate (84-inch gate) is the end of the canal and unable to be controlled. Thus, 7 pools are controlled by 6 gates and it is almost impossible to achieve this with classic control methods. But MPC can perform the optimization for 7 pools and solve the problem.

1.3 Research objectives

The research objectives of this master thesis are to develop MPC controllers based on different internal models to control the water level in an irrigation canal, distribute the water more efficiently and deal with the supply and demand mismatches of irrigation water. The district is considering building a reservoir beside the canal. After the research, the reservoir information may be presented. The following research work is executed:

- Setup the model of the Central Main Canal in SOBEK to perform unsteady flow simulations and develop two different internal models for the MPC controller in MATLAB.
- The controller is tuned via the trial-and-error method and the tuning experience could be a support to other applications
- Verify the applicability of the internal model based on the Saint Venant equations
- Model Predictive Controller is tested on the Central Main Canal model by using the one week water supply and demand schedule.
- Provide suggestions on the location and the size of the reservoir if possible.

1.4 The outline of the thesis

Chapter 1 gives an overview of this thesis. The problem and the objectives are stated here. Chapter 2 introduces the basic control theories on irrigation canals, especially for those classic methods, like feedforward control, feedback control, and their combination. Chapter 3 provides the entire theory of advanced control method – Model Predictive Control (MPC). Its implementation on actual irrigation canals has been finished in several researches. This chapter includes detailed descriptions of different components of MPC. It gives a preparation for applying two different models. Before starting the application of MPC on the real system, Chapter 4 gives the first impression to the Central Main Canal where MPC is applied, and its characteristics. Following this, the first application of MPC on the Central Main Canal based on the Integrator Delay (ID) model is introduced in chapter 5. The detailed ID model descriptions are presented with the preparation of pool properties determination and some assumptions. The results of one scenario are demonstrated in this chapter followed by short discussions and model tuning. Chapter 6 is the application of MPC on the Central Main Canal based on the

Saint Venant model. The Saint Venant equations and its descretization will be introduced, followed by the internal model and its simulation results. A detailed discussion of the model and its results is the main focus in this chapter. Following this is Chapter 7 which compares the advantages and disadvantages for both models and provides some ideas on the applicability of the more complicated model. The conclusions and recommendations are in chapter 9. All the results of other scenarios for the one week water supply and demand schedule are shown in the appendix, together with the tools used in the research and all the deduction of theory formulations in details.

2 Classic control methods on irrigation canals

2.1 General control theory

In the recent water management, the control objectives are becoming more and more complex. Hence the more sophisticated control is necessary. Generally, a controlled water system includes the water process itself, the controller, the input and the output which is the results of control actions exerting on the water system by using a certain controller. The input can be the desired output behavior or the disturbances, like the rainfall, the prescheduled offtakes, etc. The output signal comes to the controller via several processes. First, the signal should be detected by a sensor which measures variables of the water system, like water level and flow. Before the information is sent to the controller, it passes the A/D convertor which converts the analog signals into digitals, convenient for calculation. Then the controller calculates the required control actions based on the incoming signals, and the control actions are translated from digitals back into analogs via D/A convertor. Finally it exert on the actuator in order to bring the water system back to the desired output. The actuator is a device used to execute the control actions and manipulate the water system. Due to the development of sensors, communication systems, control algorithms and prediction tools, sophisticated controls become possible. The interconnections of all these components forming a system configuration are shown in Figure 2.1.

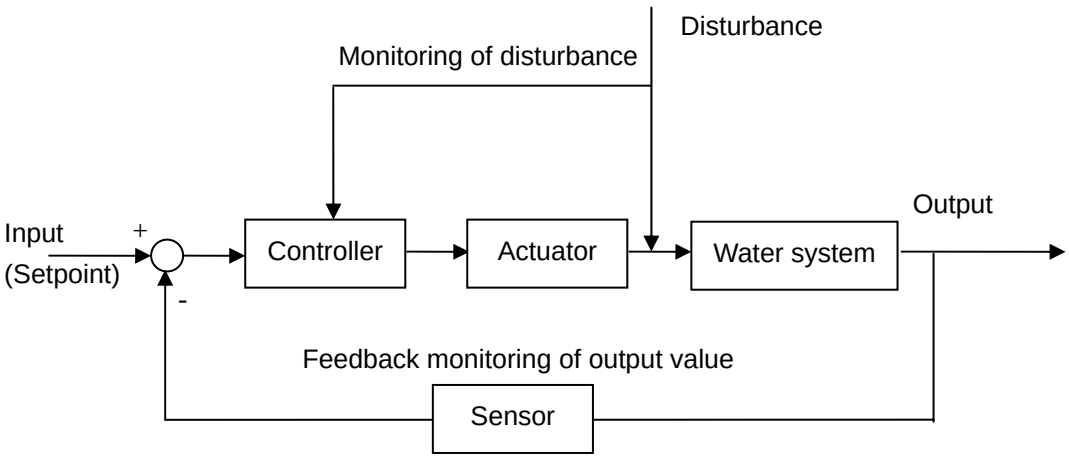

Figure 2.1, Interconnection of all the components of a controlled water system

The above figure is a vivid description of the controlled water system. In order to analysis the system and its control method, it is convenient to use the block diagram to represent the processes. The next paragraph will introduce the configuration of block diagrams as a preparation of control method analysis.

2.2 Block diagram configuration

A block diagram is a system representation using blocks connected by arrows. The blocks represent the relation of the systems and the arrows represent the variables. The block that transfers the variable from one to another is the transfer function, which is defined by the

output signal divided by the input signal. The block diagram is especially useful for the linear systems (Brouwer R. 2005). The signals can be summed or subtracted. Three basic situations are used, which are blocks in series, parallel and a closed loop.

- Series. Assume there are two blocks placed in series with the input signal x and the output signal y. The transfer function functions are H1 and H2. Then the equivalent block diagram has the transfer function of H1 • H2, shown in the Figure 2.2.

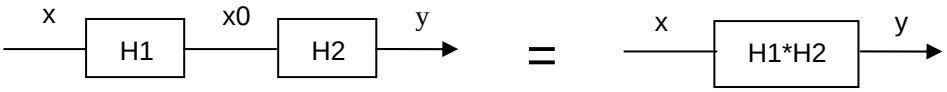

Figure 2.2, Block diagram in series

Proof:

$x0 = x \bullet H1$

$y = x0 \bullet H2$

then, $y = x*H1*H2$

Transfer function = $y / x = H1*H2$

- Parallel. Assume two input signals, x1 and x2, coming from signal x, are parallel, which pass transfer function H1 and H2 separately, and finally combine (sum or subtract) together. The transfer function of the equivalent block diagram is $H1 \pm H2$.

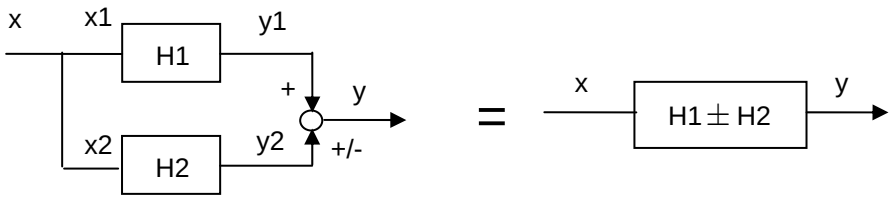

Figure 2.3, Block diagram in parallel

proof:

$x = x1 = x2$

$y1 = x1 \bullet H1$

$y2 = x2 \bullet H2$

$y = y1 \pm y2$

then, $y = x1 \bullet H1 \pm x2 \bullet H2 = x \bullet (H1 \pm H2)$

Transfer function = $y / x = H1 \pm H2$

- Closed loop. Assume the output signal y is connected to the input signal x via the transfer function H2, which creates a closed feedback loop of the system. The open loop from input to output is via the transfer function H1, then the equivalent block diagram consists the transfer function of $H1 / (1 \pm H1 \bullet H2)$.

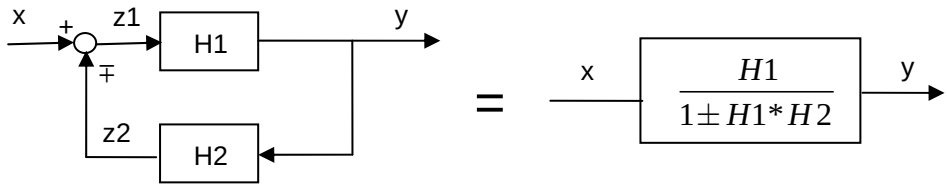

Figure 2.4, Block diagram in a closed loop

proof:

z1 = x∓z2

y = z1•H1 = (x∓z2)•H1

z2 = y•H2

then, y = (x∓y•H2)•H1

so, y = x•H1 / (1±H1•H2)

Transfer function = y / x = H1 / (1±H1•H2)

2.3 Classic control methods

A lot of different control algorithms for the irrigation canal regulation have been developed and applied throughout the world. Based on the control type and the direction of control links, these control algorithms can be categorized into different groups (P.O. Malaterre et al. 1998). As to the control type, there are feedback control, feedforward control and their combination, while downstream control and upstream control belong to the other category. Control variables, like water level, discharge and volume, are commonly used in the irrigation canal control. The following part of this chapter will present all these different methods and their comparisons.

2.3.1 Feedforward control

Feedforward control is also called open-loop control. The control action is independent to the output, but it is calculated from the disturbances, the target variables and the process simulation. In the irrigation canals, disturbances can be the incoming flow from the most upstream, and the farmer offtakes along the canal. If these disturbances are already known in advance or can be anticipated, the feedforward control can improve the control performance considerably. It can compensate for the time delay, especially in those long canals. But in reality, the single feedforward control is not so practical, because of the change in the irrigation system or the inaccuracy of anticipations. The block diagram of the feedforward control is shown in figure 2.5:

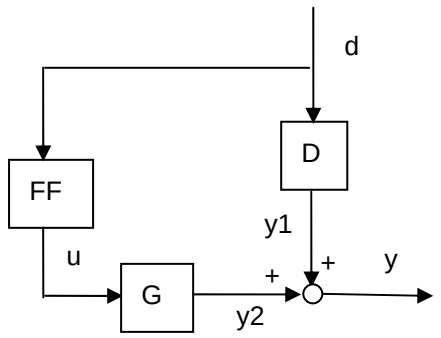

Figure 2.5, Block diagram of feedforward control

The control action has to compensate the influence of disturbances on the water system in order to keep the total output unchanged. The disturbance is measured and imposed to the system, and the output is y1 determined by the transfer function D. It is also sent to the feedforward controller and the control action u is computed. The output y2 is determined by another process G. The signals of y1 and y2 are supposed to have the same number but the opposite sign. Based on the preparation of the block diagram, the feedforward controller should have the function of – D/G.

proof:

$y1+y2=0$

$y1=d \bullet D$

$y2=d \bullet FF \bullet G$

then, $d \bullet D + d \bullet FF \bullet G=0$

So the controller FF = – D/G

In summary, the limitations of the feedforward control are obvious:

- the accurate control is difficult due to inaccurate anticipation
- the performance of feedforward control is sensitive to the system changes
- it reacts only on the known disturbances

Therefore, feedforward control always combines with the feedback control, in order to overcome its limitations.

2.3.2 Feedback control

Feedback control is a closed-loop control which takes the output variables into account. It is thought to be a very robust control algorithm. In the feedback control, the controlled variables, water level and discharge, are obtained from the measurements. Those deviations from the setpoints are calculated and sent back into the controller which will compute the control actions to correct the deviations. After the control actions are executed, the output variables are measured again and the new control actions are generated. This creates a closed loop. It is obvious that the shorter the loop time, the faster the control is. The well known and mostly used simple feedback controller for the irrigation canal system is Proportional Integral (PI) controller, whose control action is the function of deviation and the integral of deviations. The

controller function is listed below:

$$u = K_p \bullet e + K_i \bullet \int e \bullet dt$$

Here u is the control action, e is the deviation from setpoint, Kp is the proportional gain factor, Ki is the integral gain factor, t is time index.

The feedback control algorithm is shown here in the block diagram:

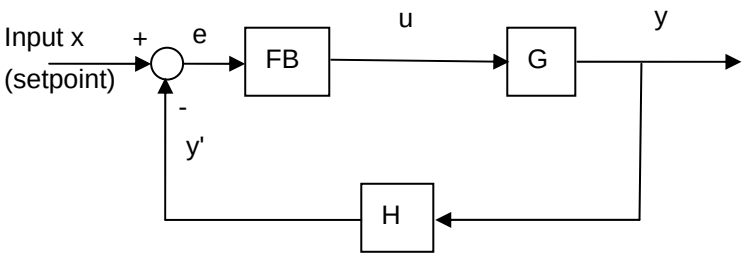

Figure 2.6, Block diagram of feedback control

Based on the aforementioned closed loop block diagram, the equivalent transfer function is y/x = FB•G / (1+FB•G•H). The setpoint is given to the irrigation system, and the output is measured, represent by H in the block diagram. If the measurements are accurate enough, H should be close to 1. Then it's easy to calculate the function of feedback controller.

In summary, there are many advantages by using the feedback control. They are:

- the accurate control is possible due to the consecutive correctness of deviations
- the performance is not sensitive to the system changes
- the deviations caused by any factors (known or unknown) can be compensated

But the feedback control has one big limitation that it does not anticipate the disturbance, thus, it can not provide a relatively quick response. Only after the deviation occurs, the control actions are triggered. In practice, most of the feedback control is indispensable, but if the irrigation system needs the anticipation of disturbances, a combination of feedback and feedforward control is useful (Brouwer R. 2005).

2.3.3 Combination of Feedback and Feedforward control

Because of both the advantages and the disadvantages of feedback and feedforward controllers, a combination is often used to control the irrigation canal system. The advantages are added together and compensate for the disadvantages each other. If the disturbances are already known, it is recommended to use the information by applying the feedforward controller in order to make a quick response. The controller does not need to be very accurate, because the feedback can compensate for the deviation. The properties of the combined feedforward and feedback control system are:

- the disturbances can be anticipated due to feedforward control
- the accurate control is possible due to the feedback control
- the performance is not sensitive to the system changes

- the deviations caused by both known and unknown disturbances are corrected

2.3.4 Downstream control

The downstream control means that a structure is operated to control the variable located downstream of the canal pool. Figure 2.7 shows the configuration of a downstream control. Taking the downstream water level as the controlled variable, when it has a deviation from the setpoint, this information is transferred to the structure located upstream end of the reach and the structure is adjusted to pass a proper flow downstream to compensate the deviation. Downstream control is normally associated with a demand type of operation (O.S. Balogun, 1985). Upstream gate should automatically open when the downstream demand increases and close if the demand decreases. All the variables (water level, discharge, and volume) can be controlled with downstream control.

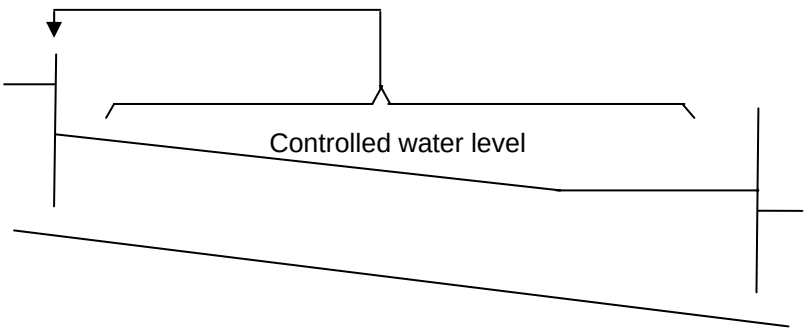

Figure 2.7, Downstream control

2.3.5 Upstream control

The upstream control is exactly the opposite. The control structure located at the downstream end of the reach is operated to control the upstream variables. Still taking the water level as an example, the deviation is detected and sent to the downstream structure and triggers the structure's adjustments. The limitation of this type of control is that only water level and volume can be controlled when flow conditions are subcritical and under the limitations of the backwater effects (P.O. Malaterre et al. 1998), which makes the downstream control of irrigation canals more interesting. Figure 2.8 shows the upstream control demonstration.

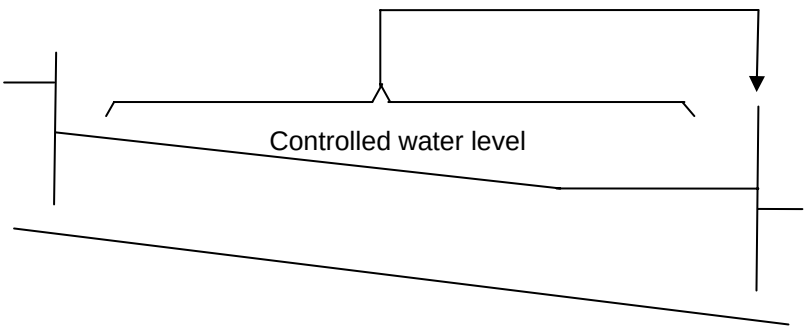

Figure 2.8, Upstream control

2.3.6 Master Slave Controller

If more than one reaches are considered, where water levels are controlled by the check structures, those reaches are interacting each other. In most of the controllers, the control action is a change in gate position. Assuming there is increases in demand at the most end of the canal, it causes the drop in water level of the last pool. This water level drop will ask for more water released from the upstream gate, which triggers the water level decrease as well in the upstream pool. Thus the water level in all the pools will decline before more water is supplied to the canal. By changing the control action to flow rate instead of the gate position, a flow rate controller is used at each gate and the influence of the demand change can be shielded (A.J. Clemmens and J. Shuurmans, 2004). When water level changes, the gate position is adjusted so that the flow rate is maintained constant (Brouwer R. 2005). So the master slave controller includes two separate parts: the water level controller (the master controller) and the flow rate controller (the slave controller). Figure 2.9 shows the configuration of a master slave controller.

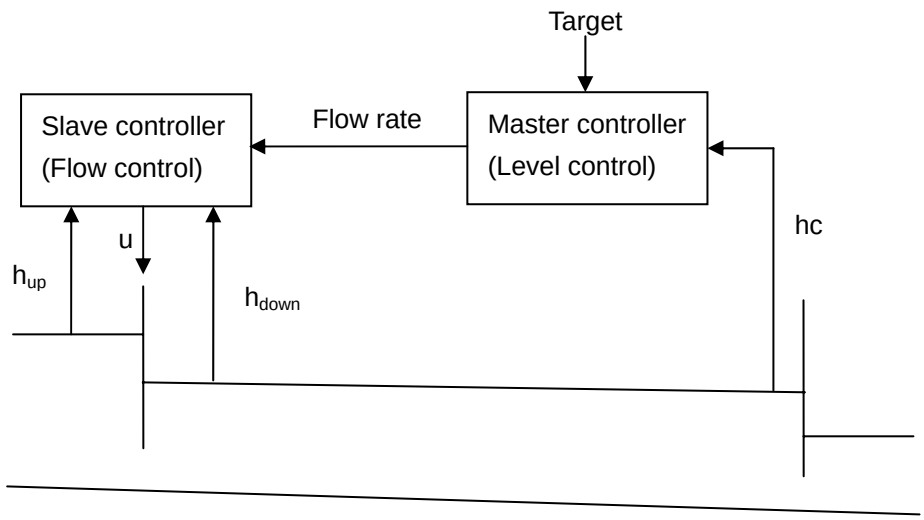

Figure 2.9, Master slave controller

The master controller uses the water level deviation to create a flow rate signal. Then the slave controller will track this flow rate and compute a control action to adjust the gate position. If the flow controller's corrective actions are quick enough (at least as fast as the feedback controller's corrective actions), then the performance of the overall controller (feedback plus flow controllers) can be as efficient as expected (Wahlin, B.T. 2006). The flow rate can be measured in two ways. First, it can be converted by the inversion of the gate-discharge relation. If this relation is not accurate enough, the second method is to measure the flow rate directly, but the cost will be more expensive (J. Schuurmans et al. 1999).

3 Model Predictive Control (MPC) on irrigation canals

3.1 General introduction

Model Predictive Control (MPC) is a practical model based control technique which emerged from the chemical process industry in the 70's. One of the biggest advantages of this controller is that it can deal with all the constraints explicitly through on-line optimization in the working process (Jay, H. Lee, et al. 1990). In the modern water management, many constraints exist in the control structures, like pumps, gates and weirs, which have the limitations to the performance of the water system and more advanced control methods, e.g. MPC, are required rather than classic feedforward and feedback control. The control flexibility also needs to be increased over time. Taking irrigation canals as an example, water delivery should guarantee all the farmers' needs at any time of the day, no matter what changes they made.

Model Predictive Control is regarded as an advanced control not only because of its use of feedforward and feedback control to the system as well, but also because it takes all the control objectives and constraints into account and applies optimization techniques. The structure diagram of the Model Predictive Control controlling a water system is shown in Figure 3.1.

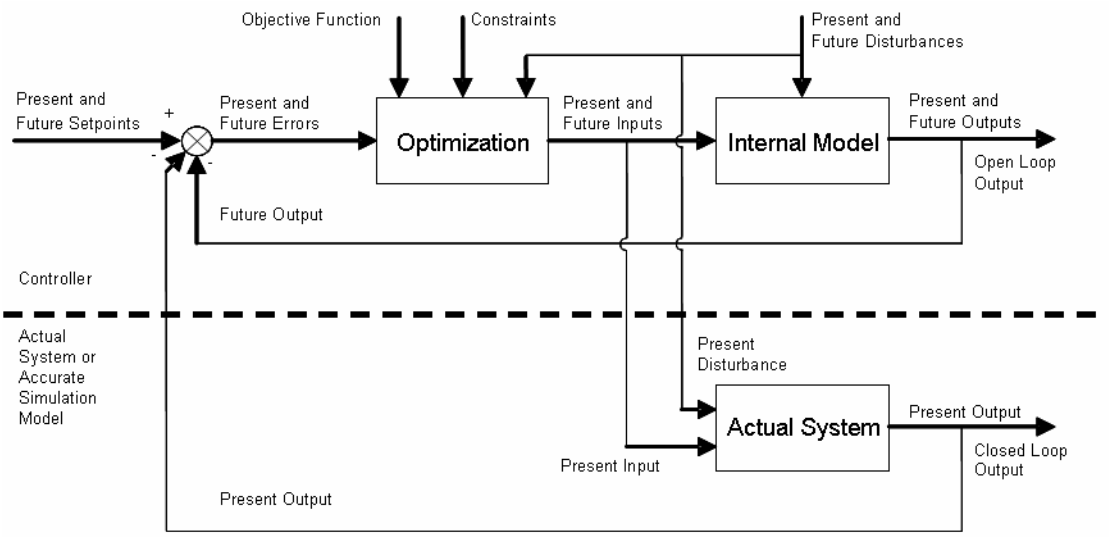

Figure 3.1, Structure diagram of Model Predictive Control controlling a water system

The model used for MPC is a representation to the actual system. When only looking at the model itself, the open loop for disturbances imposed on the internal model is the feedforward control, and the controller also takes the output values bake to the input comparing with the setpoint, which creates a closed loop called feedback control. There are some other important components in the Model Predictive Control. They are:

- Internal model.
- Objective function.
- Constraints.

- Optimization.
- Receding horizon.

The process which Model Predictive Control does is that it first takes the prediction of the system as the input together with the present and future system states. By using the internal model, the effect of these factors can be calculated and the future outputs of the water system are sent back to compare with the setpoints. The deviations from the setpoints are normally a term of the objective function subjected to the constraints. The optimization technique is used to minimize the objective function and achieve the optimized control action to the water system. When the calculation is finished, the model moves one step further according to the receding horizon and the same processes are performed until the whole simulation.

These major components construct the entire Model Predictive Control and their detailed descriptions will be discussed in the next parts. All the formulations considering the mathematical calculations and deductions will be illustrated as well. Only irrigation canal is considered.

3.2 Internal model

The internal model is used to predict the future states of a controlled irrigation canal. From the structure diagram in Figure 3.1, it is demonstrated that the inputs of the internal model have two parts. One is the present and future control actions generated from the optimization. And another one is the present and future disturbances, which could be the inflow water and the offtake pre-schedules. After the internal model, the output shows the effects of those inputs to the canal system. Normally, these outputs (present and future water levels and flows) are called state variables, which represent the state of the canal. For convenience, they are very often translated into the water level deviations and the change of flows. The linear internal models are mainly used due to the general mathematical methods (P.J. van Overloop, 2006), although the actual water system is non-linear. The commonly used state space internal model is expressed in formula 3.1.

$$\begin{aligned} x(k+1) &= A(k)\bullet x(k) + B_u(k)\bullet u(k) + B_d(k)\bullet d(k) \\ y(k) &= C\bullet x(k) \end{aligned} \qquad 3.1$$

Where:

x – States of the irrigation canal

A – System matrix

B_u – Control input matrix

B_d – Disturbance matrix

u – Control actions calculated by the controller

d – Disturbances

C – Output matrix

y – Outputs of the water system

k – Discrete time step index

The internal model should use the prediction to update the calculation upon the receding horizon. The formula for the next time step of k+2 will be:

$$x(k+2) = A(k+1)\bullet x(k+1) + B_u(k+1)\bullet u(k+1) + B_d(k+1)\bullet d(k+1) \qquad 3.2$$

Because the initial states $x(k)$ and inputs are known, the formula of the previous step is substituted into the present step, and it gets the formula 3.3:

$$\begin{aligned} x(k+2) &= A(k+1)\bullet[A(k)\bullet x(k) + B_u(k)\bullet u(k) + B_d(k)\bullet d(k)] \\ &\quad + B_u(k+1)\bullet u(k+1) + B_d(k+1)\bullet d(k+1) \\ &= A(k+1)\bullet A(k)\bullet x(k) + A(k+1)\bullet B_u(k)\bullet u(k) + B_u(k+1)\bullet u(k+1) \\ &\quad + A(k+1)\bullet B_d(k)\bullet d(k) + B_d(k+1)\bullet d(k+1) \end{aligned} \qquad 3.3$$

If continuing deriving the states in all the steps, taking n steps in total, there is no difficult to get the nth equation of $x(k+n)$. The total expression of the state space mode is:

$$\begin{aligned} X &= A\bullet x(k) + B_u\bullet U + B_d\bullet D \\ Y &= C\bullet X \end{aligned} \qquad 3.4$$

For convenience, it is recommended to write them in a systematic way of matrix and manipulating those matrices can lead to a fast solution to the problems (P.J. van Overloop, 2006). The matrix expressions representing all the variables for formula 3.4 in the internal model are shown here:

$$X = \begin{bmatrix} x(k) \\ x(k+1) \\ \vdots \\ x(k+n) \end{bmatrix} \quad U = \begin{bmatrix} u(k) \\ u(k+1) \\ \vdots \\ u(k+n) \end{bmatrix} \quad D = \begin{bmatrix} d(k) \\ d(k+1) \\ \vdots \\ d(k+n) \end{bmatrix}$$

$$A = \begin{bmatrix} I \\ A(k) \\ A(k+1)\bullet A(k) \\ \vdots \\ A(k+n-1)\bullet A(k+n-2)\bullet\cdots\bullet A(k) \end{bmatrix}$$

$$B_u = \begin{bmatrix} 0 & 0 & \cdots & 0 \\ B_u(k) & 0 & \cdots & 0 \\ A(k+1)\bullet B_u(k) & B_u(k+1) & \cdots & 0 \\ \vdots & \vdots & \ddots & \vdots \\ A(k+n-1)\bullet\cdots\bullet A(k+1)\bullet B_u(k) & A(k+n-2)\bullet\cdots\bullet A(k+1)\bullet B_u(k+1) & \cdots & B_u(k+n-1) \end{bmatrix}$$

$$B_d = \begin{bmatrix} 0 & 0 & \cdots & 0 \\ B_d(k) & 0 & \cdots & 0 \\ A(k+1)\bullet B_d(k) & B_d(k+1) & \cdots & 0 \\ \vdots & \vdots & \ddots & \vdots \\ A(k+n-1)\bullet\cdots\bullet A(k+1)\bullet B_d(k) & A(k+n-2)\bullet\cdots\bullet A(k+1)\bullet B_d(k+1) & \cdots & B_d(k+n-1) \end{bmatrix}$$

$$C = \begin{bmatrix} C & 0 & \cdots & 0 \\ 0 & C & \cdots & 0 \\ \vdots & \vdots & \ddots & 0 \\ 0 & 0 & \cdots & C \end{bmatrix}$$

From the structure diagram, a feedback law is introduced to the controller in order to overcome the conflict towards the constraints which may cause the MPC solution infeasible. If this happens, the feedback law will bring the controlled variables back to the setpoints. The feedback law is expressed in formula 3.5:

$$u(k) = -K(k)\bullet x(k) \qquad 3.5$$

Here K is the feedback gain.

When this feedback control part is applied to the controller, formula 3.1 will come to:

$$\begin{aligned} x(k+1) &= A(k)\bullet x(k) + B_u(k)\bullet[-K(k)\bullet x(k)] + B_d(k)\bullet d(k) \\ &= [A(k) - B_u(k)\bullet K(k)]\bullet x(k) + B_d(k)\bullet d(k) \\ &= A_c(k)\bullet x(k) + B_d(k)\bullet d(k) \\ y(k) &= C\bullet x(k) \end{aligned} \qquad 3.6$$

Extending to the whole prediction horizon, it is easy to get:

$$A_c = A - B_u\bullet K \qquad 3.7$$

Here A_c is called stable matrix, because of the stability guarantee from the feedback law.

$$K = \begin{bmatrix} K(k) & 0 & \cdots & 0 \\ 0 & K(k+1) & \cdots & 0 \\ \vdots & \vdots & \ddots & 0 \\ 0 & 0 & \cdots & K(k+n) \end{bmatrix} \qquad 3.8$$

3.3 Objective function

The objective function is the formulation of goals that need to be achieved by the controller. For the irrigation system, the goals can be to set the water level to the setpoint as close and fast as possible, or to minimize the flow changes through the gates or weirs, in order to make little adjustments to the structures and avoid tear and wear. Or if there are pumps using in the canal, the energy consumption can be another goal put in the objective function. These goals

may conflict each other, for example, limiting the change of flow will affect the water level back to the setpoint. Therefore, a relative penalty should be given to each of these objectives to indicate their relative importance. The high penalty means more importance of the subjected variables. The objective function is set up by using Quadratic Programming, which has the advantage to penalize both positive and negative deviations by using the power of 2 (P.J. van Overloop, 2006). The expression is shown in formula 3.9.

$$\min_{U} J = X' \bullet Q \bullet X + U' \bullet R \bullet U \qquad 3.9$$

Where:

J – Objective function

X – State variables

U – Control actions

Q – Weight matrix on state variables

R – Weight matrix on control actions

For the state variables, they normally use the water level deviations from setpoints rather than the water level itself, the change of these deviations, while the control actions are the change of control flows or the change of structure settings, like gate height or pump flow. The weight matrices of Q and R are diagonal. They represent the balance among all the goals. The determination of these weight matrices is the way of estimation, and bad estimations can cause the system unstable. This estimate is acquired via the Maximum Allowed Value Estimate (MAVE). The maximum and minimum allowed water levels relative to the setpoints are picked up for the weight factor of water level deviation, and the maximum flow changes through gates or the maximum gate height changes or pump flows are set for the weight factors of control actions. Then the weight factor is equal to the inverse of the MAVE values to the power 2.

3.4 Constraints

The constraints are physical and operational limitations on the controlled irrigation canal. They are usually applied in the optimization to restrict the boundary of the states, like water level errors, or the check structures. Some of them have the fixed values and are never allowed to be violated, for example, the limits on the magnitude of the maximum gate opening or the maximum pump capacity. The violation of these constraints will cause the damage to the structures. Some of these constraints can be time-variant. For example, when the constraint of maximum gate opening is transferred to the maximum flow through the gate, the flow constraint is time variant due to the change of water level upstream and downstream, by using stage-discharge relation, although the gate opening is fixed to the maximum. The formulation of constraints on the states and structures are:

$$\begin{aligned} -X_{\min} &\le X \le X_{\max} \\ -U_{\min} &\le U \le U_{\max} \end{aligned} \qquad 3.10$$

In order to meet the qualification of the Quadratic Programming calculation in MATLAB, it is recommended to put the constraint formula as 3.11:

$$\begin{aligned} E \bullet X &\leq X_{\lim} \\ F \bullet U &\leq U_{\lim} \end{aligned} \qquad 3.11$$

Where:

$X_{\lim}$ – Limitations on states

$U_{\lim}$ – Limitations on structures

E, F – Take 1 or -1 values in matrices to combine the two equations for maximum and minimum values in formula 3.10

3.5 Optimization

The optimization is a certain mathematical algorithm to achieve the goals by minimizing or maximizing the objective function. For those irrigation canals, the goals are to set the water level close to the setpoint or use little adjustments of the structures, thus, it's always minimizing the objective function (formula 3.9) subjected to the constraints. In order to achieve this, the control action should include another control part Z (P.J. van Overloop, 2006). Together with the feedback part $-K \bullet X$ (here these variables are extended to the whole prediction horizon), the total control action becomes:

$$U = -K \bullet X + Z \qquad 3.12$$

Applying formula 3.12 to 3.1, it comes:

$$\begin{aligned} x(k+1) &= A(k) \bullet x(k) + B_u(k) \bullet [-K(k) \bullet x(k) + z(k)] + B_d(k) \bullet d(k) \\ &= [A(k) - B_u(k) \bullet -K(k)] \bullet x(k) + B_u(k) \bullet z(k) + B_d(k) \bullet d(k) \\ &= A_c(k) \bullet x(k) + B_u(k) \bullet z(k) + B_d(k) \bullet d(k) \end{aligned} \qquad 3.13$$

By using the same procedure deriving formula 3.4 over the whole horizon, the same type of equation can be achieved:

$$\begin{aligned} X &= A_c \bullet x(k) + B_u \bullet Z + B_d \bullet D \\ Y &= C \bullet X \end{aligned} \qquad 3.14$$

When applying Quadratic Programming, the minimum of the objective function can be found at the point where the gradient of the function is zero (Huanwen Tang and Xuezhi Qin, 2005).

$$J(Z) = \frac{1}{2} \bullet Z^{'} \bullet H \bullet Z + f \bullet Z + g$$
$$\frac{\partial J(Z)}{\partial Z} = H \bullet Z + f = 0 \qquad 3.15$$
$$Z = -\frac{f}{H}$$

The gradient can be determined by calculating the Hessian matrix H and the Lagrangian f. For optimization, the constant matrix g has no influence to the problem and can be neglected.

The Hessian matrix H and the Lagrangian f (detailed deduction of them are described in Appendix II), together with the constraints for the optimization can be derived:

$$H = 2 \bullet (B_u^{'} \bullet Q \bullet B_u - R \bullet K \bullet B_u + R + B_u^{'} \bullet K^{'} \bullet R \bullet K \bullet B_u - B_u^{'} \bullet K^{'} \bullet R)$$

$$f = 2 \bullet x(k) \bullet (A_c^{'} \bullet Q \bullet B_u + A_c^{'} \bullet K^{'} \bullet R \bullet K \bullet B_u - A_c^{'} \bullet K^{'} \bullet R)$$
$$+ 2 \bullet D^{'} \bullet (B_d^{'} \bullet Q \bullet B_u + B_d^{'} \bullet K^{'} \bullet R \bullet K \bullet B_u - B_d^{'} \bullet K^{'} \bullet R)$$

$$E \bullet (A_c \bullet x(k) + B_u \bullet Z + B_d \bullet D) \leq X_{\lim}$$
$$F \bullet (-K \bullet X + Z) \leq U_{\lim}$$

3.6 Receding horizon

The receding horizon is a moving time steps to the future. The controller uses all the components discussed above in one time step. After an optimization, the control action is calculated and acted to the system. According to the receding horizon, a new step comes and the prediction is updated by moving one step further. The same calculation is performed until the entire simulation is finished. The receding horizon keeps the controller using the most recent predictions and updating to the future.

3.7 Comparison with classic control methods

From the aforementioned both classic control methods and Model Predictive Control, the benefits of MPC are apparent. First, it can take into account the constraints imposed on the irrigation canal system and this can never be considered by the classic methods. Second, a feedforward routine is built directly into the MPC controller and a separate feedforward routine does not need to be added to the controller (Wahlin, B.T. 2006). A fixed disturbance (offtake pre-schedule) is place along the prediction horizon and the controller can predict it before the offtakes happen. Of course MPC also has its disadvantages. The most drawback is that it uses on-line optimization, which means that the optimization will be calculated in every time step

and will take much computational time. If the problem is very complex, this drawback will be severe. The second drawback is the effect of the constraints. If the constraints are too strong, for example big constraints on the water level errors of an irrigation canals, this will make a tight controller and need extremely accurate measurements. In reality, this might cause the infeasibility of the system.

In this research project, MPC is a good option for application to deal with supply and demand mismatches for irrigation water subjected to the constraints. Because the last gate (84-inch gate) is unable to be controlled and the head gate can only be changed twice a day (thought to be no control), it is difficult to control 7 pools with 6 check gates by using classic control methods. This is another reason to choose MPC for the application.

4 Introduction to the Central Main Canal

Recently, an irrigation canal automation project is conducting in Eloy district, Arizona, US, by the Central Arizona Irrigation and Drainage District (CAIDD). They are trying to automate the Central Main Canal (CMC) which is the main irrigation supply canal in that district. It takes water from the Central Arizona Project (CAP). The location of the canal is shown in the Figure 4.1. Due to the inaccurate manual operation and the limitation on head gate flow change, although the operators are well experienced, there will be some supply and demand mismatches in the canal. How MPC controls the water levels and deals with these mismatches will be modeled in the next chapter. But the basic conditions, characteristics as well as the recent operation of the Central Main Canal will be first introduced here.

Figure 4.1, Location of the Central Main Canal

4.1 Impression to the Central Main Canal

The Central Main Canal is a man-made open canal. It has the concrete bottom liner and the total length is over 28 kilometers with the design capacity of 25.47m^3/s. Figure 4.2, generated from the SOBEK model, gives the impression to the canal.

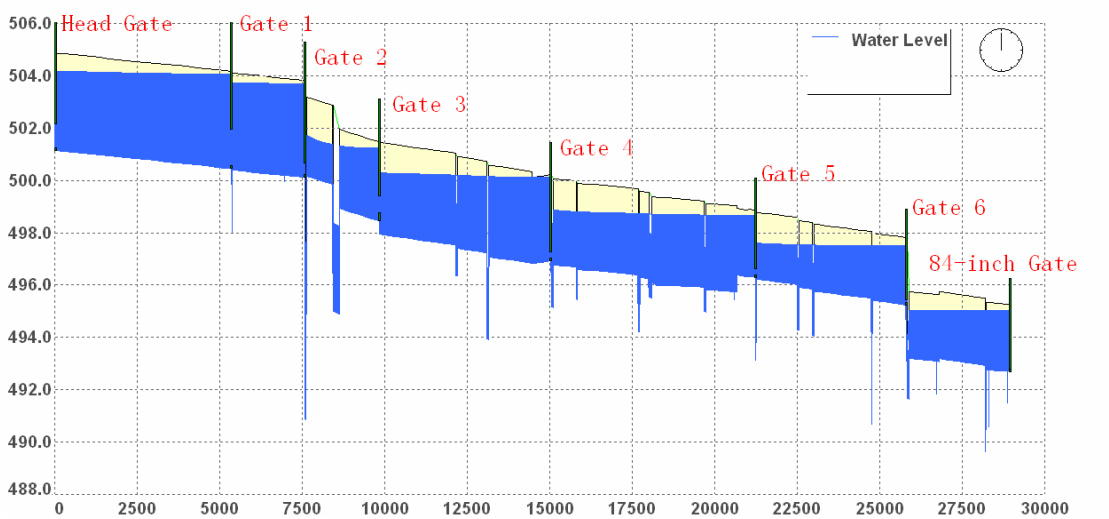

Figure 4.2, Longitudinal profile of the Central Main Canal (the horizontal axis is the distances from the inlet in Central Arizona Project, the vertical axis is the canal elevation above the reference)

Water in the canal is the gravity flow. The whole canal is divided into 7 pools with different lengths based on the 6 inline radial gates. One of the examples is shown in Figure 4.3. The free board is almost parallel to the bottom. The canal can be regarded as deep and flat, except for pool 3 which is designed as a transition and relatively short and steep. There are 20 offtakes spreading along the canal. 5 of them are pump offtakes, and others are using sluice gates. Some wells contribute additional flows to the canal, from which water is relatively cheap compared to that coming from the Central Arizona Project (CAP). It is recommended to use as much groundwater as possible until the power usage for all the pumps reaches the threshold, otherwise, the power cost will make it uneconomical. Figure 4.4 and 4.5 show the examples of a well and an undershot offtake gate. Many culverts are constructed in the canal due to the real situations that the canal passes through the rail way, big washes (drainage), roads etc. This can also been seen from the longitudinal profile of the Central Main Canal.

Figure 4.3, Example of an inline radial gate from the Central Main Canal

Figure 4.4, Example of the wells along the Central Main Canal

Figure 4.5, Example of a lateral offtake along the Central Main Canal

CAIDD is now remotely-manually operating the entire canal by using the feedforward control with the help of SCADA (Supervisory Control and Data Acquisition) system. Farmers in that district should order their water one day in advance and all the information, including the amount of water and the time of using this water, comes to the central office. Then the district orders water from the CAP based on the total farmers' order, to match their requirements. This supervisory manual control allows water master to monitor the system conditions and manipulate control structures from a headquarters office, no need to adjust the gate by driving along the canal, and usually control decisions are based on operator skills and experience (David C. Rogers and Jean Goussard, 1998). The canal operation starts with a head gate through which the inflow can only be adjusted twice a day. The operator adjusts the head gate and then water travels downstream. When the water wave arrives to the end of the first pool, the water master adjusts the first check gate to maintain the first pool condition that required for the canal. The same procedure is conducted to other pools until water rearches the end of the canal. If there are certain changes in flows, the operator needs to make new adjustment. Because all the operations are manual, depending on the operators' estimation, they must be

very experienced to the canal and flow situation; otherwise, it will take them too much time to adjust the gates to the right position and keep the right pool conditions. The inaccurate operation requires automatic control of these check gates.

4.2 Canal characteristics

Canal characteristics are the basic information describing what the canal looks like, for example, the cross section shape, slope, length, hydraulic resistance and the operational water level, etc. In order to apply a controller to the canal, these characteristics should be considered carefully, because they will influence the flow that moves from one steady state condition to another, thus, influence the pool volume (T.S.Strelkoff, et, al. 1998). The main characteristics of the Central Main Canal are listed in the tables below (better to refer to figure 4.2 (the longitudinal profile)).

Table 4.1, Physical characteristics of each canal pools

Pool NO.	Capacity (m3/s)	Length (m)	Bottom slope	Manning n
Pool 1	25.47	5217.752	0.00013	0.015
Pool 2	25.47	2207.215	0.00013	0.015
Pool 3	25.47	2269.361	0.0004	0.015
Pool 4 (I)	25.47	5204.704	0.00018	0.015
Pool 4 (II)	16.98		0.0001	0.015
Pool 5 (I)	16.98	6189.811	0.0001	0.015
Pool 5 (II)	9.9		0.00016	0.014
Pool 6	9.9	4572.390	0.00016	0.014
Pool 7 (I)	9.9	3144.862	0.00016	0.014
Pool 7 (II)	4.81		0.0001	0.014

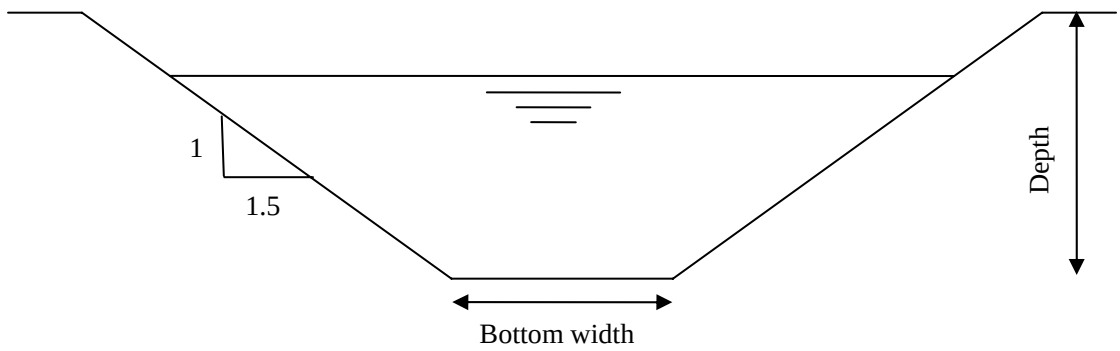

Figure 4.6, Cross section shape

Table 4.2, Cross section in each pool

Pool NO.	Invert Elevation (up) (m+Ref)	Invert Elevation (down) (m+Ref)	Bottom width (m)	Depth (m)	Side slope (V:H)
Pool 1	501.1339	500.4572	3.66	3.72	1:1.5
Pool 2	500.4572	500.1097	3.66	3.72	1:1.5
Pool 3	500.1555	498.4577	3.66	3.02	1:1.5
Pool 4 (I)	497.9396	496.8301	3.66	3.51	1:1.5
Pool 4 (II)	496.9764	496.9215	3.66	3.29	1:1.5
Pool 5 (I)	496.9215	495.7450	3.66	3.29	1:1.5
Pool 5 (II)	496.3942	496.2967	2.44	2.56	1:1.5
Pool 6	496.2967	495.2512	2.44	2.56	1:1.5
Pool 7 (I)	495.2512	493.1877	2.44	2.56	1:1.5
Pool 7 (II)	493.1877	492.6970	1.22	2.10	1:1.5

Table 4.3, Normal operational water level

Pool NO.	Setpoint (m+Ref)
Pool 1	504.024
Pool 2	503.677
Pool 3	501.231
Pool 4	500.091
Pool 5	498.613
Pool 6	497.507
Pool 7	495.060

The canal is relatively deep and flat seen from the tables above. But some of them are short, and resonance waves can probably happen there due to the flow traveling and the gate movement. Pools 4, 5 and 7 have two segments with different design capacities. That is because of the sudden cross section dimension change at those places.

5 Model Predictive Control on Central Main Canal based on the Integrator-Delay Model

5.1 Introduction of Integrator-Delay Model

Model Predictive Control (MPC) can be applied to the irrigation canals based on different models which capture the detailed knowledge of dynamics of these canals. Due to the nonlinearity of the canal, it will make the controller complicated, thus, a linear approximated model is required (Jan Schuurmans, 1997). The most commonly used model is the so called Integrator Delay (ID) model which catches the major dynamics of an irrigation canal: delay time and surface area. It is a linear approximation model with some assumptions. First, the canal pool is divided into two parts: the uniform flow part where the water profile is parallel to the canal bottom at the normal flow depth, and the backwater (reservoir) part which is caused by the check structures at the end of each pool. In the backwater part, the water level is assumed to be horizontal. T.S. Strelkoff et al. (1998) pointed that the amount of backwater at the downstream end of the pool can have huge effect on the system and are necessary to allow sufficient control. Second, when the flow travels from upstream to downstream, a certain delay time exists, but this only happens in the uniform flow part. While in the backwater part, waves travel up and down and reflect against the boundaries. The surface area becomes a key factor and the water level seems to be an integrator of the flow deviations in this part. That's the reason the model is called Integrator-Delay model. The third assumption is that all the offtakes are located at the end of each pool, where water level is controlled. One of the goals in irrigation canal control systems is to maintain constant offtake discharges. This can be achieved by automating the offtake to keep the constant flow or automating the canal to keep the water level on the upstream of the offtake constant, or both (V.M. Ruiz-Carmona et al. 1998). It is impossible to keep the canal water levels constant over the entire length of a pool due to the water surface slope changes with flow rates, and only the water level at the end of the canal pool is controlled in the Integrator Delay model. Therefore, the third assumption is a necessity. Figure 5.1 shows the representation of one canal pool.

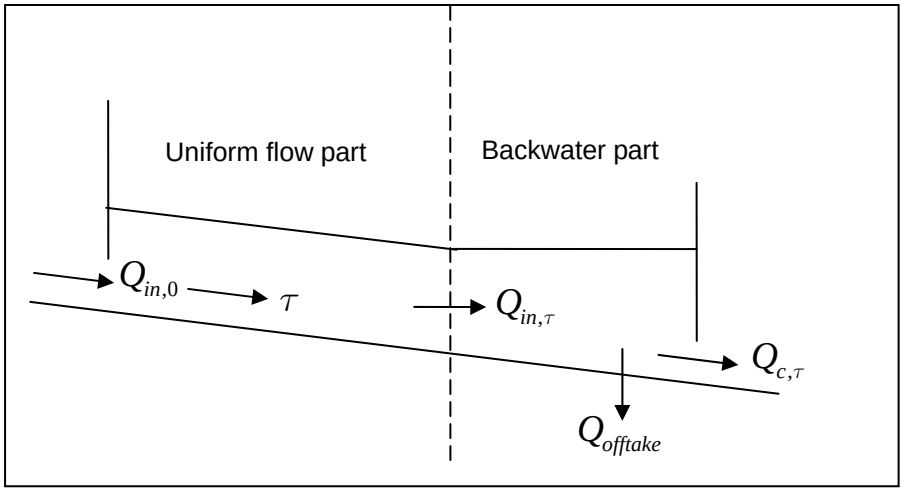

Figure 5.1, Irrigation canal pool profile

When there is a flow change at the upstream of the pool, it creates two waves with the velocities of V+c and V-c, respectively. Here V represents the flow velocity and c is the wave celerity. During traveling, the waves deform. Obviously, the wave with velocity of V-c deforms much faster than the other. The reason why delay only happens in the uniform flow part is because of the friction from the canal bottom, which is the only cause for wave dampening based on the Saint Venant equations. In the backwater part, the flow velocity is relatively small, thus, the friction from the canal bottom is less and the wave hardly deforms. Then the flow change can reach the downstream quite fast. While in the uniform part, the wave deformation is essential due to the high flow velocity, thus, the high friction (J. Schuurmans et, al. 1999).

Based on this analysis and combined with the figure 5.1, the Integrator Delay model can have two approximations to the uniform flow part and backwater part, separately.

- Approximation for the uniform flow part (a pure delay model): the inflow at the upstream is the same as the outflow at the end of uniform flow part after a certain delay. Therefore, it is easy to get the equation:

  $$Q_{in,0} = Q_{in,\tau} \qquad 5.1$$

  Where:

  $Q_{in,0}$ – Upstream inflow [m^3/s]

  $Q_{in,\tau}$ – Downstream outflow at the end of uniform flow part [m^3/s]

  τ – Delay time [s]

- Approximation for the backwater part (a reservoir model): the surface is assumed to be completely horizontal and the main characteristic is represented by the surface area. A mass balance can be applied to this part. Considering the cross-sectional view of the process, a trapezoidal shaped canal looks like this:

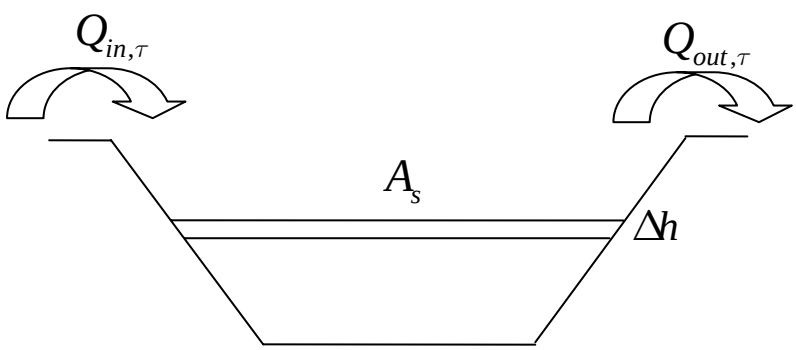

Figure 5.2, Cross-sectional view of the reservoir part

When the inflow from the uniform flow part reaches downstream, it becomes the inflow of the reservoir part. There will be a small water level increase Δh due to the big surface

area A_s. The volume increase can be approximated by using $A_s \bullet \Delta h$. Therefore, the mass balance can be applied:

$$\frac{dV}{dt} = Q_{in,\tau} - Q_{out,\tau}$$
$$so, \quad A_s \bullet \frac{dh}{dt} = Q_{in,\tau} - Q_{out,\tau} = Q_{in,\tau} - (Q_{c,\tau} + Q_{offtake}) \qquad 5.2$$

Where:

V – Volume [m^3]

$Q_{c,\tau}$ – Control flow through gate [m^3/s]

$Q_{offtake}$ – Offtake flow [m^3/s]

If the pool is completely backed up, only the reservoir model is needed. Otherwise, a combination should be used.

5.2 Determination of pool properties

From the analysis to the Integrator Delay model, there are mainly two hydraulic parameters representing the canal dynamics: delay time and backwater surface area. Thus, the determination of these two factors becomes a critical issue of applying the ID model. There are two ways to solve the problem: first, it can be calculated from the geometry of the canal, the flow rates and water levels under steady state conditions. This is tedious work and becoming impossible when the data is lacking. The second and more practical method is through unsteady flow simulations (J. Schuurmans et al. 1999). The model's response to a flow change upstream can be fitted by using the measured water level downstream. The detailed procedures are presented blow;

- A steady state condition is achieved under a certain capacity with the laterals on before the unsteady flow simulation in SOBEK starts.
- Separate the canal pools by shut down all the check gates, and all the lateral offtakes are closed as well. With a step inflow, the water passes through the fixed pump station at the downstream of each pool. The pump capacity is the same as the capacity in steady state condition. An example of inflow and outflow is shown in Figure 5.3 and 5.4 (60% of the design capacity).

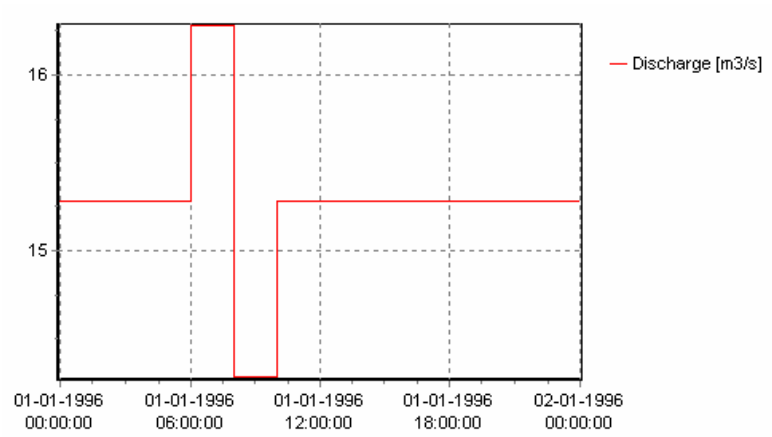

Figure 5.3, Example of inflow for pool properties determination

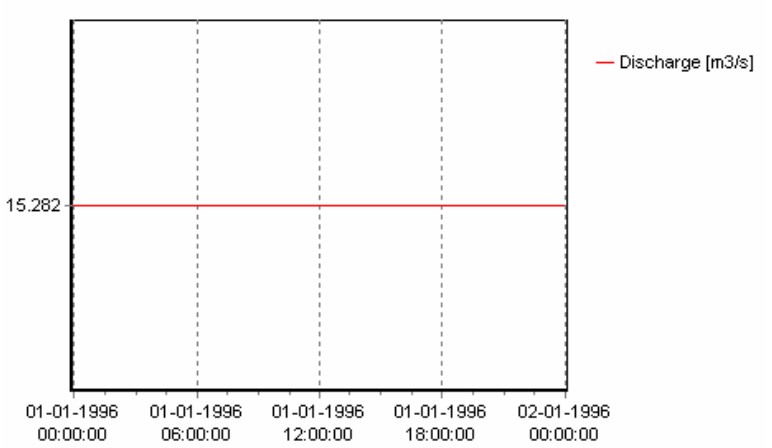

Figure 5.4, Example of pump outflow for pool properties determination

- An unsteady flow simulation starts in SOBEK and the water levels at the end of each pool are detected with the aforementioned inflow and outflow, taking the first pool as an example:

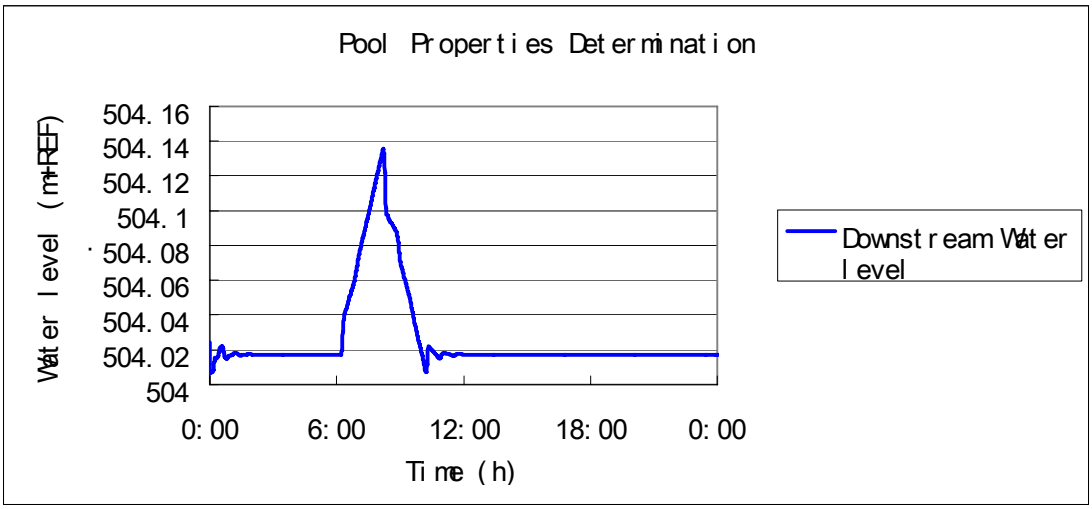

Figure 5.5, Downstream water level of the first pool with the aforementioned inflow and outflow

The delay time can be seen from the time difference between the step flow change and the downstream water level change. The mass balance provides a function of determining the surface area:

$$A_s = \frac{\Delta Q \cdot \Delta t}{\Delta h} \qquad 5.3$$

If the flow change of ΔQ is set up to 1 m^3/s, the surface area A_s will be inverted to the slope of the rising line referring to figure 5.5. Therefore, the next step is to calculate its trend line, and the delay time can also be determined by moving the trend line passing through the 6:00 point (time of inflow change) in this example.

The unsteady flow simulation provides the method of determining canal pool properties, and with these information, the internal model can be configured.

Because different inflows will cause different flow conditions in the canal, pool properties will also be affected to a certain degree. Figure 5.6 shows different water level profiles from the Central Main Canal in different flow conditions. The differences are obvious. Therefore, pool properties should be determined for specific flow capacities and big flow change is not allowed in the Integrator Delay model.

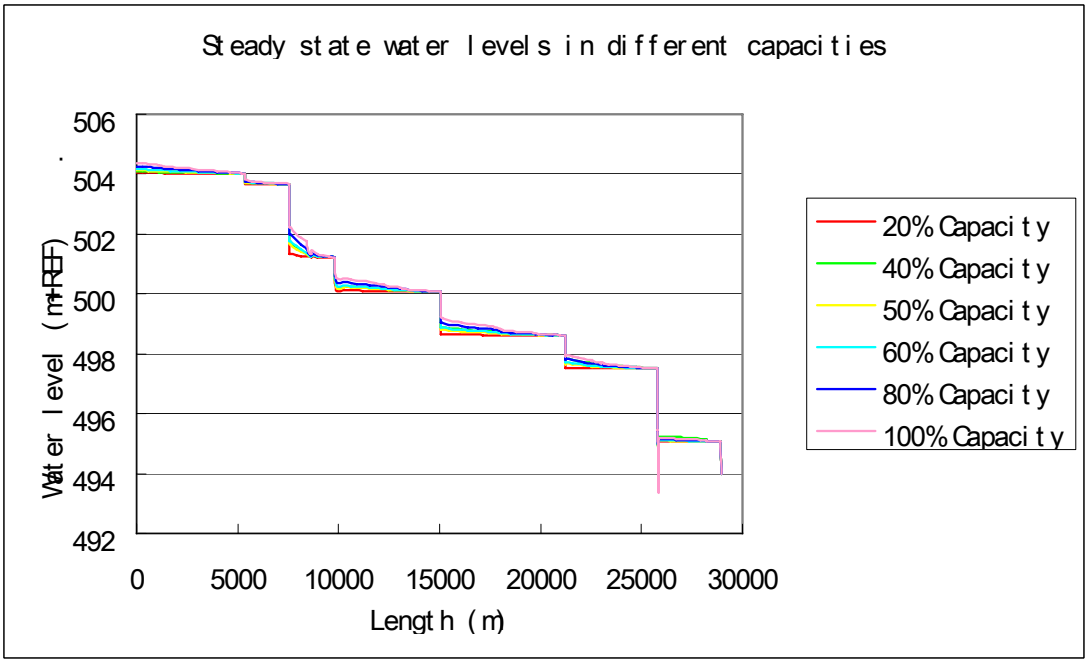

Figure 5.6, Steady state water levels in different capacities

The pool properties of the Central Main Canal on different inflow capacities are listed in the table 5.1, 5.2 and 5.3:

Table 5.1, Delay time in different pools and different inflow capacities (Unit: seconds)

Pool NO.	100%	80%	60%	50%	40%	20%
1	315	225	210	180	165	135
2	30	30	30	15	12	12
3	255	225	210	180	150	120
4	585	510	420	375	315	210
5	930	855	705	645	540	315
6	720	690	540	510	450	255
7	330	300	285	270	195	135

Considering the scale of the system, the requirement of accuracy and the implementation in the field, 2 minutes control time is chosen. The delay time is translated into delay time steps based on this control time. The number of delay time steps in the state matrix is determined by dividing the delay time by the control time step and always rounding up (Wahlin, B.T. and A.J. Clemmens, 2006).

Table 5.2, Delay time steps in different pools and different inflow capacities

Pool NO.	100%	80%	60%	50%	40%	20%
1	3	2	2	2	2	2
2	1	1	1	1	1	1
3	3	2	2	2	2	1
4	5	5	4	4	3	2
5	8	8	6	6	5	3
6	6	6	5	5	4	3
7	3	3	3	3	2	2

Table 5.3, Surface areas in different pools and different inflow capacities (Unit: m^2)

Pool NO.	100%	80%	60%	50%	40%	20%
1	57084	61609	65230	67016	68439	70346
2	28989	29460	30123	30218	30492	30506
3	18264	18254	18246	18750	18948	19276
4	47552	52750	56439	57776	59659	62745
5	44221	48838	55051	57036	58856	62114
6	27450	28471	31010	31708	32099	33930
7	20759	21370	21981	22739	22978	23456

The delay time and the surface areas are plotted against different inflow capacities in the figure 5.7 and 5.8. There is an obvious trend in these two figures that the delay time increases and the surface area decreases as the inflow is becoming higher. The reason to explain this phenomenon should come to the irrigation canal pool profile. As the inflow increases, the water level goes up, which means the length of uniform flow part gets longer. Although the water travels faster, the impact of length increase is much bigger than the flow velocity. Hence the delay time increases. While in the backwater part, because the length is getting shorter,

and the effect is stronger than the top water width increase, the surface area decreases as the inflow gets higher.

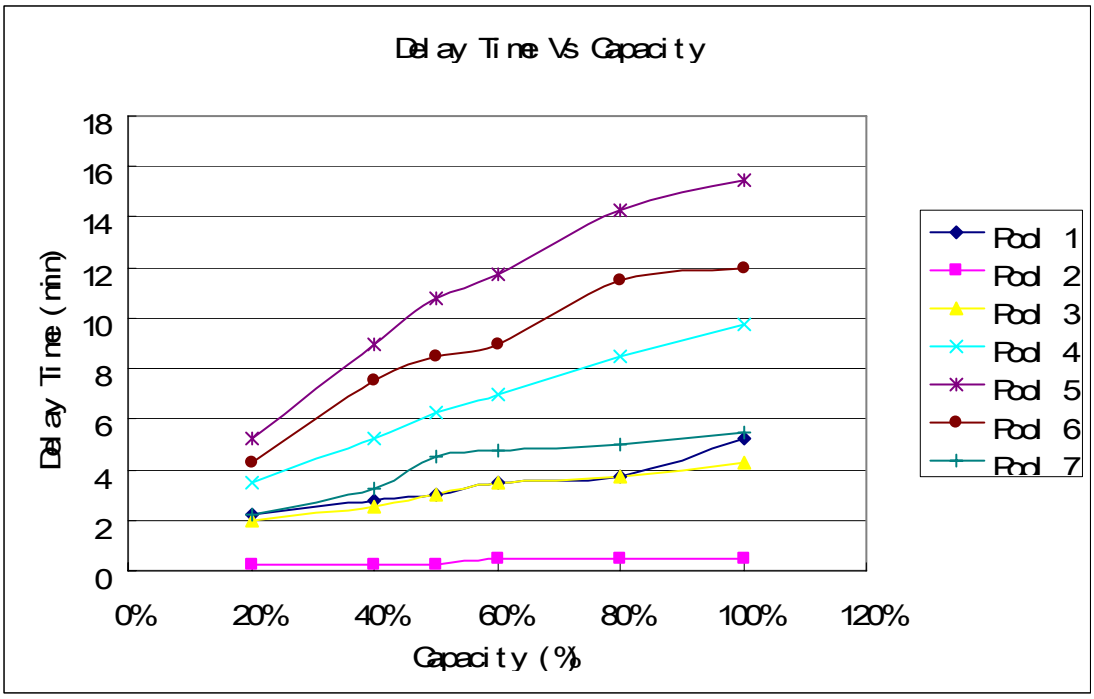

Figure 5.7, Plot of Delay time Versus Inflow Capacity in different pools

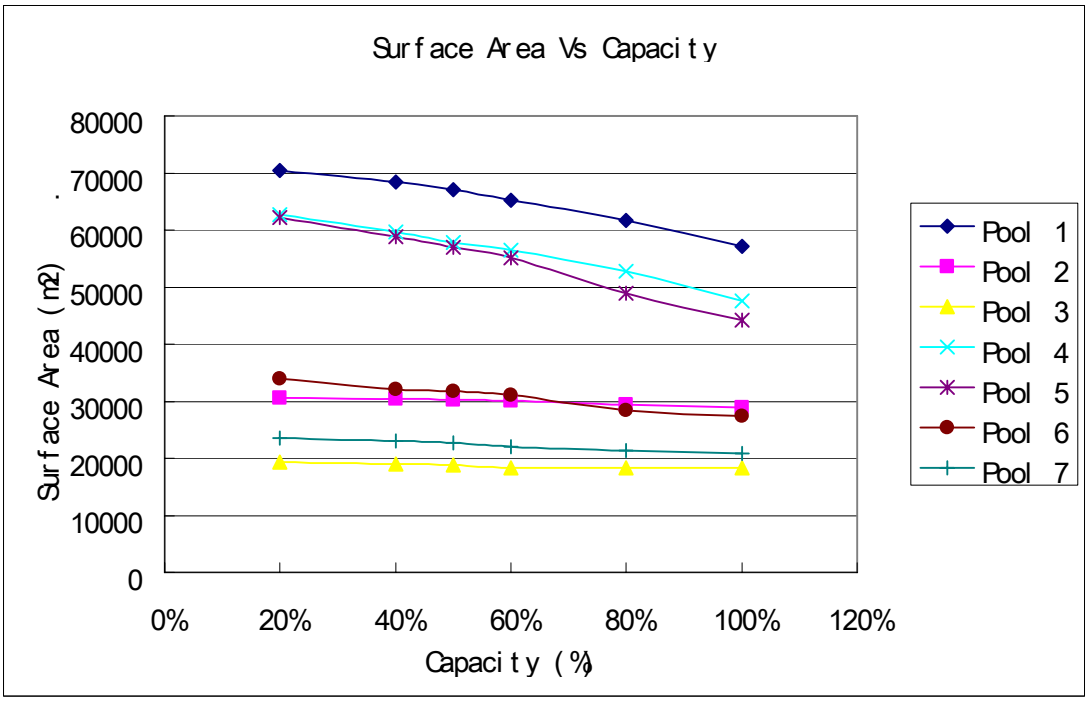

Figure 5.8, Plot of Surface area Versus Inflow Capacity in different pools

5.3 Internal model

With the above preparations, Model Predictive Control based on the Integrator Delay model can now be applied on the Central Main Canal. Water level error e and the change of flow ΔQ are commonly used in the internal model, instead of water level and flow themselves. The change of water level error Δe is also used to limit the rate of water level fluctuation, and the flows at previous time steps based on the delay time steps are considered to be the terms in the state matrix. The internal model derived here is only for one pool and extended to two. The Full model is shown in Appendix III, for convenience.

5.3.1 Internal model on one pool

The first pool of the Central Main Canal is considered and it has both the uniform flow part and the backwater part. Therefore, the approximations should be applied on both parts. The discretization of the combined approximations on two parts becomes:

$$\begin{aligned}\Delta h = h(k+1) - h(k) &= \frac{T_c}{A_s}[Q_{in}(k-k_d) - Q_{out}(k)] \\ &= \frac{T_c}{A_s}\{Q_{in}(k-k_d) - [Q_c(k) + Q_{offtake}(k)]\}\end{aligned} \qquad 5.4$$

Where:

k – Time step [-]

k_d – Delay time steps [-]

T_c – Control time [s]

There are:

$$\begin{aligned} e(k) &= h(k) - h_{ref} \\ e(k+1) &= h(k+1) - h_{ref} \end{aligned} \quad \Rightarrow \quad h(k+1) - h(k) = e(k+1) - e(k) \qquad 5.5$$

Where h_{ref} is the water level setpoint.

Then, considering two consecutive time steps, formula 5.4 becomes:

$$e(k+1) - e(k) = \frac{T_c}{A_s}\{Q_{in}(k-k_d) - [(Q_c(k) + Q_{offtake}(k)]\} \qquad 5.6$$

$$e(k) - e(k-1) = \frac{T_c}{A_s}\{Q_{in}(k-1-k_d) - [(Q_c(k-1) + Q_{offtake}(k-1)]\} \qquad 5.7$$

Substituting 5.7 into formula 5.6 gets:

$$e(k+1)=e(k)+[(e(k)-e(k-1)]+\frac{T_c}{A_s}[Q_{in}(k-k_d)-Q_{in}(k-1-k_d)] \\ -\frac{T_c}{A_s}\{[Q_c(k)-Q_c(k-1)]+[Q_{offtake}(k)-Q_{offtake}(k-1)]\} \quad 5.8$$

With the definitions:

$$\begin{aligned} &\Delta e(k+1)=e(k+1)-e(k) \\ &\Delta e(k)=e(k)-e(k-1) \\ &\Delta Q_c(k)=Q_c(k)-Q_c(k-1) \\ &\Delta Q_{in}(k)=Q_{in}(k)-Q_{in}(k-1) \\ &\Delta Q_{offtake}(k)=Q_{offtake}(k)-Q_{offtake}(k-1) \end{aligned} \quad 5.9$$

The two equations for the state-space model, taking the change of water level error Δe into account, can be derived from equation 5.8:

$$e(k+1)=e(k)+\Delta e(k)+\frac{T_c}{A_s}\Delta Q_{in}(k-k_d)-\frac{T_c}{A_s}[\Delta Q_c(k)+\Delta Q_{offtake}(k)] \quad 5.10$$

$$\Delta e(k+1)=\Delta e(k)+\frac{T_c}{A_s}\Delta Q_{in}(k-k_d)-\frac{T_c}{A_s}[\Delta Q_c(k)+\Delta Q_{offtake}(k)] \quad 5.11$$

Because the head gate inflow of the Central Main Canal can only be changed twice a day, this is held to be another disturbance in the model which has the opposite sign to the offtakes. Together, they comprise of the disturbance matrix ΔQ_d :

$$\Delta Q_d(k)=Q_d(k)-Q_d(k-1) \quad 5.12$$

Considering the flow of 60 percent of the design capacity, there are 2 delays steps in the first pool that consists of 3 offtakes. Thus,

$$\begin{pmatrix} e(k+1) \\ \Delta e(k+1) \\ \Delta Q_H(k) \\ \Delta Q_H(k-1) \end{pmatrix} = \begin{pmatrix} 1 & 1 & 0 & \frac{T_c}{A_{s1}} \\ 0 & 1 & 0 & \frac{T_c}{A_{s1}} \\ 0 & 0 & 0 & 0 \\ 0 & 0 & 1 & 0 \end{pmatrix} \begin{pmatrix} e(k) \\ \Delta e(k) \\ \Delta Q_H(k-1) \\ \Delta Q_H(k-2) \end{pmatrix} + \begin{pmatrix} -\frac{T_c}{A_{s1}} \\ -\frac{T_c}{A_{s1}} \\ 0 \\ 0 \end{pmatrix} [\Delta Q_c(k)]$$

$$+ \begin{pmatrix} 0 & -\frac{T_c}{A_{s1}} & -\frac{T_c}{A_{s1}} & -\frac{T_c}{A_{s1}} \\ 0 & -\frac{T_c}{A_{s1}} & -\frac{T_c}{A_{s1}} & -\frac{T_c}{A_{s1}} \\ 1 & 0 & 0 & 0 \\ 0 & 0 & 0 & 0 \end{pmatrix} \begin{pmatrix} \Delta Q_H(k) \\ \Delta Q_{d1}(k) \\ \Delta Q_{d2}(k) \\ \Delta Q_{d3}(k) \end{pmatrix} \qquad 5.13$$

Here ΔQ_H is the flow change of head gate, A_{s1} represents the surface area of the first pool.

5.3.2 Internal model on two pools

As an irrigation canal is always divided into several pools with different delay time, it is necessary to know how they structure the internal model during modeling. From the figure of a canal profile of two pools, the outflow of the control gate from the first pool becomes the inflow of the second pool with a certain delay.

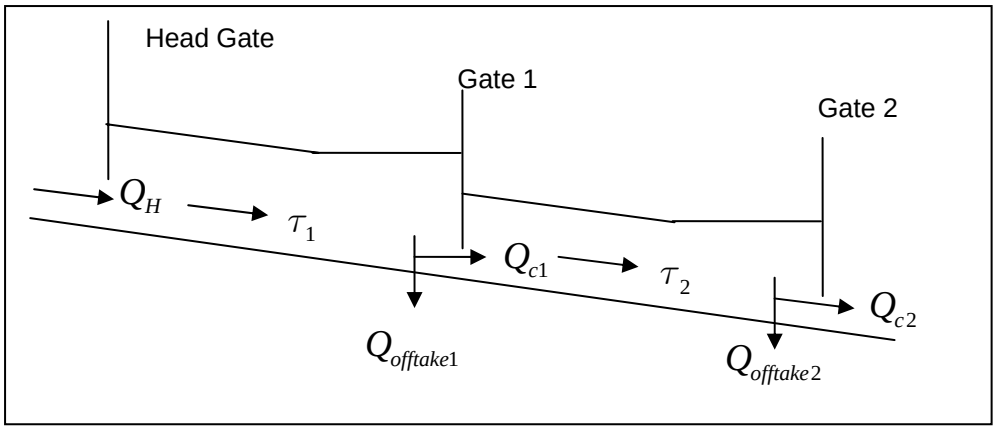

Figure 5.9, Irrigation canal profile of two pools

There are 2 offtakes and 1 delay step in the second pool. The internal model can be expanded like this:

$$
\begin{pmatrix} e_1(k+1) \\ \Delta e_1(k+1) \\ \Delta Q_H(k) \\ \Delta Q_H(k-1) \\ e_2(k+1) \\ \Delta e_2(k+1) \\ \Delta Q_{c1}(k) \end{pmatrix}
=
\begin{pmatrix}
1 & 1 & 0 & \frac{T_c}{A_{s1}} & 0 & 0 & 0 \\
0 & 1 & 0 & \frac{T_c}{A_{s1}} & 0 & 0 & 0 \\
0 & 0 & 0 & 0 & 0 & 0 & 0 \\
0 & 0 & 1 & 0 & 0 & 0 & 0 \\
0 & 0 & 0 & 0 & 1 & 1 & \frac{T_c}{A_{s2}} \\
0 & 0 & 0 & 0 & 0 & 1 & \frac{T_c}{A_{s2}} \\
0 & 0 & 0 & 0 & 0 & 0 & 0
\end{pmatrix}
\begin{pmatrix} e_1(k) \\ \Delta e_1(k) \\ \Delta Q_H(k-1) \\ \Delta Q_H(k-2) \\ e_2(k) \\ \Delta e_2(k) \\ \Delta Q_{c1}(k-1) \end{pmatrix}
+
\begin{pmatrix} -\frac{T_c}{A_{s1}} \\ -\frac{T_c}{A_{s1}} \\ 0 \\ 0 \\ -\frac{T_c}{A_{s2}} \\ -\frac{T_c}{A_{s2}} \\ 1 \end{pmatrix}
\begin{pmatrix} \Delta Q_{c1}(k) \\ \Delta Q_{c2}(k) \end{pmatrix}
$$

$$
+
\begin{pmatrix}
0 & -\frac{T_c}{A_{s1}} & -\frac{T_c}{A_{s1}} & -\frac{T_c}{A_{s1}} & 0 & 0 \\
0 & -\frac{T_c}{A_{s1}} & -\frac{T_c}{A_{s1}} & -\frac{T_c}{A_{s1}} & 0 & 0 \\
1 & 0 & 0 & 0 & 0 & 0 \\
0 & 0 & 0 & 0 & 0 & 0 \\
0 & 0 & 0 & 0 & -\frac{T_c}{A_{s2}} & -\frac{T_c}{A_{s2}} \\
0 & 0 & 0 & 0 & -\frac{T_c}{A_{s2}} & -\frac{T_c}{A_{s2}} \\
0 & 0 & 0 & 0 & 0 & 0
\end{pmatrix}
\begin{pmatrix} \Delta Q_H(k) \\ \Delta Q_{d1}(k) \\ \Delta Q_{d2}(k) \\ \Delta Q_{d3}(k) \\ \Delta Q_{d4}(k) \\ \Delta Q_{d5}(k) \end{pmatrix}
\qquad 5.14
$$

From formula 5.13 and 5.14, it is obvious to see that the state variables will become quite large when the number of pool and delay step increases.

5.3.3 Flow controller

All the water level errors can be determined by measuring the water levels and comparing with the setpoints. Then the change of error is not difficult to calculate. As to the flow change at check or lateral gates, direct flow measurements are not economic and flow controllers are used to convert the flow change into gate position change. So in practice, by monitoring the gate position, the flow can be easily calculated. There are four discharge equations used for the flow controller depending on the different flow conditions categorized into orifice flow and weir flow (SOBEK 2000). Figure 5.10 shows the geometrical shape of an orifice. The detailed formulations are as follows.

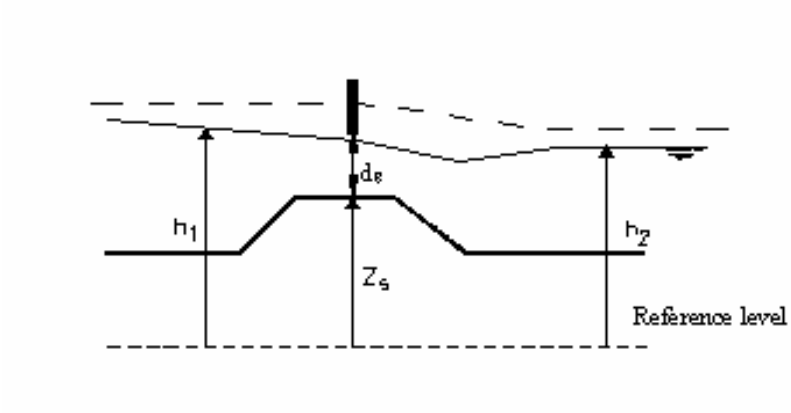

Figure 5.10, Geometrical shape of an orifice

- Free orifice flow

$$Q = c_w \bullet W_s \bullet \mu \bullet d_g \bullet \sqrt{2 \bullet g \bullet (h_1 - (z_s + \mu \bullet d_g))} \qquad 5.14$$

With the flow conditions:

$$h_1 - z_s \geq \frac{3}{2} \bullet d_g \quad \text{and} \quad h_2 \leq z_s + d_g$$

Where:

Q – Discharge through orifice [m3/s]

c_w – Lateral contraction coefficient [-]

W_s – Crest width [m]

μ – Contraction coefficient [-], taking 0.63

d_g – Gate opening height [m]

g – Gravity acceleration [m/s2], taking 9.81

h_1 – Upstream water level [m]

z_s – Crest level [m]

h_2 – Downstream water level [m]

- Submerged orifice flow

$$Q = c_w \bullet W_s \bullet \mu \bullet d_g \bullet \sqrt{2 \bullet g \bullet (h_1 - h_2)} \qquad 5.15$$

With the flow conditions:

$$h_1 - z_s \geq \frac{3}{2} \bullet d_g \quad \text{and} \quad h_2 > z_s + d_g$$

- Free weir flow

$$Q = \frac{2}{3} \bullet c_w \bullet W_s \bullet \sqrt{\frac{2}{3} \bullet g} \bullet (h_1 - z_s)^{\frac{3}{2}} \qquad 5.16$$

The flow conditions are:

$$h_1 - z_s < \frac{3}{2} \bullet d_g \quad \text{and} \quad h_1 - z_s > \frac{3}{2} \bullet (h_2 - z_s)$$

- Submerged weir flow

$$Q = c_w \bullet W_s \bullet (h_1 - z_s - \frac{u_s^2}{2 \bullet g}) \bullet \sqrt{2 \bullet g \bullet (h_1 - h_2)} \qquad 5.17$$

The flow conditions are:

$$h_1 - z_s < \frac{3}{2} \bullet d_g \quad \text{and} \quad h_1 - z_s \leq \frac{3}{2} \bullet (h_2 - z_s)$$

5.3.4 Filter

In reality, there are many input signals coming with the noises, which can influence the system. Getting rid of these noises will be one of the key factors to achieve a successful control. Therefore, filter is an important device in control systems. The commonly used filter is called the low pass filter that only the signals with low frequency can pass, and the high frequency signals will be filtered out. The filter equation is presented in formula 5.18.

$$X(k) = X(k-1) + (1 - T_f) X(k)_{measure} \qquad 5.18$$

T_f is calculated with the equation: $T_f = \frac{T_s}{T_s + T_c}$ 5.19

Where: $X(k-1)$ is the previous value, $X(k)$ is the present value, $X(k)_{measure}$ is the measurement at present time step and T_f is the filter factor, T_s is the sampling time, T_c is the control time.

The low pass filter is also applied in this modeling due to the occurrence of resonance wave that travel in the canal up and down. Because the frequency of resonance wave is higher than the normal flow, it needs to be filtered in order to avoid its influences. The sampling time can be acquired from the period of oscillation by performing the simulation without any filters.

5.4 Results of MPC based on the Integrator Delay model

The objectives are to set water level errors and the flow changes. Different penalties are imposed to them depending on the importance of these factors. The constraints are using time-variant values. The model calculates the maximum and minimum flows in each time step based on the maximum and minimum gate position, the water levels upstream and downstream of the gate. When water levels change, the flow constraints also change. The model runs in different schedules coming from the previous water order by farmers. One of the scenarios is listed in table 5.4 for the date of 07 August, 2006, which was one of the most severe days having small initial flow and big flow change at the head gate.

Table 5.4, Scheduled water order for the date of 07 August, 2006

	Initial time	0:00-10:00	10:00-14:00	14:00-18:00	18:00-24:00
Offtake	Flow (m3/s)	Flow (m3/s)	Flow (m3/s)	Flow (m3/s)	Flow (m3/s)
C-A	0.3962	0.3962	0.3962	0.3962	0.3962
C-B	0	0	0	0	0
C-C	0	0	0	0	0
C-D	1.4999	2.3489	2.264	2.2923	2.2923
C-E	0	0	0	0	0
C-32	0	0	0	0	0
C-F	0.8207	2.0093	1.5565	1.5565	1.5565
C-56	0	0	0	0	0
C-57	0	0	0	0	0
C-58	0	0.4245	0.4245	0.4245	0.4245
C-G	1.63291	2.08571	2.11401	2.11401	2.11401
C-H	0.6226	0.6262	0.6262	0.6262	0.6262
C-101	0	0.1981	0.1981	0.1981	0.1981
C-102	0.283	0.283	0.283	0.283	0.283
C-102B	0.4245	0.4245	0	0	0
C-J	0	0.1132	0.1132	0.1132	0.1132
C105	0.2547	0.2547	0.2547	0.2547	0.2547
C-K	1.96968	1.77158	1.77158	1.77158	1.77158
C-114	0	0	0	0	0
C-115	0	0	0	0	0
Unit 4	1.1886	2.1791	2.1791	2.1791	2.1791
Sum	9.09	13.11	12.18	12.21	12.21

The inflow from the head gate can only be changed twice a day. Here the changing time is set up to 4:30 in the morning and 12:00 in the afternoon. Before 4:30, the inflow is equal to the head gate flow of the end of previous day (06 August), because there is no change in the midnight. The head gate flow is listed in table 5.5.

Table 5.5, Head gate flows on 07 August, 2006

Time period	0:00-4:30	4:30-12:00	12:00-24:00
Parameter	Flow (m3/s)	Flow (m3/s)	Flow (m3/s)

Head gate	9.26	13.71	12.74

Comparing table 5.4 and 5.5, it is obvious to see the flow mismatches between head gate and offtakes. The mismatches in each time period of a day are presented in table 5.6. The difference at the beginning of the day is quite big. That might because the previous day has large water level deviation. Then the operator has to order extra water to bring them up, which causes the big flow change of the head gate flow.

Table 5.6, Flow mismatches (07 August, 2006)

Flow(m3/s)	0:00-4:30	4:30-10:00	10:00-11:00	11:00-12:00	12:00-14:00	14:00-24:00
Mismatch	-3.23	0.60	1.11	1.53	0.56	0.53

(Here negative value means that the head gate flow is smaller than the sum of offtake flows)

The modeled results are showing how the canal responds to the water order. Below, the control flows through check gates, check gate openings, water levels in all the canal pools and the offtake flows are demonstrated in figures.

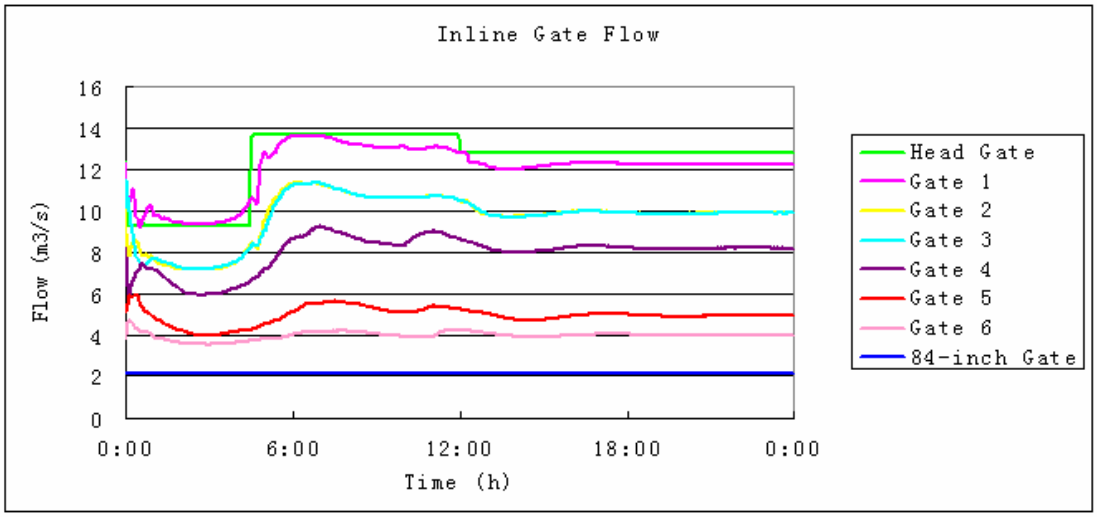

Figure 5.11, Control flows through check gates

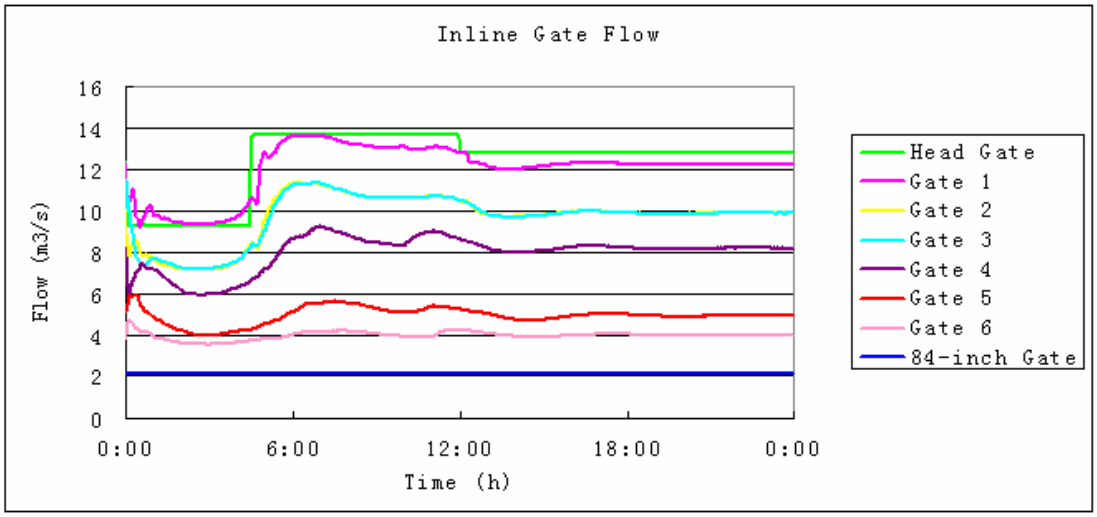

Figure 5.12, Check gate openings

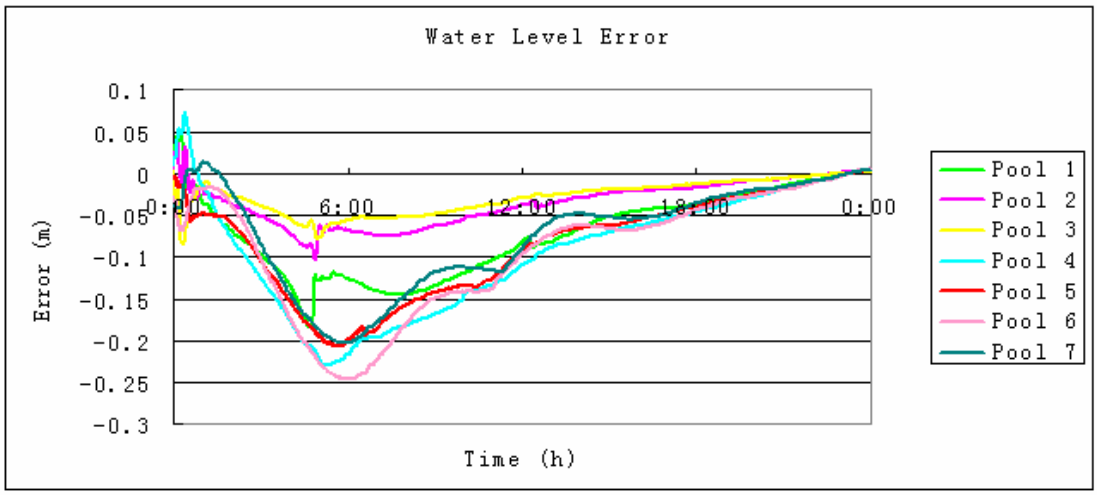

Figure 5.13, Water level errors from the setpoints

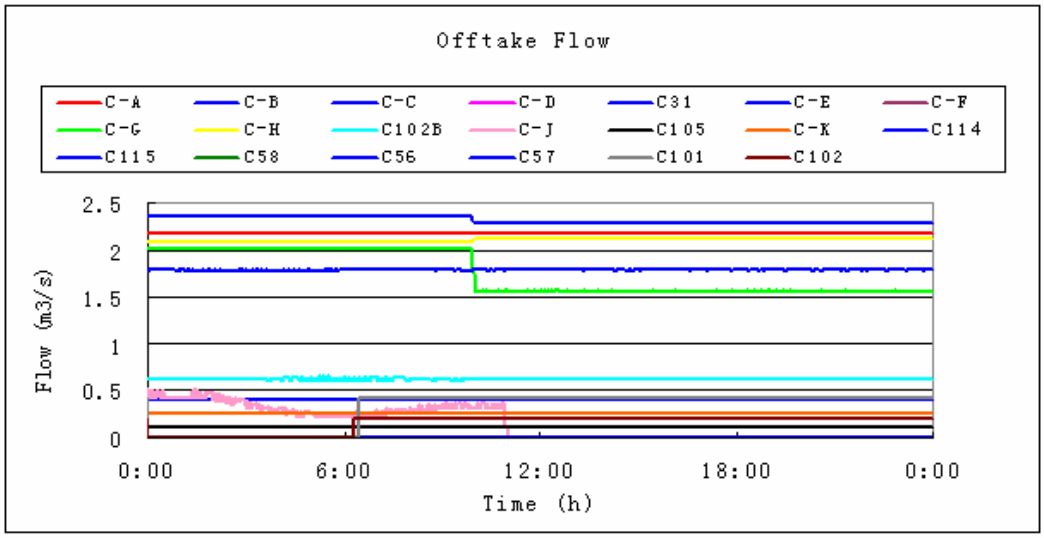

Figure 5.14, Offtake flows

Another scenario needs to be mentioned as well, which is 08th August, 2006. The district ordered 31284 m3 less than the sum of offtakes. This can be calculated from the flow mismatch table 5.7. In addition to the big flow mismatch at the beginning, some of the water levels drop below the minimum limitations. But from the figure of offtake flows, all the farmer demands can be fulfilled.

Table 5.7, Flow mismatches (08 August, 2006)

Flow(m3/s)	0:00-5:00	5:00-10:00	10:00-12:00	12:00-14:00	14:00-18:00	18:00-24:00
Mismatch	-2.95	0.48	0.74	0.17	-0.25	0.17

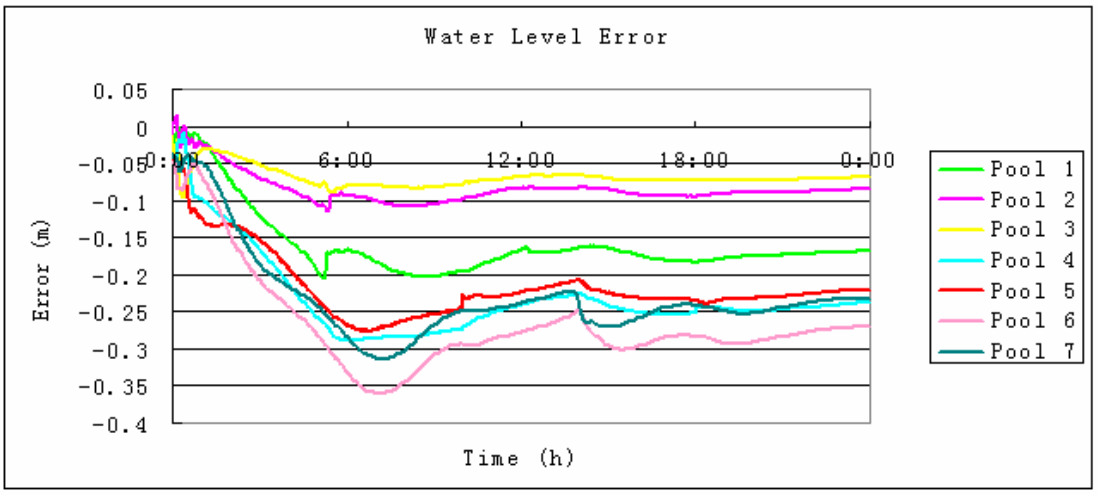

Figure 5.15, Water level deviations

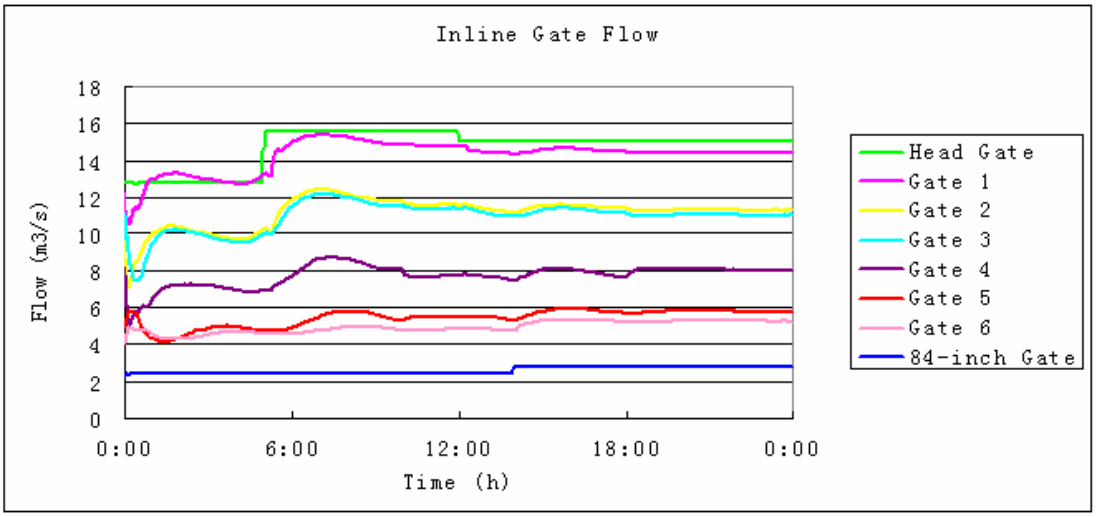

Figure 5.16, Control flows through inline gates

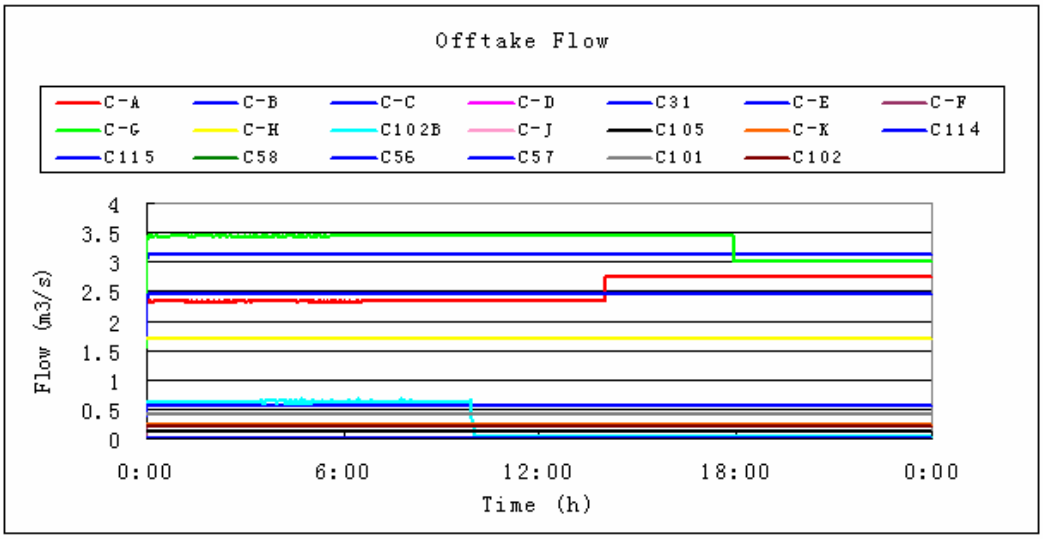

Figure 5.17, Offtake flows

5.5 Discussion on results of Integrator Delay model

From the figure of water level error, it is obvious that the simulation starts a bit below setpoints. There are two flow changes for the head gate. The first change makes an extremely large step, 4.45m3/s in the first day, which is 48.1% of the flow. This step change creates significant problems. The selected internal model at the beginning can not represent the model after the step change. When considering how the controller can deal with the flow mismatch, the water level errors in each pool should compare with their physical limits. Table 5.8 listed the water level limitations for each pool.

Table 5.8, Water level limitations (unit: m)

Pool No.	1	2	3	4	5	6	7
Below setpoints	0.152	0.152	0.305	0.366	0.122	0.213	0.305
Above setpoints	0.213	0.213	0.152	0.244	0.152	0.213	0.305

Based on the comparison between figure 5.13 and table 5.7, the controller can not deal with this mismatch, and pools 1, 5 and 6 violate the minimum limitations. The reason causing this violation might be the extremely big flow mismatch at the beginning of the day. Although the large flow after the step change tries to bring the water levels up, the big mismatch has already triggered the water level violation in some pools. The same situation happened on the 08th August, 2006 as well.

When analyzing each pool in detail, it comes that pools 2 and 3 can always be well controlled, because they are quite short and water flows relatively fast to compensate the deviation at the end. By contrast, pools 5 and 6 are long and low flow. They have more delay time; in addition, the limitations are small there, which make them easy to be violated when big flow mismatches happen, like in these examples, the minimum limitations are violated. Pool 4 also has long delay time, but the minimum limitation is big enough to keep the water level within the range, same as pool 7. As to the first pool, it's a long reach with high flow, but the minimum limitation

is small. The situation is in between. It's also sensitive to big flow mismatches. The district is now considering building a reservoir along the canal in order to balance the mismatch and easily operate the canal. These results and analysis provide the suggestion of the reservoir location. The best place may be beside pool 5. It can directly affect on the most sensitive pools.

It is obvious to see that water levels vary in accordance with the flow mismatch. When the mismatch gets larger, water levels drift away their setpoints more and faster. But the controllers can optimize the water usage and take actions in advance of the actual disturbance changes as long as the prediction horizon is longer than the delay time. It shows the feedforward control part of MPC.

Although there are some violations in certain pools, most of the offtakes are controlled very well by using flow controllers and their on-demand water deliveries are guaranteed, see offtake flow figure 5.14 and 5.17. Only the turnout C102B has some problems. The reason causing this may be because of the physical offtake condition. See offtake profile figure 5.18. The downstream is using pipe flow, and the most downstream is set to 609.1m constant elevation boundary. The upstream water level of the gate (in Central Main Canal) is not high enough (setpoint in this reach is 497.507), and then the pipe is not submerged. This can not guarantee the required flow downstream, but no relation to the controller. This does not influence the main goal of controlling the Central Main Canal.

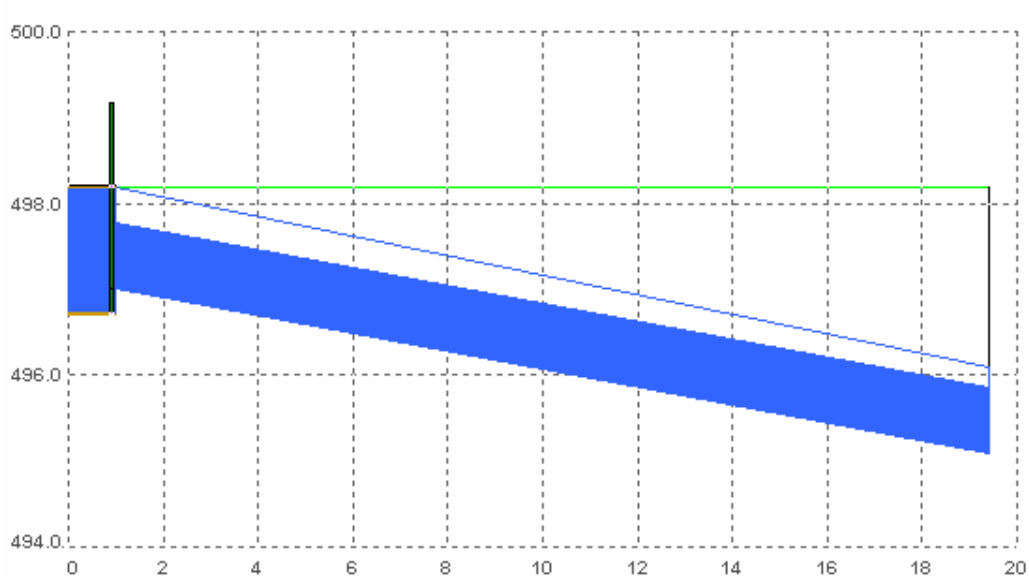

Figure 5.18, Profile of offtake C102B

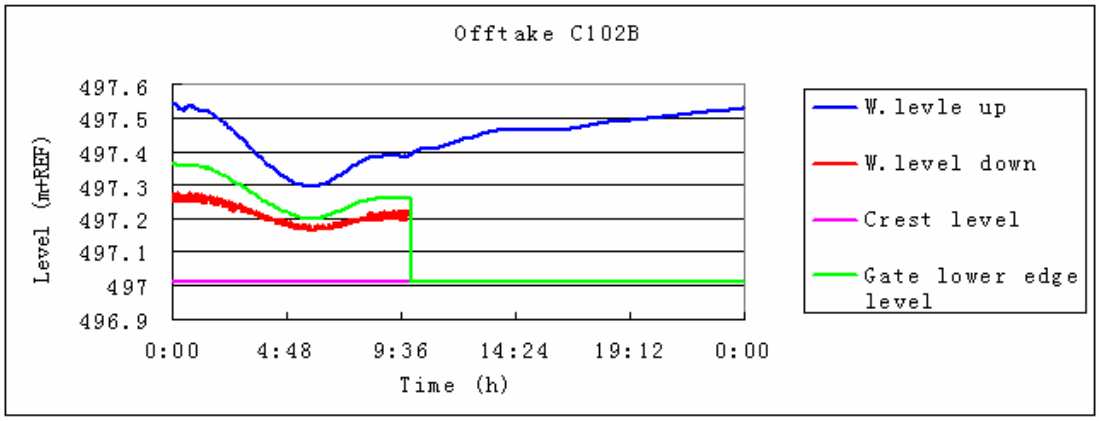

Figure 5.19, Offtake C102B

5.6 Tuning

Model tuning is extremely important to acquire proper parameters, and it is better to have automatic tuning methods or rules which easily identify these parameters. Many different tuning rules, like Ziegler-Nichols rule, Astrom-Hagglung rule, etc, are proposed for classic PI or PID controllers (X. Litrico, et, al. 2007). Unfortunately, there is no specific rule of tuning MPC now, and most of them are performed by the trial-and-error procedure, which is time consuming. Another difficult is that tuning the controller for one flow condition does not guarantee the satisfactory control in other flow conditions (P.J. van Overloop, et al. 2005). This research is trying to provide some experience and suggestions to the MPC tuning, which might be helpful to its formulization in the future.

There are several tuning parameter in MPC: First, prediction horizon, which should be long enough to cover the whole dynamics; second, control time step, which should be shorter than the prediction horizon (Wahlin, B.T. 2006). The choice of control time step also depends on the scale of the system. Large reservoir system with slow responses can select long control time step, while for small irrigation canal system, it should be relatively short; third, weight factors on water level errors and control flows. Tuning of these weight factors normally uses the trial-and-error procedure, and their values provide a trade-off between minimizing water level errors and minimizing flow changes. The following will focus on how to choose them.

From section 3.6, those MAVE (Maximum Allowed Value Estimate) factors are used to give penalties on water level errors and control actions. The big the MAVE factor, the small the penalty is, which means small restriction on that parameter. In this research, the MAVE factor on water level error (MAVEe) is selected by using the minimum limit above or below setpoint, which represents the maximum allowed water level deviation. Then by tuning the factor on control actions (MAVEdQ), chosen as a certain percentage of the flow through each controlled check gate in maximum inflow (Qmax) conditions, the model will have different performances and finally it will becomes unstable with extremely tight restrictions. The critical value of 0.03Qmax for MAVEdQ is then found (here ‘critical means that the controller gets unstable with

this value).

Table 5.7, Flows through each controlled check gate in maximum inflow conditions

Gate No.	1	2	3	4	5	6
Maximum flow	23.55	19.81	19.13	13.70	7.36	5.55

The same procedure can be applied to find the critical value of MAVEe by assuming proper MAVEdQ within its limitation. It is recommended to select the values close to the limitation due to the need for high performance. The critical value of MAVEe is detected to be 0.1. From the above description, it is obvious to see that high penalty on water level errors and low penalty on control actions will lead a tight control, thus, there is high risk to create an unstable control system.

The specific relation of these MAVE factors is difficult to formulate. But with this method, the proper MAVE values providing high performance are finally decided.

Table 5.8, Final MAVE factors in ID model

Factor	MAVEe(1,2,3,4,6,7)	MAVEe(5)	MAVEdQ
Values	0.152	0.122	0.02*Qmax

6 Model Predictive Control on Central Main Canal based on the Saint Venant model

6.1 Introduction to the Saint Venant model

The aforementioned Integrator Delay model is a lumped-parameter linear transfer function model of the Saint Venant equations. It only captures the main hydrodynamic characteristics, and the controller based on the ID model only allows small flow changes in the canal. Otherwise, the pool properties determined at previous flow conditions can not be correct in the present situations. These two drawbacks limit the accuracy of the model. In order to achieve more accurate results, more complicated internal model should be applied. Therefore, the full Saint Venant equations are considered, which describes the whole dynamics of an open channel. It contains two equations: continuity equation (mass balance) and momentum (balance) equation.

$$\frac{\partial Q}{\partial x}+\frac{\partial A_f}{\partial t}=q_{lat} \qquad 6.1$$

$$\frac{\partial Q}{\partial t}+\frac{\partial}{\partial x}\left(\frac{Q^2}{A_f}\right)+g\bullet A_f\bullet\frac{\partial h}{\partial x}+\frac{g\bullet Q\bullet|Q|}{C^2\bullet R_f\bullet A_f}=0 \qquad 6.2$$

Where:

Q – Flow in the canal [m^3/s]

x – Distance [m]

A_f – Wetted area of the flow [m^2]

q_{lat} – Lateral inflow per unit length [m^3/s/m]

t – Time [s]
g – Gravity acceleration [m/s^2] 9.81
h – Water level above the reference [m]
C – Chezy coefficient [m$^{1/2}$/s]

R_f – Hydraulic radius [m].

R_f is calculated from wetted area A_f divided by wetted perimeter P_f

Formula 6.2 has four terms on the left hand side, which are the inertia, advection, gravity force and friction force, separately from left to right. The inertia represents the slope of the energy grade due to the variations of flow in time; advection is the slope corresponding to the variations of velocity head in space; the third term, gravity force, is the slope of water surface itself; while the friction force represents the slope due to the resistance opposing to the flow (J.A. Cunge et al. 1980). Based on the different flow conditions and the canal itself, these terms have relatively different importance and can be simplified by ignoring one ore more terms in the complete equations for some numerical models. Failure to solve the complete Saint Venant equations can produce inaccurate results to some unsteady flow problems (The ASCE Task Committee on Irrigation Canal System Hydraulic Modeling, 1994).

6.2 Discretization

The Saint Venant equations are nonlinear, partial differential equations. This makes the direct application extremely difficult in the model. Thus linearized version of the Saint Venant equations is required. Formula 6.2 can be rewritten:

$$\frac{\partial Q}{\partial t} + u \bullet \frac{\partial Q}{\partial x} + Q \bullet \frac{\partial u}{\partial x} + g \bullet A_f \bullet \frac{\partial h}{\partial x} + \frac{g \bullet Q \bullet |Q|}{C^2 \bullet R_f \bullet A_f} = 0 \qquad 6.3$$

With the continuity equation 6.1, lateral flows are assumed to be zero, because they are already assigned as disturbances in MATLAB code. These turnouts are distributed throughout the length of the pool, thus, they are fitted with the discharge-rate regulators to provide a constant flow rate under variable depth in the supply canal (J. Mohan Reddy, et al. 1991). There is:

$$\frac{\partial Q}{\partial t} = A_f \bullet \frac{\partial u}{\partial t} + u \bullet \frac{\partial A_f}{\partial t} = A_f \bullet \frac{\partial u}{\partial t} - u \bullet \frac{\partial Q}{\partial x} \qquad 6.4$$

Substituting equation 6.4 into 6.3 and divided by A_f gets:

$$\frac{\partial u}{\partial t} + u \bullet \frac{\partial u}{\partial x} + g \bullet \frac{\partial h}{\partial x} + \frac{g \bullet u \bullet |u|}{C^2 \bullet R_f} = 0 \qquad 6.5$$

Where: u represents the flow velocity.

The Saint Venant equations are simplified to equation 6.5. In order to solve this partial differential equation, a proper discretization in time and space is needed. The spatial derivatives are discretized by finite-difference approximations by dividing each canal pool into several segments based on its length. Each segment has a representative water level and inflow and outflow. For convenience the segment lengths in one pool are made equal, although it is not a compulsory requirement. The number of segments required in a pool is determined by the trade off between the desired accuracy of linearized system equations and the nodes and states variables used in the model, namely, the computational time (O.S. Balogun, et al. 1988). Stelling, G.S. and Duinmeyer, S.P.A. (2003) presented the detailed spatial discretizations for the momentum equation:

$$\frac{du_{l+1/2}}{dt} + u_{l+1/2} \bullet \frac{u_{l+1} - u_l}{\Delta x} + g \bullet \frac{h_{l+1} - h_l}{\Delta x} + \frac{g \bullet u_{l+1/2} \bullet |u_{l+1/2}|}{C^2 \bullet R_f} = 0 \qquad 6.6$$

Where: l represent the space index.

The flow or velocity between two water level locations l and $l+1$ is then formulated:

$$Q_l = A_f \bullet [f_u \bullet (h_l - h_{l+1}) + r_u] \qquad 6.7$$

Or $$u_l = f_u \bullet (h_l - h_{l+1}) + r_u \qquad 6.8$$

For convenience, taking the following equations:

$$f_u = \frac{c_u}{b_u}$$
$$r_u = \frac{d_u}{b_u} - advec \qquad 6.9$$

In which:

$$b_u = \frac{1}{\Delta t} + \frac{g \bullet |u_l|}{C^2 \bullet R_f}$$
$$c_u = \frac{g}{\Delta x} \qquad 6.10$$
$$d_u = \frac{u_l}{\Delta t}$$

$$advec = u_l \bullet (u_{l+1} - u_l) \bullet \frac{\Delta t}{\Delta x}$$

6.3 Internal model

When applying the formula 6.7 to the mass balance $\frac{dh}{dt} = \frac{1}{A_s} \bullet (Q_{in} - Q_{out} - Q_{lat})$ on the first segment of the first pool with the equivalent discrete-time, there is:

$$h_1(k+1) = h_1(k) - \frac{T_c \bullet A_{f1} \bullet f_{u1}}{A_{s1}}(h_1(k) - h_2(k)) - \frac{T_c \bullet A_{f1} \bullet r_{u1}}{A_{s1}} + \frac{T_c \bullet (Q_{in} - Q_{lat1})}{A_{s1}} \qquad 6.11$$

Here Q_{in} is the head gate flow which is treated as a disturbance; Q_{lat1} represents the total offtakes in the first segment.

The same procedure can be applied to the other segments. The only difference is that the outflow of the previous segment becomes the inflow to the next one instead of disturbance, and this should be embodied in the system matrix as well. Attentions should also be paid to the last segment of each pool, where control flows of the gates are used. The internal model for the first pool is derived (it is divided into five segments and has 4 disturbances including the head gate), and the number of segments in each pool is listed in table 6.1:

$$\begin{pmatrix} h_1(k+1) \\ h_2(k+1) \\ h_3(k+1) \\ h_4(k+1) \\ h_5(k+1) \\ Q_{c1}(k) \end{pmatrix} =$$

$$\begin{pmatrix} 1-\frac{T_c \bullet A_{f1} \bullet f_{u1}}{A_{s1}} & \frac{T_c \bullet A_{f1} \bullet f_{u1}}{A_{s1}} & 0 & 0 & 0 & 0 \\ \frac{T_c \bullet A_{f1} \bullet f_{u1}}{A_{s2}} & 1-\frac{T_c \bullet A_{f1} \bullet f_{u1}}{A_{s2}} - \frac{T_c \bullet A_{f2} \bullet f_{u2}}{A_{s2}} & \frac{T_c \bullet A_{f2} \bullet f_{u2}}{A_{s2}} & 0 & 0 & 0 \\ 0 & \frac{T_c \bullet A_{f2} \bullet f_{u2}}{A_{s3}} & 1-\frac{T_c \bullet A_{f2} \bullet f_{u2}}{A_{s3}} - \frac{T_c \bullet A_{f3} \bullet f_{u3}}{A_{s3}} & \frac{T_c \bullet A_{f3} \bullet f_{u3}}{A_{s3}} & 0 & 0 \\ 0 & 0 & \frac{T_c \bullet A_{f3} \bullet f_{u3}}{A_{s4}} & 1-\frac{T_c \bullet A_{f3} \bullet f_{u3}}{A_{s4}} - \frac{T_c \bullet A_{f4} \bullet f_{u4}}{A_{s4}} & \frac{T_c \bullet A_{f4} \bullet f_{u4}}{A_{s4}} & 0 \\ 0 & 0 & 0 & \frac{T_c \bullet A_{f4} \bullet f_{u4}}{A_{s5}} & 1-\frac{T_c \bullet A_{f4} \bullet f_{u4}}{A_{s5}} & -\frac{T_c}{A_{s5}} \\ 0 & 0 & 0 & 0 & 0 & 1 \end{pmatrix} \bullet$$

$$\begin{pmatrix} h_1(k) \\ h_2(k) \\ h_3(k) \\ h_4(k) \\ h_5(k) \\ Q_{c1}(k-1) \end{pmatrix} + \begin{pmatrix} 0 \\ 0 \\ 0 \\ 0 \\ -\frac{T_c}{A_{s5}} \\ 1 \end{pmatrix} [\Delta Q_{c1}(k)] + \begin{pmatrix} \frac{T_c}{A_{s1}} & 0 & 0 & 0 & 0 \\ 0 & \frac{T_c}{A_{s2}} & 0 & 0 & 0 \\ 1 & 0 & \frac{T_c}{A_{s1}} & 0 & 0 \\ 0 & 0 & 0 & \frac{T_c}{A_{s1}} & 0 \\ 0 & 0 & 0 & 0 & \frac{T_c}{A_{s1}} \\ 0 & 0 & 0 & 0 & 0 \end{pmatrix} \begin{pmatrix} -A_{f1} \bullet r_{u1} + Q_H(k) \\ A_{f1} \bullet r_{u1} - A_{f2} \bullet r_{u2} - Q_1(k) \\ A_{f2} \bullet r_{u2} - A_{f3} \bullet r_{u3} \\ A_{f3} \bullet r_{u3} - A_{f4} \bullet r_{u4} - Q_2(k) \\ A_{f4} \bullet r_{u4} - Q_3(k) \end{pmatrix}$$

6.12

Table 6.1, Number of segments in each pool

Pool NO.	1	2	3	4	5	6	7
Seg. NO.	5	2	2	5	5	5	3

6.4 Results of MPC based on the Saint Venant model

Taking the same case of 07th of August, 2006, as used in the Integrator Delay model, the results of water levels and check gate flows are demonstrated in the figures below, with 1 hour and 2 hours prediction horizon, separately. The corresponding weight factors of Q and R used for tuning are presented in table 6.2. Within the Q matrix, only the first and the last segments of each pool are weighted. The factors of MAVEe and MAVEdQ are considered.

- One hour prediction horizon:

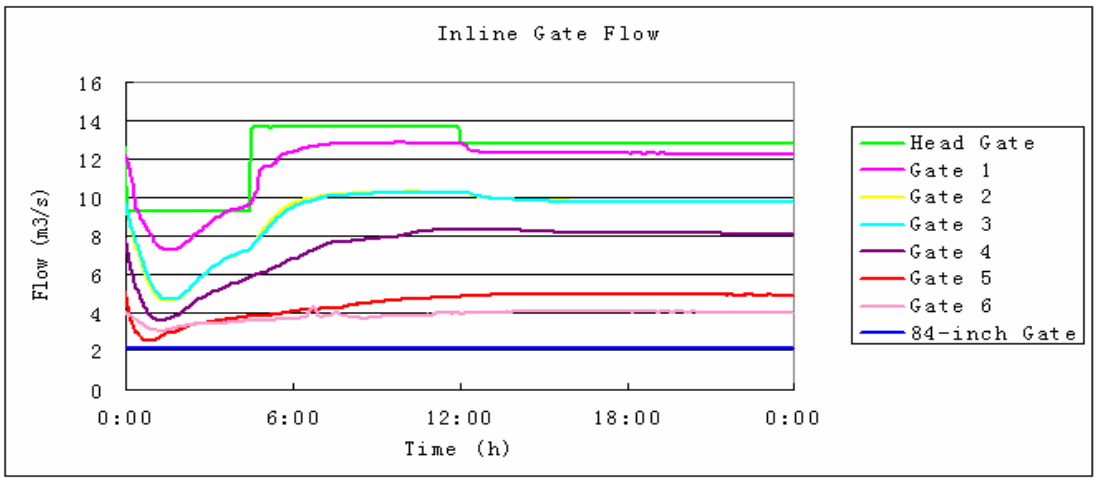

Figure 6.1, Control flows from the check gates

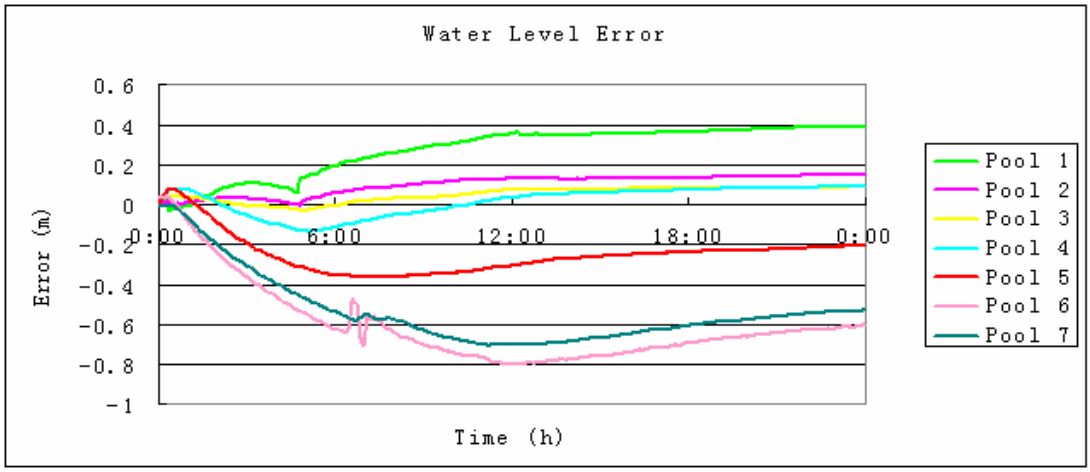

Figure 6.2, Water levels from the canal pools

- Two-hour prediction horizon:

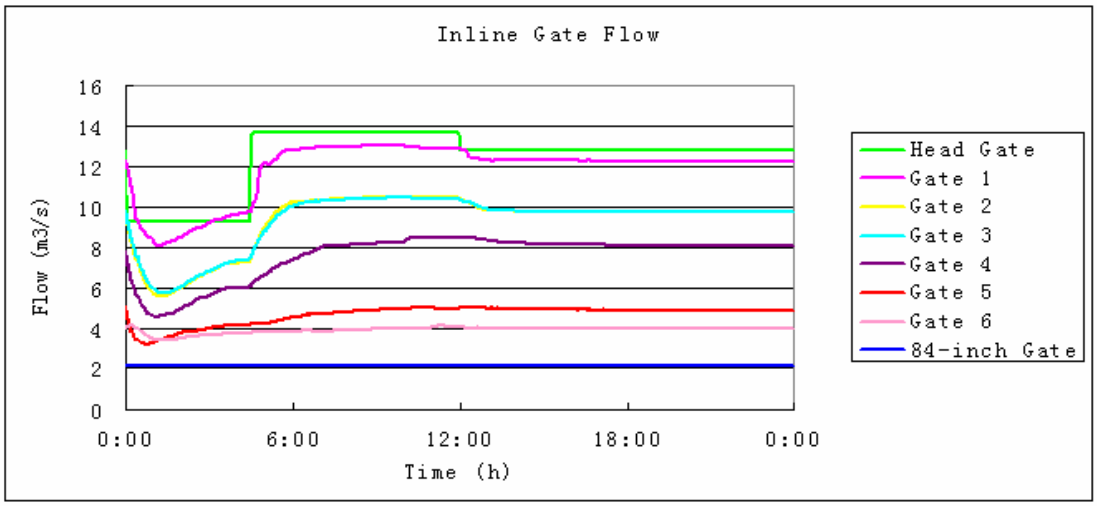

Figure 6.3, Control flows from the check gates

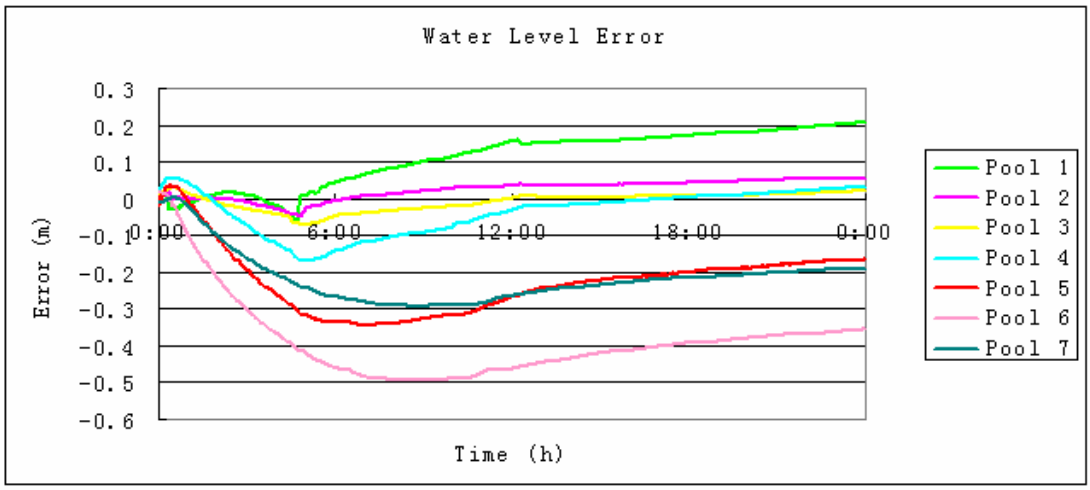

Figure 6.4, Water levels from the canal pools

Table 6.2, Weight factor in Saint Venant model

Factor	MAVEe	MAVEdQ
Value	0.02	0.01Qmax

6.5 Discussion on MPC results based on the Saint Venant model

From the results generated from the Saint Venant model simulation, they do not meet the needs of expectation, which requires the water distribution along the canal to be optimized. What we see in the results above is that more water is retained in the upstream pools and water levels are even higher than their setpoints in the end, while water levels in the downstream pools largely drift away from the their equilibriums. Comparing with results of the Integrator Delay model (figure 5.11), check gate flows are much smaller in the Saint Venant model. The reason causing these problems may come to the canal characteristics, flow conditions and the internal model. The Central Main Canal is a relatively flat and deep canal, which has a large capacity compared to the normal operational flow. This will make the water level profile considerably flat. See figure 6.5. When we hold the internal model back again, it is obvious to see that this situation will weaken the connections between the adjacent segments, and the prediction to the future outputs is considered less accurate. For convenience, equation 6.11 is presented here again:

$$h_1(k+1) = h_1(k) - \frac{T_c \bullet A_{f1} \bullet f_{u1}}{A_{s1}}(h_1(k) - h_2(k)) - \frac{T_c \bullet A_{f1} \bullet r_{u1}}{A_{s1}} + \frac{T_c \bullet (Q_{in} - Q_{lat1})}{A_{s1}}$$

When the two adjacent segments have the same water level, the connection even comes to zero. Because of this weak relationship, the optimization does not have enough relevant information to correct the water level deviations downstream. If the problem is extended to a pool or even the whole canal, the upstream structure can have less connection to the downstream water level at the moment of flat water level profile. This means when the deviation happens at the downstream, upstream structure can not efficiently deal with the situation, and it just meets the needs of upstream segments. This explains why check gate flows are much smaller than these in the ID model and more water is retained in the upstream pools.

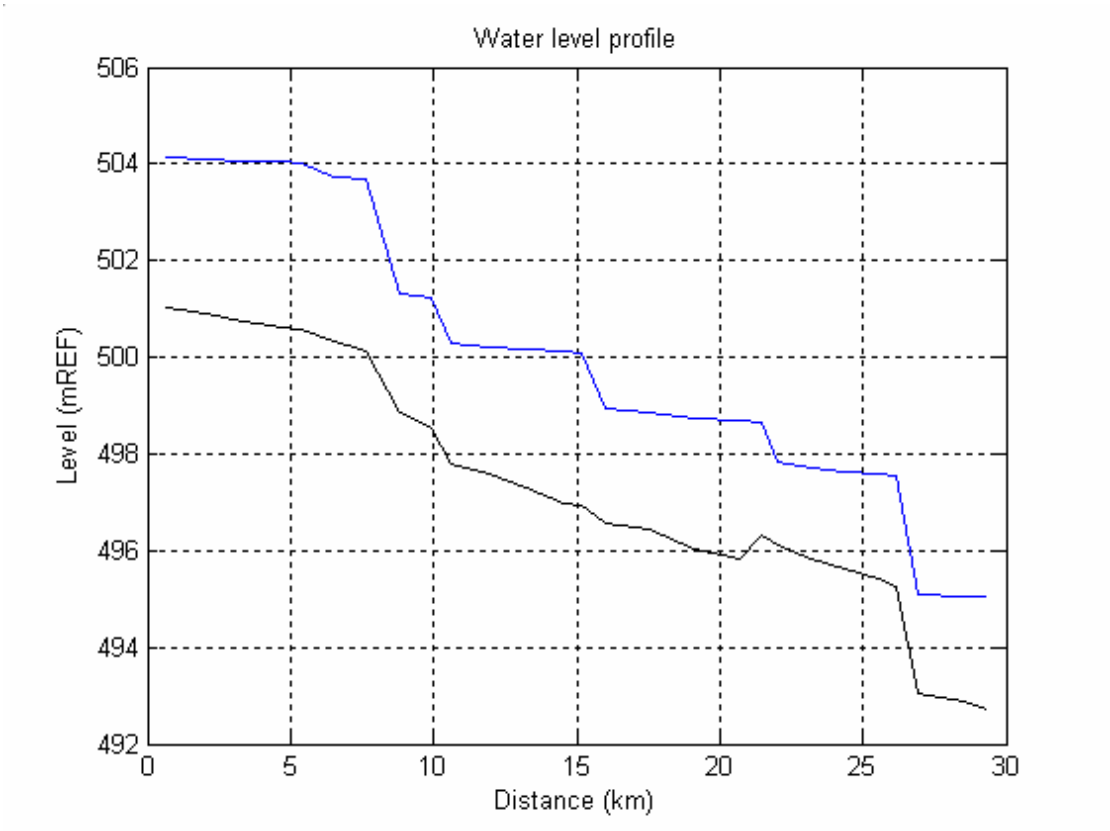

Figure 6.5, Water level profile

The two-hour prediction horizon makes the results better than those of one-hour prediction. The reason is apparent, that longer prediction provides more accurate information. But due to the weak connection between upstream structure and downstream water level, although the disturbance term becomes relatively important in the above equation, longer prediction horizon still can not compensate for this influence.

7 Comparison between two models

Every coin has its two sides. The two models have their own advantages and disadvantages, embodied on the simplicity and accuracy, in addition to the simulation time. First, the Integrator Delay model uses lumped parameters to get a linear response model, which makes the process model mathematically easier to handle but only captures two characteristics: delay

time and surface area. In order to simplify the model, some assumptions are needed and provide restrictions to the model use. For example, MPC based on the ID model does not allow big flow change in order to avoid switching between two internal models. Due to the simplicity, in theory, the model is less accurate compared with a fully linearized version of the Saint Venant equations which includes the whole dynamics and are more complex. The Saint Venant model can also model the long waves. These resonance waves will cause unforeseen water level deviations in the canal and will be dealt with in the Saint Venant model. Second, the Integrator Delay model is fixed once the internal model is generated, called time-invariant. The flow change at the upstream structure can always reach to downstream and correct the error there. But the Saint Venant model is time-variant; its elements of f_u in system matrix and r_u in disturbance variables change over the prediction horizon every time step. The relationship between segments can be influenced due to the flow and canal situation. In this example, it generates bad results. Another factor needs to be considered for the implementation is the computational time. There is a big difference between two models. The simulation with two-hour prediction horizon of the Saint Venant model takes almost 20 hours to run the one day schedule, which makes it less applicable. Therefore, comparing all these aspects, the Integrator Delay model is suitable for the Central Main Canal project, and its accuracy can meet the requirement within a certain range. The comparisons are listed in the table 7.1.

Table 7.1, Comparisons between two models

	Advantage	Disadvantage
Integrator Delay Model (Time-invariant)	1. Simple to handle 2. Short computational time 3. It functions in these pools	1. No big flow change during simulation 2. Only capture the main properties (delay time and surface area) 3. No wave modeling (filter needed) 4. Less accurate
Saint Venant model (Time-variant)	1. Simulate the whole dynamics, including the resonance waves 2. Accurate (in theory) 3. Any flow condition change is possible (in theory)	1. Complex 2. Can be influenced by the water profile situation (may be suitable for steep canal) 3. Extremely long computational time

8 Conclusions and Recommendations

From the whole description above, some conclusions and recommendations are useful to generalize the points, and help for the further study.

8.1 Conclusions

- Model Predictive Control is proved to be a good control technique to apply on the Central Main Canal compared to the classic control methods, and the requirements of efficiently distributing water and maintaining water levels can be successfully met.
- Different methods within MPC are mostly based on their internal models. Here the Integrator Delay model and the Saint Venant model capture the canal properties differently, which makes them have different performances.
- Two models have their own benefits and drawbacks. Although the Saint Venant model is more accurate in theory and can simulate the flow characteristics better but more complex. Integrator Delay model is more suitable for the application to the Central Main Canal due to the short computational time, and its accuracy can also meet the requirement.
- The biggest risk of running Integrator Delay model lies in the flow change. It is not allowed to make large flow jumps during the simulation, in order to avoid wrong representation of the internal model.
- Good initial conditions can help the simulation a lot, especially to the Saint Venant model. It reduces the number of iterations to reach stabilized states.
- The Saint Venant model is a time-variant model, and changes every time step. From this above case, it shows that the results are worse than the ID model, and the model is not applicable to the canal with flat water level profile. But more researches are needed to make further improvement.

8.2 Recommendations

- It is recommended to find a proper filter first to get rid of the resonance wave, then to identify the canal properties, due to the extra delay time caused by the filter.
- Further researches are needed for the application and implementation of the Saint Venant model, and then the internal model are no longer relevant to the flow conditions.
- A better optimization may help to reduce the computational time and make the Saint Venant model applicable
- There might be a necessity for the study of non-linear model due to the non-linearity of the channel flow.

References

A.J. Clemmens and J. Shuurmans, (2004), "Simple Optimal Downstream Feedback Canal Controllers: Theory", Journal of Irrigation and Drainage Engineering, 130(1), 26-34.

A.J. Clemmens and J. Shuurmans, (2004), "Simple Optimal Downstream Feedback Canal Controllers: ASCE Test Case Results", Journal of Irrigation and Drainage Engineering, 130(1),

35-46.

Brouwer R. (2005), "Operational Water Management", Lecture Notes, Delft University of Technology.

David C. Rogers and Jean Goussard, (1998), "Canal Control Algorithms Currently in Use", Journal of Irrigation and Drainage Engineering, ASCE. 124(1), 11-15.

Huanwen Tang and Xuezhi Qin, (2005), "Practical Methods of Optimization", the Third Edition, in Chinese, Dalian University of Technology Press.

J. Mohan Reddy, Amadou Dia and Ahmed Oussou, (1991), "Design of Control Algorithm for Operation of Irrigation Canals", Journal of Irrigation and Drainage Engineering, 118(6), 852-867.

J.A. Cunge, F.M. Holly and A. Verwey, (1980), "Practical Aspects of Computational River Hydraulics", Pitman Advanced Publishing Program.

J. Schuurmans, A.J. Clemmens, S. Dijkstra, A. Hof and R. Brouwer, (1999), "Modeling of Irrigation and Drainage Canals for Controller Design", Journal of Irrigation and Drainage Engineering, ASCE. 125(6), 338-344.

J. Schuurmans, O.H. Bosgra and R. Brouwer, (1995), "Open-Channel Flow Model Approximation for Controller Design", Applied Mathematical Modeling. 19, 525-530.

J. Schuurmans, A. Hof, S. Dijkstra, O.H. Bosgra and R. Brouwer, (1999), "Simple Water Level Controller for Irrigation and Drainage Canals", Journal of Irrigation and Drainage Engineering, 125(4), 189-195.

Jan Schuurmans, (1997), "Control of Water Levels in Open Channels", PhD dissertation, Delft University of Technology, the Netherlands.

Jay, H. Lee, Manfred Morari and Carlos E. Garcia, (1990), "State-Space Interpretation of Model Predictive Control", Automatica, 30(4), 707-717.

MathWorks (1992), “Matlab User Guider”, The MathWorks, Inc. Natick, Massachusetts.

O.S. Balogun, M. Hubbard and J.J. DeVries, (1988) "Automatic Control of Canal Flow Using Linear Quadratic Regulator Theory", Journal of Irrigation and Drainage Engineering, 114(1), 75-101.

O.S. Balogun, (1985), "Design of Real-time Feedback Control for Canal Systems Using Linear Quadratic Regulator Theory", PhD dissertation, University of California, at Davis, Calif.

P.J. van Overloop, (2006), “Model Predictive Control on Open Water Systems”, PhD dissertation, Delft University of Technology, the Netherlands.

P.J. van Overloop, J. Schuurmans, R. Brouwer and C.M. Burt, (2005), "Multiple-Model Optimization of Proportional Integral Controllers on Canals", Journal of Irrigation and Drainage Engineering, ASCE. 131(2), 190-196.

Pierre-Olivier Malaterre, David C. Rogers and Jan Schuurmans, (1998), "Classification of Canal Control Algorithms", Journal of Irrigation and Drainage Engineering, ASCE. 124(1). 3-10.

SOBEK (2000), “Manual and Technical Reference”, WL|Delft Hydraulics, Delft, the Netherlands.

Stelling, G.S. and Duinmeyer, S.P.A. (2003), "A Staggered Conservative Scheme for Every Froude Number in Rapidly Varied Shallow Water Flows", International Journal for Numerical Methods in Fluids, 43, 1329-1354.

The ASCE Task Committee on Irrigation Canal System Hydraulic Modeling, (1994), "Unsteady-Flow Modeling of Irrigation Canals", Journal of Irrigation and Drainage Engineering, 119(4), 615-630.

T.S.Strelkoff, J.L. Deltour, C.M. Burt, A.J. Clemmens and J.P. Baume, (1998), "Influence of Canal Geometry and Dynamics on Controllability", Journal of Irrigation and Drainage Engineering, ASCE. 124(1), 16-22.

V.M. Ruiz-Carmona, A.J. Clemmens and J. Schuurmans, (1998), "Canal Control Algorithm Formulations", Journal of Irrigation and Drainage Engineering, ASCE. 124(1), 31-39.

Wahlin, B.T. (2006), "Remote downstream feedback control of branching-canal networks", PhD dissertation, Arizona State University, USA.

Wahlin, B.T. and A.J. Clemmens, (2006), "Automatic Downstream Water-Level Feedback Control of Branching Canal Networks: Theory", Journal of Irrigation and Drainage Engineering, ASCE. 132(3), 198-207.

Wahlin, B.T. and A.J. Clemmens, (2006), "Automatic Downstream Water-Level Feedback Control of Branching Canal Networks: Results", Journal of Irrigation and Drainage Engineering, ASCE. 132(3), 208-219.

X. Litrico; P.O. Malaterre; J.P. Baume and J.Ribot-Bruno, (2007), "Automatic Tuning of PI Controllers for an Irrigation Canal Pool", Journal of Irrigation and Drainage Engineering, ASCE. 133(1), 27-37.

Appendices

Appendix I SOBEK introduction

SOBEK (version 2.10) is an integrated software package for river, canal and sewer systems modeling in rural and urban water management (SOBEK 2000). It contains a variety of different modules that can be used for both water quantity and water quality simulation. The

Channel Flow (CF) module and the Real-Time Control (RTC) module are used to perform the whole simulation in this project. SOBEK-CF does unsteady flow simulation and SOBEK-RTC allows the inline structures (e.g. gates and pumps) from SOBEK-CF to be controlled by MATLAB. The working processes are like this: All the canal properties are set up in the SOBEK-CF module, and the MPC is written in the MATLAB m-files which are connected to the SOBEK-CF through the SOBEK-RTC. SOBEK-RTC passes the canal properties from SOBEK-CF to the MATLAB code. MATLAB does all the calculations with the input information, and the calculated results or adjustments to these inline structures are read back to the SOBEK-CF by SOBEK-RTC and the control actions are implemented.

SOBEK uses the Delft Hydraulics Library scheme to solve the Saint Venant equations. It is an implicit, staggered scheme based on the concept of nodes where the water stages are computed. These nodes are connected to the left and right adjacent nodes through discharge equations. Thus, the computational grids include both h-point (water level) and Q-point (discharge), which are arranged as computational nodes and links between them separately in SOBEK schematization. The staggered grids are shown in the Figure I.1.

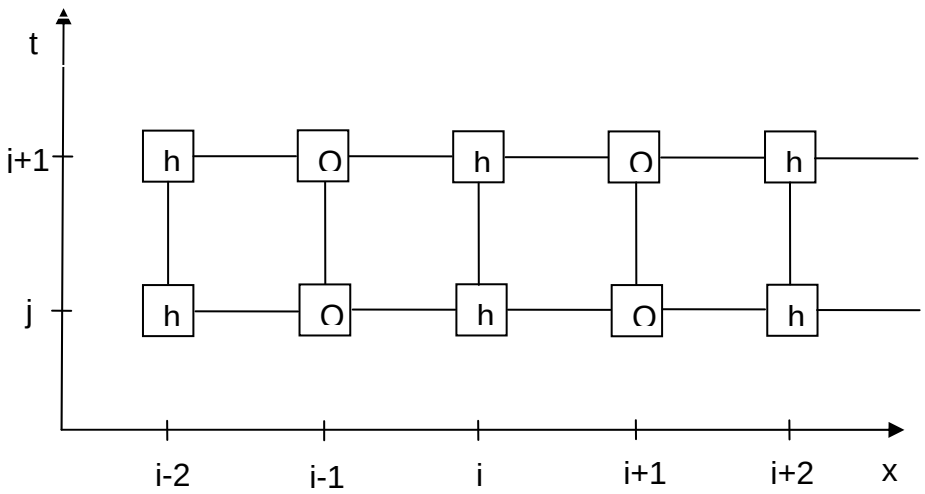

Figure I.1, the staggered grids in time and space

The space derivatives are weighted between two time lines by using a weighting coefficient θ (J.A. Cunge et al. 1980):

$$\frac{\partial f}{\partial x} = \theta \bullet \frac{f_{i+1}^{j+1} - f_{i-1}^{j+1}}{2\Delta x} + (1-\theta) \bullet \frac{f_{i+1}^{j} - f_{i-1}^{j}}{2\Delta x} \qquad 10.1$$

Here f is a continuous function.

Appendix II Deduction of Hessian matrix H and Lagrangian f

The objective function of the controlled system is:

$$\min_{U} J = X' \bullet Q \bullet X + U' \bullet R \bullet U \qquad 10.2$$

The state variables and the control action are:

$$X = A_c \bullet x(k) + B_u \bullet Z + B_d \bullet D$$
$$U = -K \bullet X + Z = -K \bullet [A_c \bullet x(k) + B_u \bullet Z + B_d \bullet D] + Z \qquad 10.3$$

Substituting 10.3 into formula 10.2 gets the equation:

$$\min_U J = [A_c \bullet x(k) + B_u \bullet Z + B_d \bullet D]' \bullet Q \bullet [A_c \bullet x(k) + B_u \bullet Z + B_d \bullet D]$$
$$+\{-K \bullet [A_c \bullet x(k) + B_u \bullet Z + B_d \bullet D] + Z\}' \bullet R \bullet \{-K \bullet [A_c \bullet x(k) + B_u \bullet Z + B_d \bullet D] + Z\} \qquad 10.4$$

Based on the formation of $J(Z) = \frac{1}{2} \bullet Z' \bullet H \bullet Z + f \bullet Z + g$, only the terms consisting of Z or Z' should be considered from the formula 10.4. Therefore, rewriting 10.4 by neglecting the constant matrix g , for convenience, get the function of $J'(Z)$:

$$J'(Z) = x(k)' A_c' Q B_u Z + Z' B_u' Q [A_c x(k) + B_d D] + Z' B_u' Q B_u Z + D' B_d' Q B_u Z + x(k)' A_c' K' R K B_u Z$$
$$-x(k)' A_c' K' R Z + Z' B_u' K' R K [A_c x(k) + B_d D] + Z' B_u' K' R K B_u Z - Z' B_u' K' R Z$$
$$+D' B_d' K' R K B_u Z - D' B_d' K' R Z + Z' R [-K A_c x(k) + B_d D] - Z' R K B_u Z + Z' R Z \qquad 10.5$$

Putting the terms containing Z and Z' together will create the Hessian matrix, while extracting the terms only comprising Z or Z' will generate the Lagrangian. There is another rule needs to be mentioned here is that the penalties of Q and R are diagonal matrices, which means that: $\begin{array}{l} Q = Q' \rightarrow M \bullet Q \bullet N = N' \bullet Q' \bullet M' = N' \bullet Q \bullet M' \\ R = R' \rightarrow M \bullet Q \bullet N = N' \bullet R' \bullet M' = N' \bullet R \bullet M' \end{array}$ when M and N' have the same dimension. This gives many combinations of the above terms. For example the second term: $Z' B_u' Q A_c x(k) = [A_c x(k)]' Q' [Z' B_u']' = x(k)' A_c' Q B_u Z$, which is the same as the first term. By using this method, $J'(Z)$ can be written as $\frac{1}{2} \bullet Z' \bullet H \bullet Z + f \bullet Z$, and the Hessian matrix

$$H = 2 \bullet (B_u' \bullet Q \bullet B_u - R \bullet K \bullet B_u + R + B_u' \bullet K' \bullet R \bullet K \bullet B_u - B_u' \bullet K' \bullet R)$$

The Lagrangian $\begin{array}{l} f = 2 \bullet x(k) \bullet (A_c' \bullet Q \bullet B_u + A_c' \bullet K' \bullet R \bullet K \bullet B_u - A_c' \bullet K' \bullet R) \\ \quad +2 \bullet D' \bullet (B_d' \bullet Q \bullet B_u + B_d' \bullet K' \bullet R \bullet K \bullet B_u - B_d' \bullet K' \bullet R) \end{array}$

Appendix III State space Integrator Delay model on Central Main Canal

The state-space internal model of MPC is described as:

$$x(k+1) = A(k) \bullet x(k) + B_u(k) \bullet u(k) + B_d(k) \bullet d(k)$$
$$y(k) = C \bullet x(k)$$

where:
x – the states of the water system
A – the system matrix
B_u – the control input matrix
B_d – the disturbance matrix
u – the control actions calculated by the controller
d – the disturbances
C – the output matrix
y – the outputs of the water system
k – the discrete time step index

Here only the model with 60 % of the design capacity is presented. The last inline gate called 84-inch gate is considered as an additional offtake (disturbance) through which the flow called “Unit 4” passes and continues downstream.

$$x(k)=\begin{pmatrix} e_1(k) \\ \Delta e_1(k) \\ \Delta Q_H(k-1) \\ \Delta Q_H(k-2) \\ e_2(k) \\ \Delta e_2(k) \\ \Delta Q_{c1}(k-1) \\ e_3(k) \\ \Delta e_3(k) \\ \Delta Q_{c2}(k-1) \\ \Delta Q_{c2}(k-2) \\ e_4(k) \\ \Delta e_4(k) \\ \Delta Q_{c3}(k-1) \\ \vdots \\ \Delta Q_{c3}(k-4) \\ e_5(k) \\ \Delta e_5(k) \\ \Delta Q_{c4}(k-1) \\ \vdots \\ \Delta Q_{c4}(k-6) \\ e_6(k) \\ \Delta e_6(k) \\ \Delta Q_{c5}(k-1) \\ \vdots \\ \Delta Q_{c5}(k-5) \\ e_7(k) \\ \Delta e_7(k) \\ \Delta Q_{c6}(k-1) \\ \Delta Q_{c6}(k-2) \\ \Delta Q_{c6}(k-3) \end{pmatrix} \qquad u(k)=\begin{pmatrix} \Delta Q_{c1}(k) \\ \Delta Q_{c2}(k) \\ \Delta Q_{c3}(k) \\ \Delta Q_{c4}(k) \\ \Delta Q_{c5}(k) \\ \Delta Q_{c6}(k) \end{pmatrix} \qquad d(k)=\begin{pmatrix} \Delta Q_H(k) \\ \Delta Q_{d1}(k) \\ \Delta Q_{d2}(k) \\ \Delta Q_{d3}(k) \\ \Delta Q_{d4}(k) \\ \Delta Q_{d5}(k) \\ \Delta Q_{d6}(k) \\ \Delta Q_{d7}(k) \\ \Delta Q_{d8}(k) \\ \Delta Q_{d9}(k) \\ \Delta Q_{d10}(k) \\ \Delta Q_{d11}(k) \\ \Delta Q_{d12}(k) \\ \Delta Q_{d13}(k) \\ \Delta Q_{d14}(k) \\ \Delta Q_{d15}(k) \\ \Delta Q_{d16}(k) \\ \Delta Q_{d17}(k) \\ \Delta Q_{d18}(k) \\ \Delta Q_{d19}(k) \\ \Delta Q_{d20}(k) \\ \Delta Q_{84-inch}(k) \end{pmatrix}$$

For convenience, the system matrix, the control input matrix and the disturbance matrix are presented in a concise way that all the locations of those non-zero values are marked in their own figures, but their values are given separately. The first number represents the row, while the second number is the column.

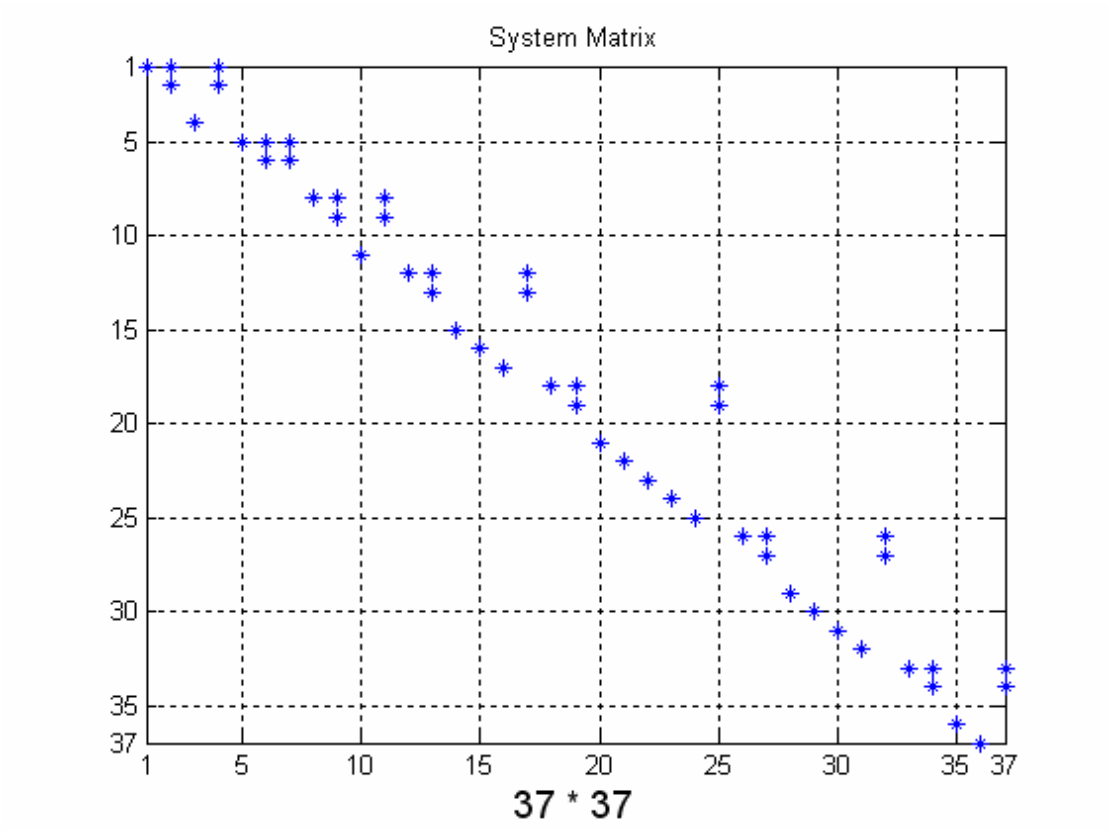

Figure III.1, System Matrix

$$A[1,1]=1,\ A[1,2]=1,\ A[1,4]=\frac{T_c}{A_{s1}},\ A[2,2]=1,\ A[2,4]=\frac{T_c}{A_{s1}},\ A[4,3]=1,$$

$$A[5,5]=1,\ A[5,6]=1,\ A[5,7]=\frac{T_c}{A_{s2}},\ A[6,6]=1,\ A[6,7]=\frac{T_c}{A_{s2}},$$

$$A[8,8]=1,\ A[8,9]=1,\ A[8,11]=\frac{T_c}{A_{s3}},\ A[9,9]=1,\ A[9,11]=\frac{T_c}{A_{s3}},\ A[11,10]=1,$$

$$A[12,12]=1,\ A[12,13]=1,\ A[12,17]=\frac{T_c}{A_{s4}},\ A[13,13]=1,\ A[13,17]=\frac{T_c}{A_{s4}},$$

$$A[15,14]=1,\ A[16,15]=1,\ A[17,16]=1,\ A[18,18]=1,\ A[18,19]=1,\ A[18,25]=\frac{T_c}{A_{s5}},$$

$$A[19,19]=1,\ A[19,25]=\frac{T_c}{A_{s5}},\ A[21,20]=1,\ A[22,21]=1,\ A[23,22]=1,\ A[24,23]=1,$$

$$A[25,24]=1,\ A[26,26]=1,\ A[26,27]=1,\ A[26,32]=\frac{T_c}{A_{s6}},\ A[27,27]=1,\ A[27,32]=\frac{T_c}{A_{s6}},$$

$$A[29,28]=1,\ A[30,29]=1,\ A[31,30]=1,\ A[32,31]=1,\ A[33,33]=1,\ A[33,34]=1,$$

$$A[33,37]=\frac{T_c}{A_{s7}},\ A[34,34]=1,\ A[34,37]=\frac{T_c}{A_{s7}},\ A[36,35]=1,\ A[37,36]=1$$

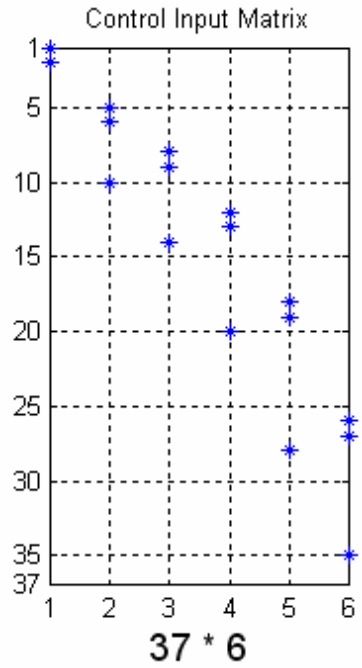

Figure III.2, Control Input Matrix

$$B_u[1,1] = -\frac{T_c}{A_{s1}},\ B_u[2,1] = -\frac{T_c}{A_{s1}},$$

$$B_u[5,2] = -\frac{T_c}{A_{s2}},\ B_u[6,2] = -\frac{T_c}{A_{s2}},\ B_u[7,1] = 1,$$

$$B_u[8,3] = -\frac{T_c}{A_{s3}},\ B_u[9,3] = -\frac{T_c}{A_{s3}},\ B_u[10,2] = 1,$$

$$B_u[12,4] = -\frac{T_c}{A_{s4}},\ B_u[13,4] = -\frac{T_c}{A_{s4}},\ B_u[14,3] = 1,$$

$$B_u[18,5] = -\frac{T_c}{A_{s5}},\ B_u[19,5] = -\frac{T_c}{A_{s5}},\ B_u[20,4] = 1,$$

$$B_u[26,6] = -\frac{T_c}{A_{s6}},\ B_u[27,6] = -\frac{T_c}{A_{s6}},\ B_u[28,5] = 1,$$

$$B_u[35,6] = 1$$

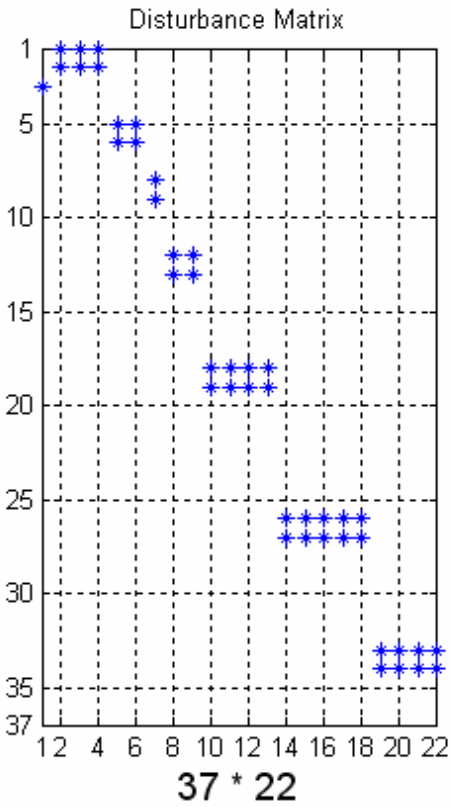

Figure III.3, Disturbance Matrix

$$B_d[3,1]=1,$$

$$B_d[1,2]=B_d[1,3]=B_d[1,4]=B_d[2,2]=B_d[2,3]=B_d[2,4]=-\frac{T_c}{A_{s1}},$$

$$B_d[5,5]=B_d[5,6]=B_d[6,5]=B_d[6,6]=-\frac{T_c}{A_{s2}},$$

$$B_d[8,7]=-\frac{T_c}{A_{s3}},$$

$$B_d[12,8]=B_d[12,9]=B_d[13,8]=B_d[13,9]=-\frac{T_c}{A_{s4}},$$

$$B_d[18,10]=B_d[18,11]=B_d[18,12]=B_d[18,13]$$

$$=B_d[19,10]=B_d[19,11]=B_d[19,12]=B_d[19,13]=-\frac{T_c}{A_{s5}},$$

$$B_d[26,14]=B_d[26,15]=B_d[26,16]=B_d[26,17]=B_d[26,18]$$

$$=B_d[27,14]=B_d[27,15]=B_d[27,16]=B_d[27,17]=B_d[27,18]=-\frac{T_c}{A_{s6}},$$

$$B_d[33,19]=B_d[33,20]=B_d[33,21]=B_d[33,22]$$

$$=B_d[34,19]=B_d[34,20]=B_d[34,21]=B_d[34,22]=-\frac{T_c}{A_{s7}},$$

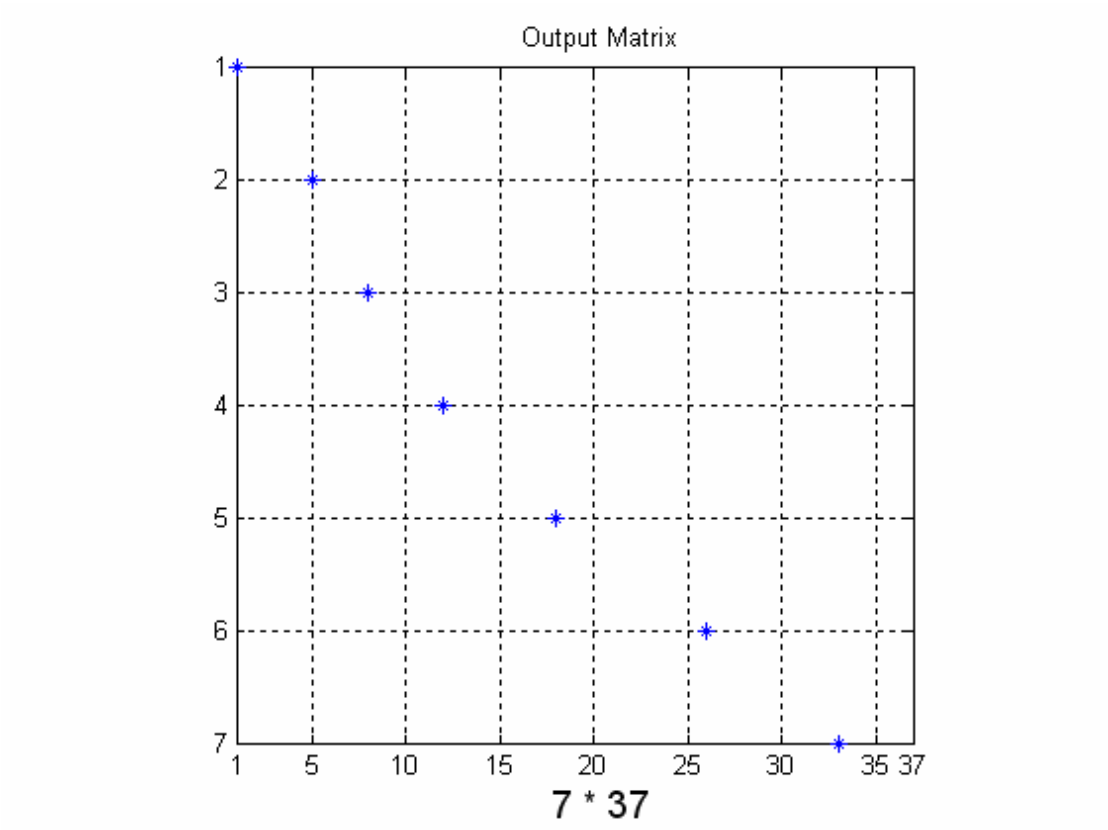

Figure III.4, Output Matrix

$$C[1,1]=1,\ C[2,5]=1,\ C[3,8]=1,\ C[4,12]=1,\ C[5,18]=1,\ C[6,26]=1,\ C[7,33]=1$$

Appendix IV State space Saint Venant model on Central Main Canal

The Saint Venant model has the same state-space internal model of MPC as the ID model, which is described as:

$$x(k+1) = A(k)\bullet x(k) + B_u(k)\bullet u(k) + B_d(k)\bullet d(k)$$
$$y(k) = C\bullet x(k)$$

$$x(k) = \begin{pmatrix} h_{1,1}(k) \\ \vdots \\ h_{1,5}(k) \\ Q_{c1}(k-1) \\ h_{2,1}(k) \\ h_{2,2}(k) \\ Q_{c2}(k-1) \\ h_{3,1}(k) \\ h_{3,2}(k) \\ Q_{c3}(k-1) \\ h_{4,1}(k) \\ \vdots \\ h_{4,5}(k) \\ Q_{c4}(k-1) \\ h_{5,1}(k) \\ \vdots \\ h_{5,5}(k) \\ Q_{c5}(k-1) \\ h_{6,1}(k) \\ \vdots \\ h_{6,5}(k) \\ Q_{c6}(k-1) \\ h_{7,1}(k) \\ \vdots \\ h_{7,5}(k) \end{pmatrix} \qquad u(k) = \begin{pmatrix} \Delta Q_{c1}(k) \\ \Delta Q_{c2}(k) \\ \Delta Q_{c3}(k) \\ \Delta Q_{c4}(k) \\ \Delta Q_{c5}(k) \\ \Delta Q_{c6}(k) \end{pmatrix} \qquad d(k) = \begin{pmatrix} -A_{f1,1}\bullet r_{u1,1} + Q_H(k) \\ A_{f1,1}\bullet r_{u1,1} - A_{f1,2}\bullet r_{u1,2} - Q_1(k) \\ A_{f1,2}\bullet r_{u1,2} - A_{f1,3}\bullet r_{u1,3} \\ A_{f1,3}\bullet r_{u1,3} - A_{f1,4}\bullet r_{u1,4} - Q_2(k) \\ A_{f1,4}\bullet r_{u1,4} - Q_3(k) \\ -A_{f2,1}\bullet r_{u2,1} \\ A_{f2,2}\bullet r_{u2,2} - Q_4(k) - Q_5(k) \\ -A_{f3,1}\bullet r_{u3,1} \\ A_{f3,2}\bullet r_{u3,2} - Q_6(k) \\ -A_{f4,1}\bullet r_{u4,1} \\ A_{f4,1}\bullet r_{u4,1} - A_{f4,2}\bullet r_{u4,2} \\ A_{f4,2}\bullet r_{u4,2} - A_{f4,3}\bullet r_{u4,3} \\ A_{f4,3}\bullet r_{u4,3} - A_{f4,4}\bullet r_{u4,4} \\ A_{f4,4}\bullet r_{u4,4} - Q_7(k) - Q_8(k) \\ -A_{f5,1}\bullet r_{u5,1} \\ A_{f5,1}\bullet r_{u5,1} - A_{f5,2}\bullet r_{u5,2} \\ A_{f5,2}\bullet r_{u5,2} - A_{f5,3}\bullet r_{u5,3} - Q_9(k) \\ A_{f5,3}\bullet r_{u5,3} - A_{f5,4}\bullet r_{u5,4} - Q_{10}(k) \\ A_{f5,4}\bullet r_{u5,4} - Q_{11}(k) - Q_{12}(k) \\ -A_{f6,1}\bullet r_{u6,1} \\ A_{f6,1}\bullet r_{u6,1} - A_{f6,2}\bullet r_{u6,2} - Q_{13}(k) \\ A_{f6,2}\bullet r_{u6,2} - A_{f6,3}\bullet r_{u6,3} - Q_{14}(k) - Q_{15}(k) \\ A_{f6,3}\bullet r_{u6,3} - A_{f6,4}\bullet r_{u6,4} - Q_{16}(k) \\ A_{f6,4}\bullet r_{u6,4} - Q_{17}(k) \\ -A_{f7,1}\bullet r_{u7,1} \\ A_{f7,1}\bullet r_{u7,1} - A_{f7,2}\bullet r_{u7,2} - Q_{18}(k) \\ A_{f7,4}\bullet r_{u7,4} - Q_{19}(k) - Q_{20}(k) - Q_{84-inch}(k) \end{pmatrix}$$

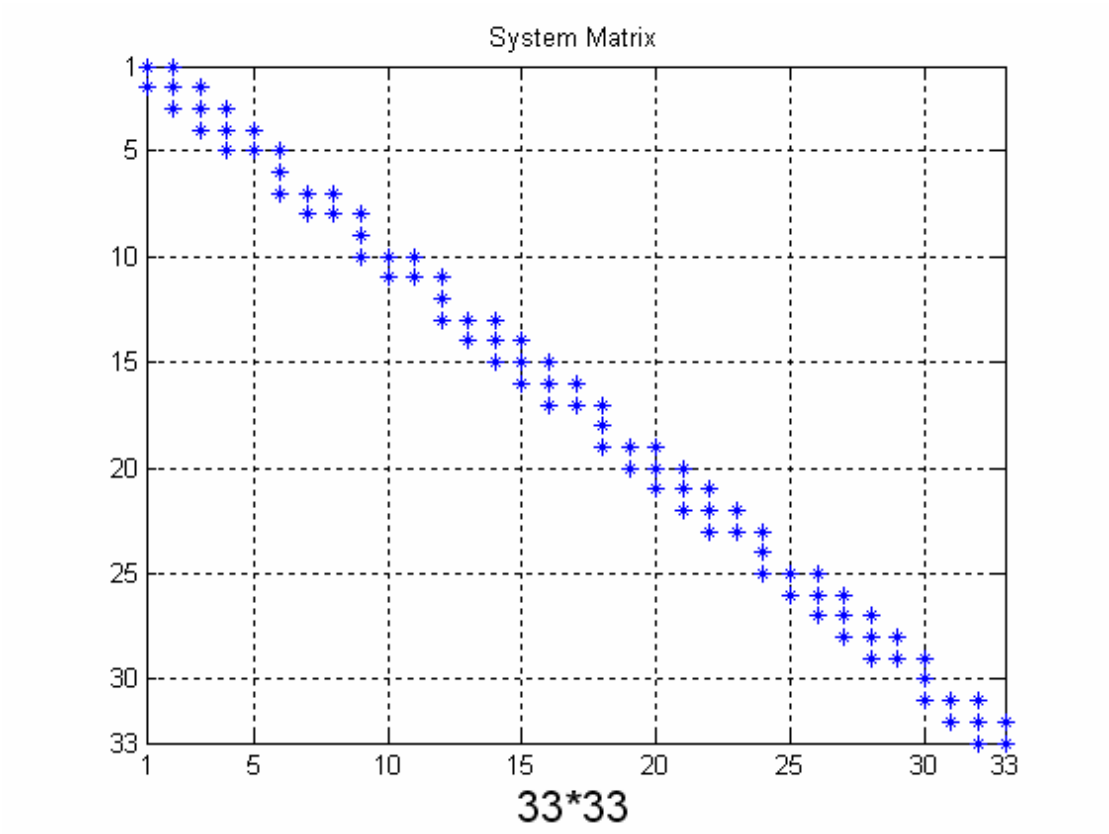

Figure IV.1, System matrix

$$A[1,1]=1-\frac{T_c\bullet A_{f1}\bullet f_{u1}}{A_{s1}},\ A[1,2]=\frac{T_c\bullet A_{f1}\bullet f_{u1}}{A_{s1}},$$

$$A[2,1]=\frac{T_c\bullet A_{f1}\bullet f_{u1}}{A_{s2}},\ A[2,2]=1-\frac{T_c\bullet A_{f1}\bullet f_{u1}}{A_{s2}}-\frac{T_c\bullet A_{f2}\bullet f_{u2}}{A_{s2}},\ A[2,3]=\frac{T_c\bullet A_{f2}\bullet f_{u2}}{A_{s2}},$$

$$A[3,2]=\frac{T_c\bullet A_{f2}\bullet f_{u2}}{A_{s3}},\ A[3,3]=1-\frac{T_c\bullet A_{f2}\bullet f_{u2}}{A_{s3}}-\frac{T_c\bullet A_{f3}\bullet f_{u3}}{A_{s3}},\ A[3,4]=\frac{T_c\bullet A_{f3}\bullet f_{u3}}{A_{s3}},$$

$$A[4,3]=\frac{T_c\bullet A_{f3}\bullet f_{u3}}{A_{s4}},\ A[4,4]=1-\frac{T_c\bullet A_{f3}\bullet f_{u3}}{A_{s4}}-\frac{T_c\bullet A_{f4}\bullet f_{u4}}{A_{s4}},\ A[4,5]=\frac{T_c\bullet A_{f4}\bullet f_{u4}}{A_{s4}},$$

$$A[5,4]=\frac{T_c\bullet A_{f4}\bullet f_{u4}}{A_{s5}},\ A[5,5]=1-\frac{T_c\bullet A_{f4}\bullet f_{u4}}{A_{s5}},\ A[5,6]=-\frac{T_c}{A_{s5}},$$

$$A[6,6]=1,$$

$$A[7,6]=\frac{T_c}{A_{s6}},\ A[7,7]=1-\frac{T_c\bullet A_{f6}\bullet f_{u6}}{A_{s6}},\ A[7,8]=\frac{T_c\bullet A_{f6}\bullet f_{u6}}{A_{s6}},$$

$$A[8,7]=\frac{T_c\bullet A_{f6}\bullet f_{u6}}{A_{s7}},\ A[8,8]=1-\frac{T_c\bullet A_{f6}\bullet f_{u6}}{A_{s7}},\ A[8,9]=-\frac{T_c}{A_{s7}},$$

$$A[9,9]=1,$$

$$A[10,9]=\frac{T_c}{A_{s8}},\ A[10,10]=1-\frac{T_c\bullet A_{f8}\bullet f_{u8}}{A_{s8}},\ A[10,11]=\frac{T_c\bullet A_{f8}\bullet f_{u8}}{A_{s8}},$$

$$A[11,10]=\frac{T_c\bullet A_{f8}\bullet f_{u8}}{A_{s9}},\ A[11,11]=1-\frac{T_c\bullet A_{f8}\bullet f_{u8}}{A_{s9}},\ A[11,12]=-\frac{T_c}{A_{s9}},$$

$$A[12,12]=1,$$

$$A[13,12]=\frac{T_c}{A_{s10}},\ A[13,13]=1-\frac{T_c\bullet A_{f10}\bullet f_{u10}}{A_{s10}},\ A[13,14]=\frac{T_c\bullet A_{f10}\bullet f_{u10}}{A_{s10}},$$

$$A[14,13]=\frac{T_c\bullet A_{f10}\bullet f_{u10}}{A_{s11}},\ A[14,14]=1-\frac{T_c\bullet A_{f10}\bullet f_{u10}}{A_{s11}}-\frac{T_c\bullet A_{f11}\bullet f_{u11}}{A_{s11}},\ A[14,15]=\frac{T_c\bullet A_{f11}\bullet f_{u11}}{A_{s11}},$$

$$A[15,14]=\frac{T_c\bullet A_{f11}\bullet f_{u11}}{A_{s12}},\ A[15,15]=1-\frac{T_c\bullet A_{f11}\bullet f_{u11}}{A_{s12}}-\frac{T_c\bullet A_{f12}\bullet f_{u12}}{A_{s12}},\ A[15,16]=\frac{T_c\bullet A_{f12}\bullet f_{u12}}{A_{s12}},$$

$$A[16,15]=\frac{T_c\bullet A_{f12}\bullet f_{u12}}{A_{s13}},\ A[16,16]=1-\frac{T_c\bullet A_{f12}\bullet f_{u12}}{A_{s13}}-\frac{T_c\bullet A_{f13}\bullet f_{u13}}{A_{s13}},\ A[16,17]=\frac{T_c\bullet A_{f13}\bullet f_{u13}}{A_{s13}},$$

$$A[17,16]=\frac{T_c\bullet A_{f13}\bullet f_{u13}}{A_{s14}},\ A[17,17]=1-\frac{T_c\bullet A_{f13}\bullet f_{u13}}{A_{s14}},\ A[17,18]=-\frac{T_c}{A_{s14}},$$

$$A[18,18]=1,$$

$$A[19,18]=\frac{T_c}{A_{s15}},\ A[19,19]=1-\frac{T_c\bullet A_{f15}\bullet f_{u15}}{A_{s15}},\ A[19,20]=\frac{T_c\bullet A_{f15}\bullet f_{u15}}{A_{s15}},$$

$$A[20,19]=\frac{T_c\bullet A_{f15}\bullet f_{u15}}{A_{s16}},\ A[20,20]=1-\frac{T_c\bullet A_{f15}\bullet f_{u15}}{A_{s16}}-\frac{T_c\bullet A_{f16}\bullet f_{u16}}{A_{s16}},\ A[20,21]=\frac{T_c\bullet A_{f16}\bullet f_{u16}}{A_{s16}},$$

$$A[21,20]=\frac{T_c\bullet A_{f16}\bullet f_{u16}}{A_{s17}},\ A[21,21]=1-\frac{T_c\bullet A_{f16}\bullet f_{u16}}{A_{s17}}-\frac{T_c\bullet A_{f17}\bullet f_{u17}}{A_{s17}},\ A[21,22]=\frac{T_c\bullet A_{f17}\bullet f_{u17}}{A_{s17}},$$

$$A[22,21]=\frac{T_c\bullet A_{f17}\bullet f_{u17}}{A_{s18}},\ A[22,22]=1-\frac{T_c\bullet A_{f17}\bullet f_{u17}}{A_{s18}}-\frac{T_c\bullet A_{f18}\bullet f_{u18}}{A_{s18}},\ A[22,23]=\frac{T_c\bullet A_{f18}\bullet f_{u18}}{A_{s18}},$$

$$A[23,22]=\frac{T_c\bullet A_{f18}\bullet f_{u18}}{A_{s19}},\ A[23,23]=1-\frac{T_c\bullet A_{f18}\bullet f_{u18}}{A_{s19}},\ A[23,24]=-\frac{T_c}{A_{s19}},$$

$$A[24,24]=1,$$

$$A[25,24]=\frac{T_c}{A_{s20}},\ A[25,25]=1-\frac{T_c\bullet A_{f20}\bullet f_{u20}}{A_{s20}},\ A[25,26]=\frac{T_c\bullet A_{f20}\bullet f_{u20}}{A_{s20}},$$

$$A[26,25]=\frac{T_c\bullet A_{f20}\bullet f_{u20}}{A_{s21}},\ A[26,26]=1-\frac{T_c\bullet A_{f20}\bullet f_{u20}}{A_{s21}}-\frac{T_c\bullet A_{f21}\bullet f_{u21}}{A_{s21}},\ A[26,27]=\frac{T_c\bullet A_{f21}\bullet f_{u21}}{A_{s21}},$$

$$A[27,26]=\frac{T_c\bullet A_{f21}\bullet f_{u21}}{A_{s22}},\ A[27,27]=1-\frac{T_c\bullet A_{f21}\bullet f_{u21}}{A_{s22}}-\frac{T_c\bullet A_{f22}\bullet f_{u22}}{A_{s22}},\ A[27,28]=\frac{T_c\bullet A_{f22}\bullet f_{u22}}{A_{s22}},$$

$$A[28,27]=\frac{T_c\bullet A_{f22}\bullet f_{u22}}{A_{s23}},\ A[28,28]=1-\frac{T_c\bullet A_{f22}\bullet f_{u22}}{A_{s23}}-\frac{T_c\bullet A_{f23}\bullet f_{u23}}{A_{s23}},\ A[28,29]=\frac{T_c\bullet A_{f23}\bullet f_{u23}}{A_{s23}},$$

$$A[29,28]=\frac{T_c\bullet A_{f23}\bullet f_{u23}}{A_{s24}},\ A[29,29]=1-\frac{T_c\bullet A_{f23}\bullet f_{u23}}{A_{s24}},\ A[29,30]=-\frac{T_c}{A_{s24}},$$

$$A[30,30]=1,$$

$$A[31,30]=\frac{T_c}{A_{s25}},\ A[31,31]=1-\frac{T_c\bullet A_{f25}\bullet f_{u25}}{A_{s25}},\ A[31,32]=\frac{T_c\bullet A_{f25}\bullet f_{u25}}{A_{s25}},$$

$$A[32,31]=\frac{T_c\bullet A_{f25}\bullet f_{u25}}{A_{s26}},\ A[32,32]=1-\frac{T_c\bullet A_{f25}\bullet f_{u25}}{A_{s26}}-\frac{T_c\bullet A_{f26}\bullet f_{u26}}{A_{s26}},\ A[32,33]=\frac{T_c\bullet A_{f26}\bullet f_{u26}}{A_{s26}},$$

$$A[33,32]=\frac{T_c\bullet A_{f26}\bullet f_{u26}}{A_{s27}},\ A[33,33]=1-\frac{T_c\bullet A_{f26}\bullet f_{u26}}{A_{s27}}$$

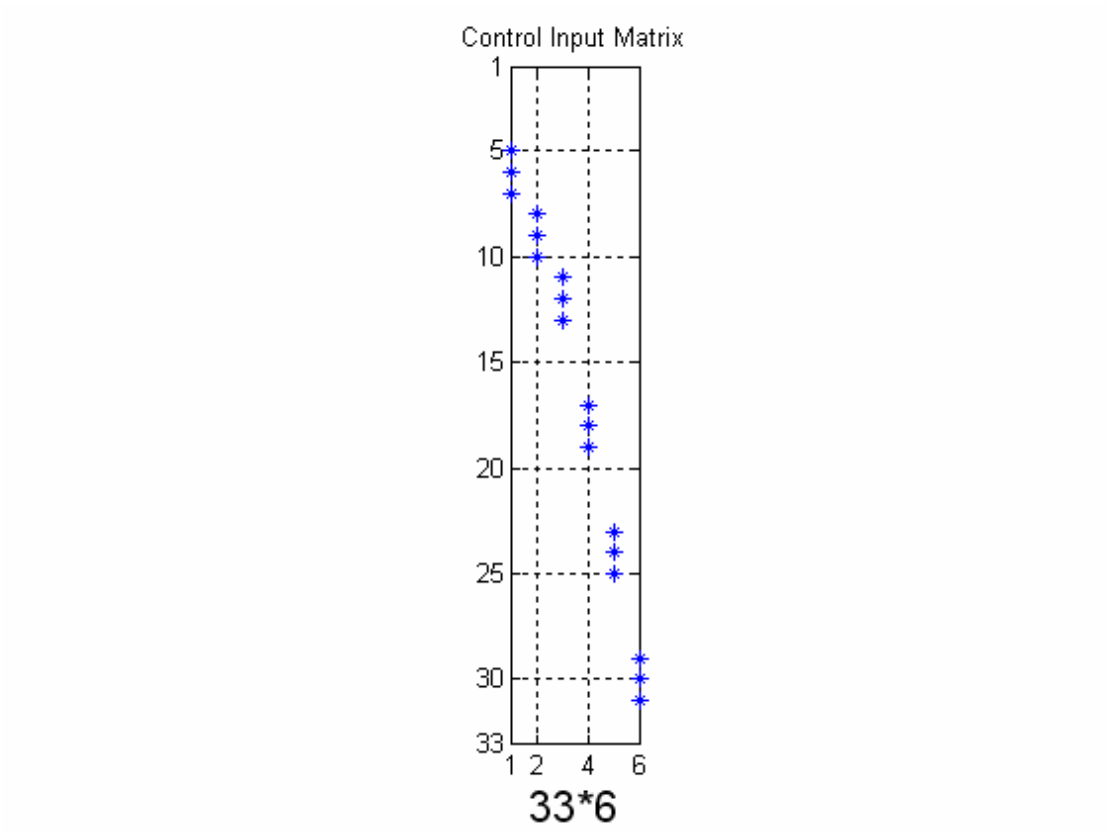

Figure IV.2, Control input matrix

$$B_u[5,1]=-\frac{T_c}{A_{s5}},\ B_u[6,1]=1,\ B_u[7,1]=-\frac{T_c}{A_{s6}},\ A[8,2]=-\frac{T_c}{A_{s7}}\ ,A[9,2]=1\ ,A[10,2]=\frac{T_c}{A_{s8}}\ ,$$

$$A[11,3]=-\frac{T_c}{A_{s9}},\ A[12,3]=1\ ,A[13,3]=\frac{T_c}{A_{s10}},\ A[17,4]=-\frac{T_c}{A_{s14}},\ A[18,4]=1\ ,A[19,4]=\frac{T_c}{A_{s15}},$$

$$A[23,5]=-\frac{T_c}{A_{s19}},\ A[24,5]=1,\ A[25,5]=\frac{T_c}{A_{s20}},\ A[29,6]=-\frac{T_c}{A_{s24}},\ A[30,6]=1,\ A[31,6]=\frac{T_c}{A_{s25}}$$

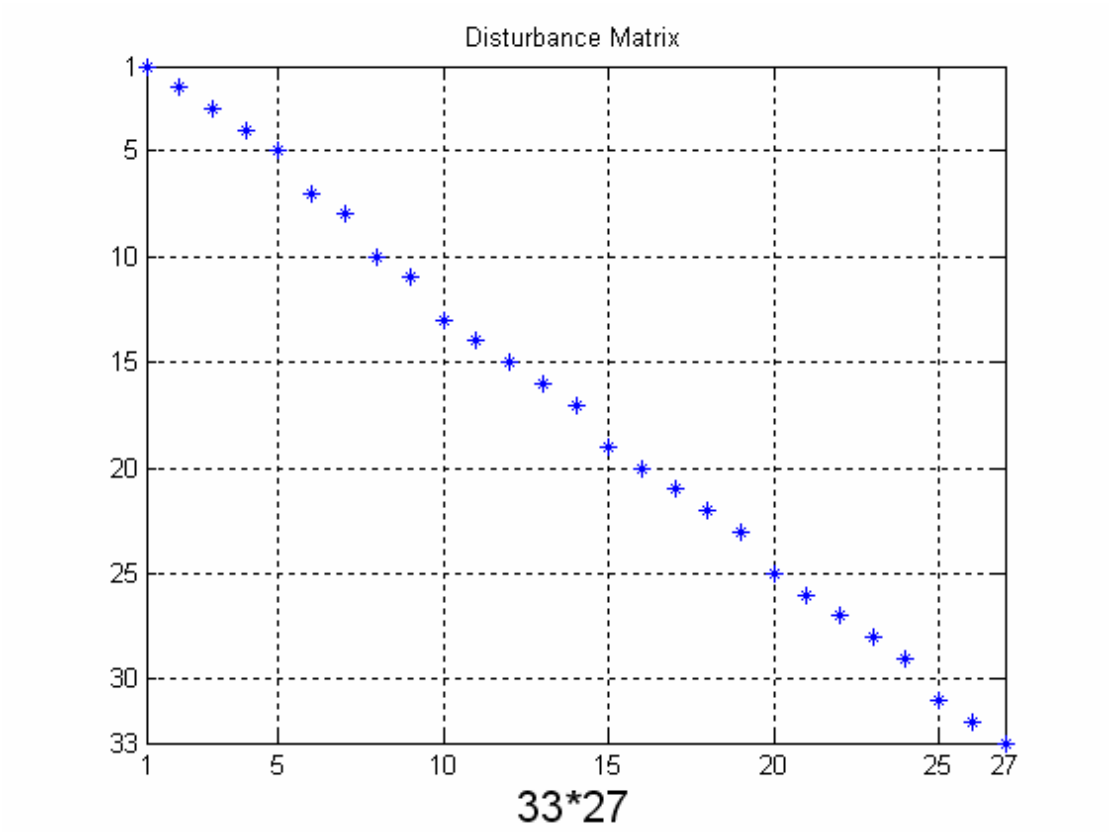

Figure IV.3, Disturbance matrix

$$B_d[1,1]=\frac{T_c}{A_{s1}},B_d[2,2]=\frac{T_c}{A_{s2}},B_d[3,3]=\frac{T_c}{A_{s3}},B_d[4,4]=\frac{T_c}{A_{s4}},B_d[5,5]=\frac{T_c}{A_{s5}},$$

$$B_d[7,6]=\frac{T_c}{A_{s6}},B_d[8,7]=\frac{T_c}{A_{s7}},$$

$$B_d[10,8]=\frac{T_c}{A_{s8}},B_d[11,9]=\frac{T_c}{A_{s9}},B_d[12,10]=\frac{T_c}{A_{s10}},$$

$$B_d[14,11]=\frac{T_c}{A_{s11}},B_d[15,12]=\frac{T_c}{A_{s12}},B_d[16,13]=\frac{T_c}{A_{s13}},B_d[17,14]=\frac{T_c}{A_{s14}},B_d[18,15]=\frac{T_c}{A_{s15}},$$

$$B_d[20,16]=\frac{T_c}{A_{s16}},B_d[21,17]=\frac{T_c}{A_{s17}},B_d[22,18]=\frac{T_c}{A_{s18}},B_d[23,19]=\frac{T_c}{A_{s19}},B_d[24,20]=\frac{T_c}{A_{s20}},$$

$$B_d[26,21]=\frac{T_c}{A_{s21}},B_d[27,22]=\frac{T_c}{A_{s22}},B_d[28,23]=\frac{T_c}{A_{s23}},B_d[29,24]=\frac{T_c}{A_{s24}},B_d[30,25]=\frac{T_c}{A_{s25}},$$

$$B_d[32,26]=\frac{T_c}{A_{s26}},B_d[33,27]=\frac{T_c}{A_{s27}}$$

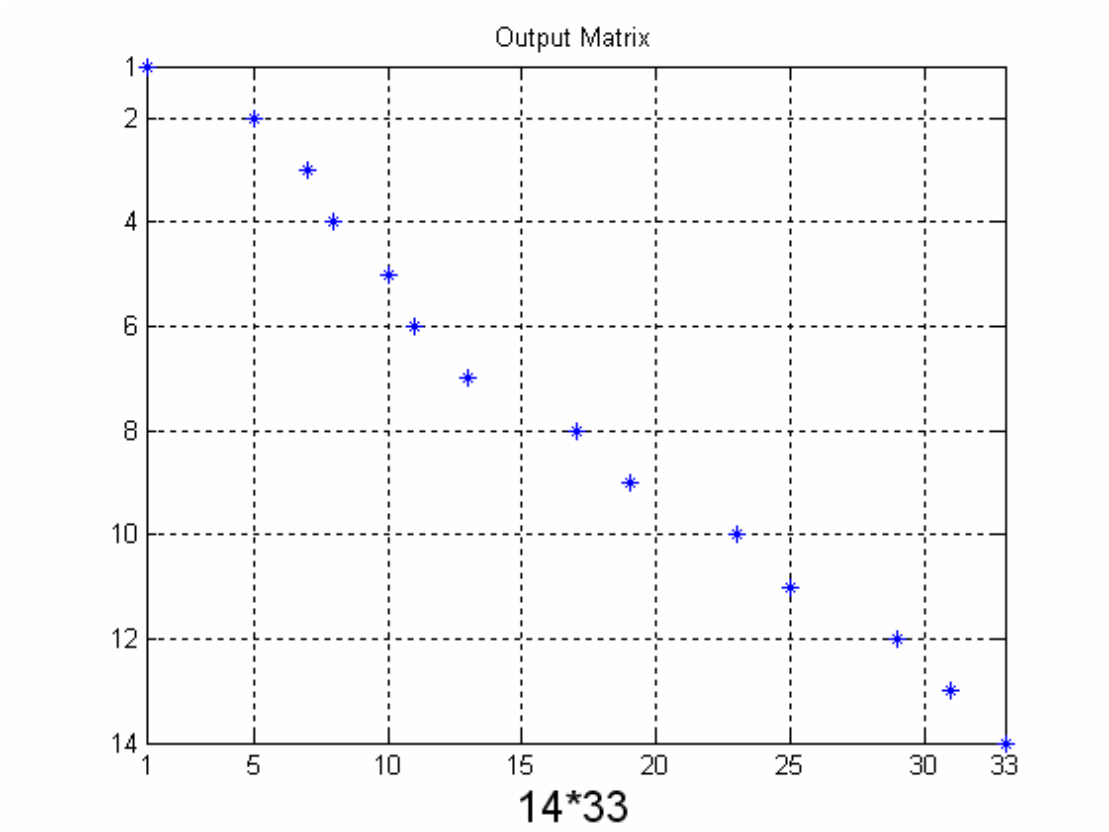

Figure IV.4, Output Matrix

$C[1,1]=1, C[2,5]=1, C[3,7]=1, C[4,8]=1, C[5,10]=1, C[6,11]=1, C[7,13]=1,$
$C[8,17]=1, C[9,19]=1, C[10,23]=1, C[11,25]=1, C[12,29]=1, C[13,31]=1, C[14,33]=1$

Appendix V Other scenarios of Integrator Delay model for water level deviations and flows

08-09-2006

Table V1, Flow mismatches (09 August, 2006)

Flow(m3/s)	0:00-5:00	5:00-10:00	10:00-13:00	13:00-14:00	14:00-18:00	18:00-24:00
Mismatch	0.17	0.34	0.20	-0.74	-0.28	0.20

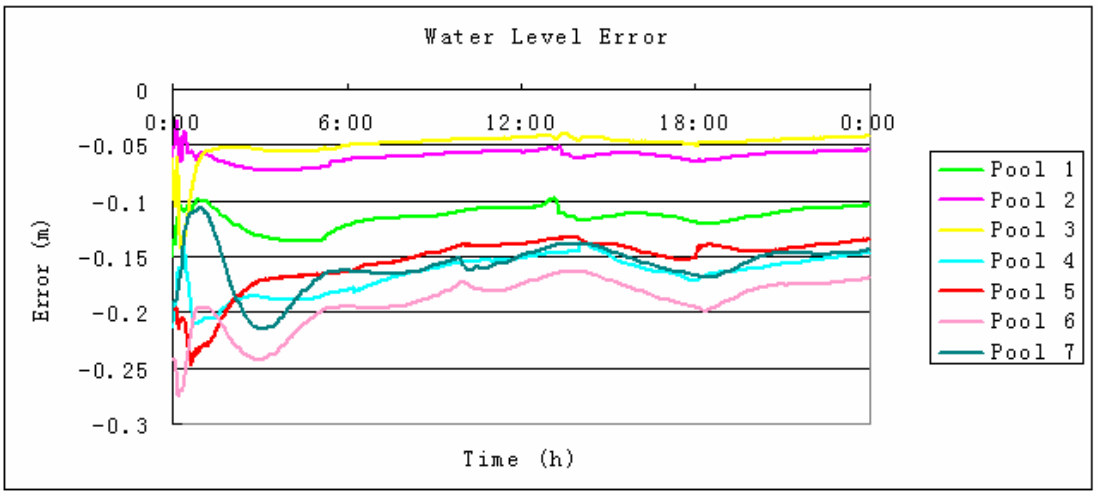

Figure V1, Water level deviations

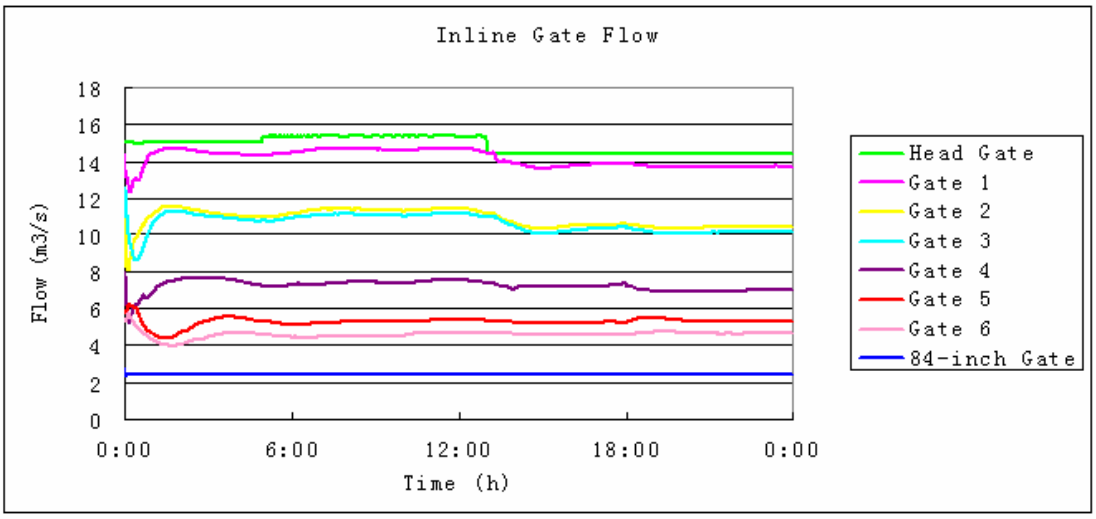

Figure V2, Control flows through inline gates

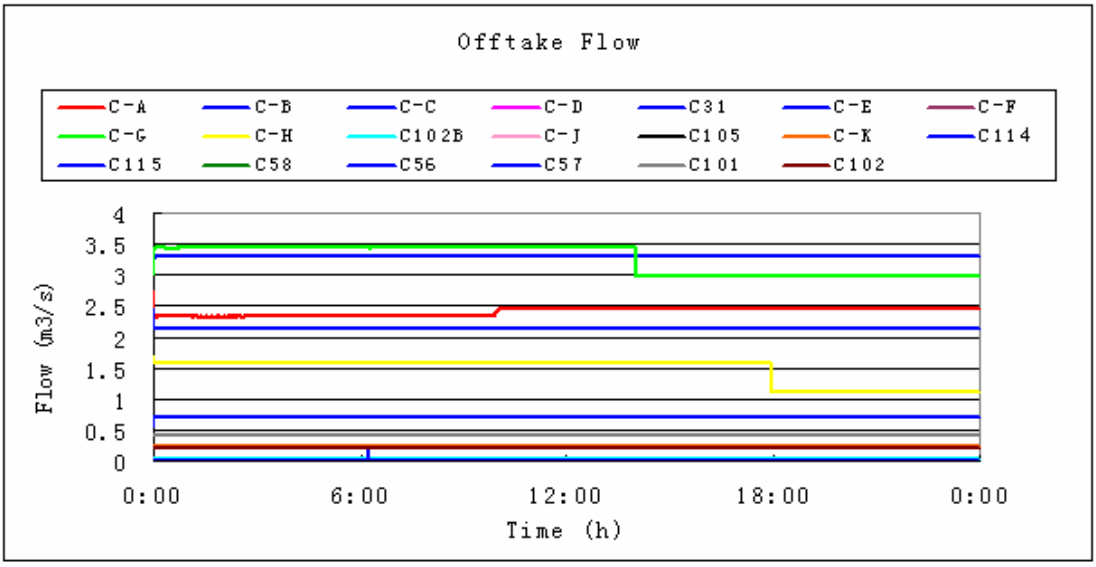

Figure V3, Offtake flows

08-10-2006

Table V2, Flow mismatches (10 August, 2006)

Flow(m3/s)	0:00-5:00	5:00-10:00	10:00-12:00	12:00-14:00	14:00-18:00	18:00-24:00
Mismatch	0.39	-0.28	0.46	-0.71	-0.06	-0.06

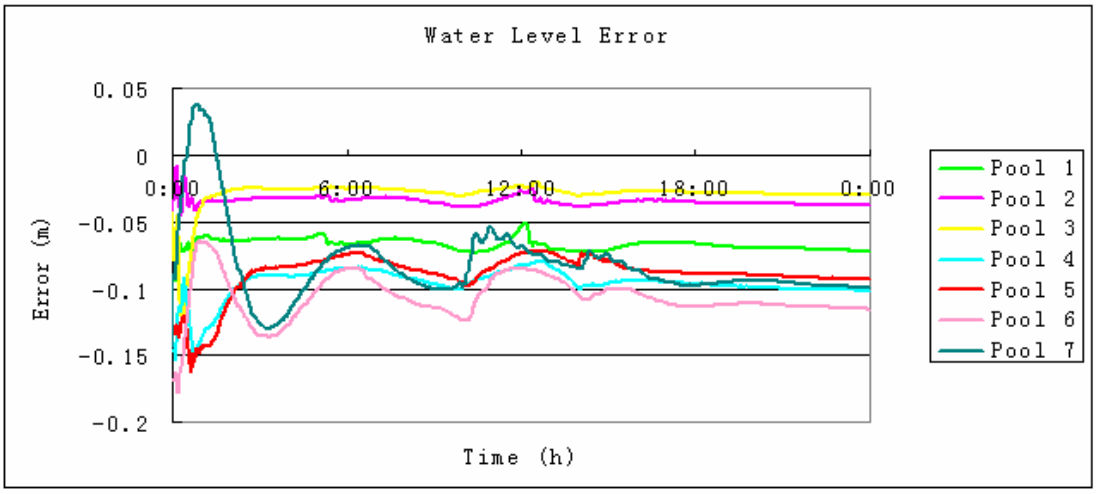

Figure V4, Water level deviations

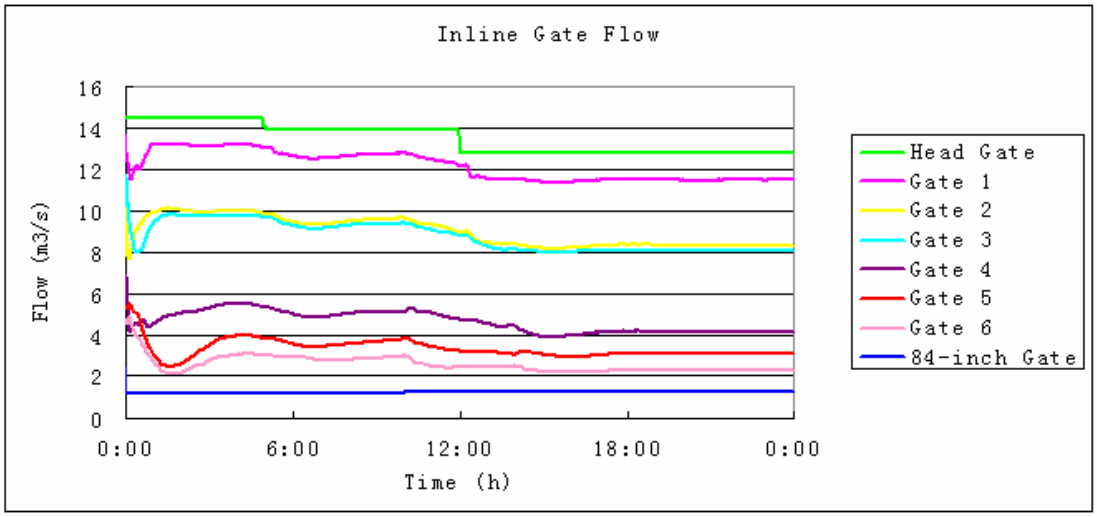

Figure V5, Control flows through inline gates

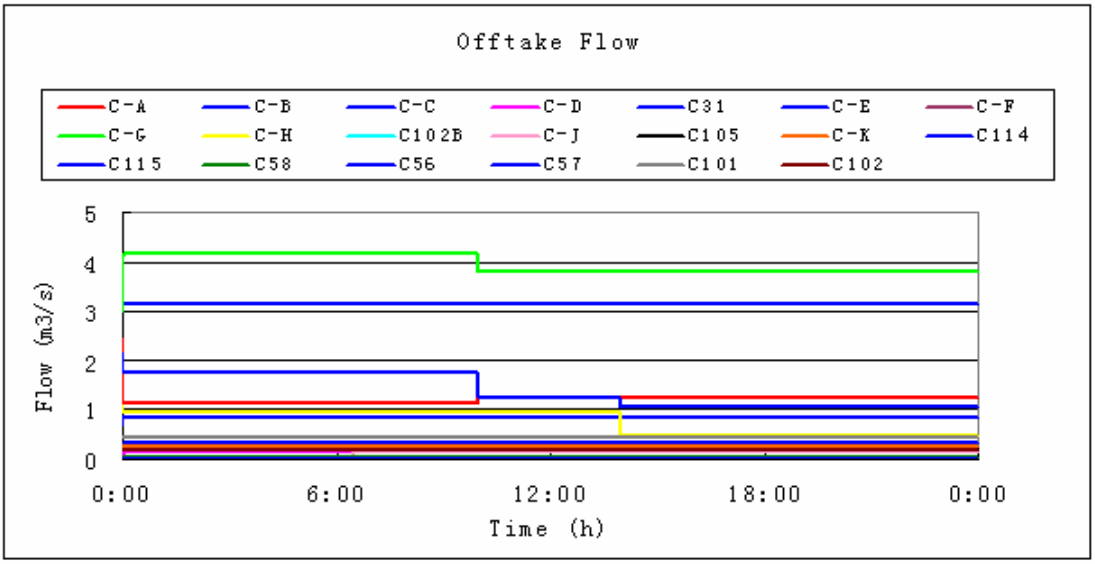

Figure V6, Offtake flows

08-11-2006

Table V3, Flow mismatches (11 August, 2006)

Flow(m3/s)	0:00-5:00	5:00-10:00	10:00-14:00	14:00-18:00	18:00-24:00
Mismatch	1.25	-0.53	-0.25	1.39	-0.78

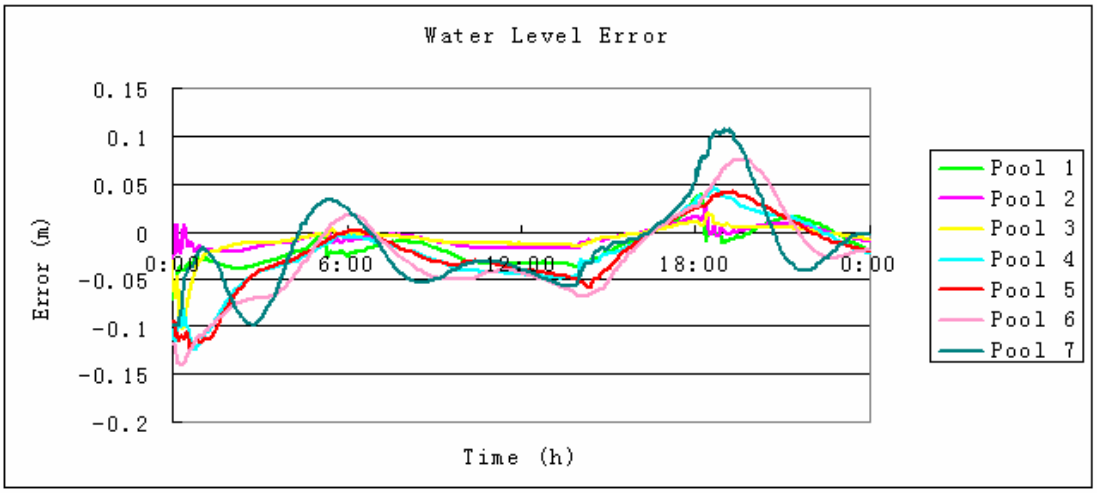

Figure V7, Water level deviations

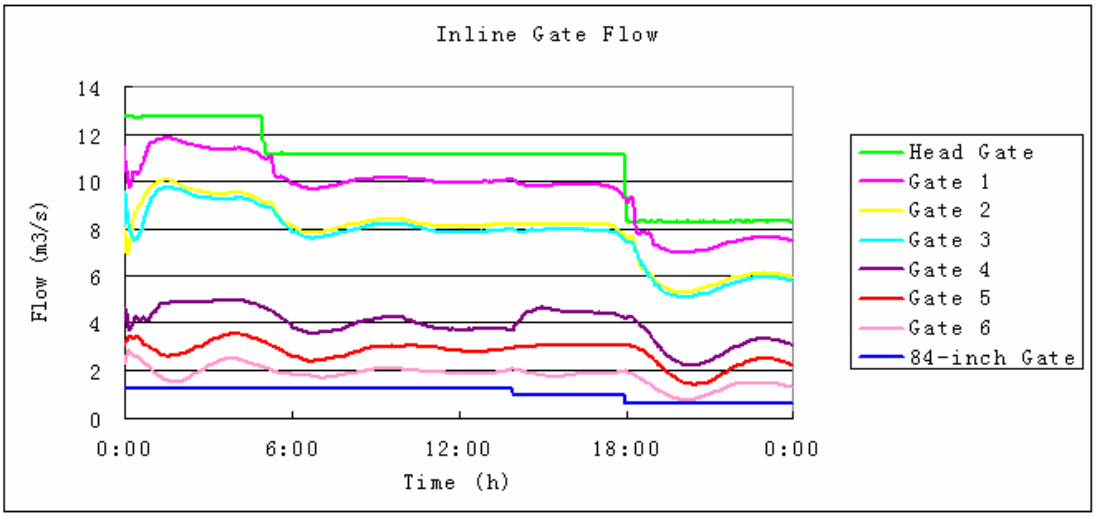

Figure V8, Control flows through inline gates

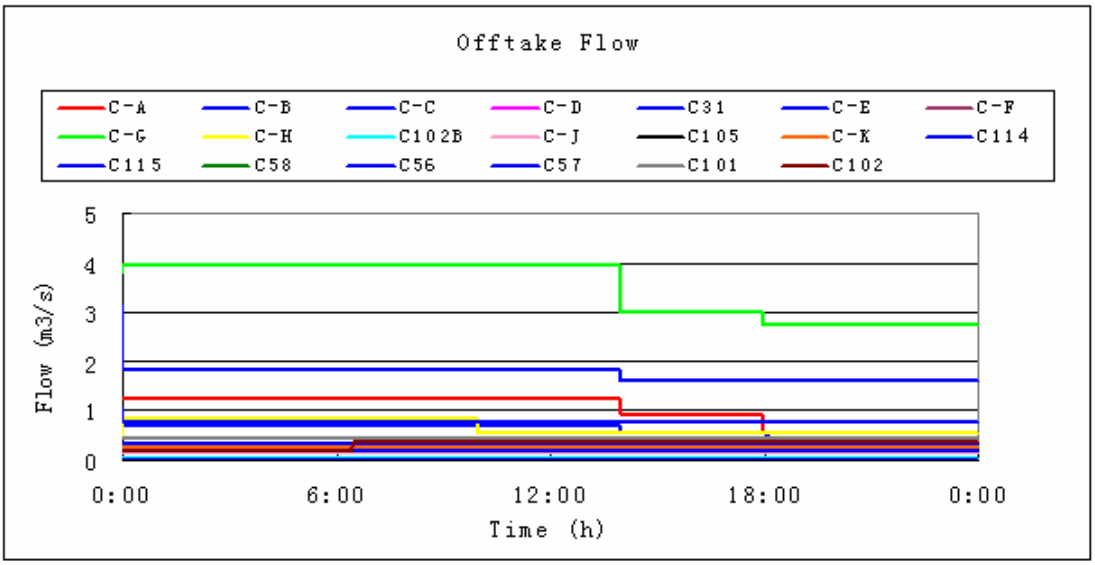

Figure V9, Offtake flows

08-12-2006

Table V4, Flow mismatches (12 August, 2006)

Flow(m3/s)	0:00-5:00	5:00-10:00	10:00-14:00	14:00-18:00	18:00-24:00
Mismatch	-0.13	-0.14	-0.14	0.76	0.76

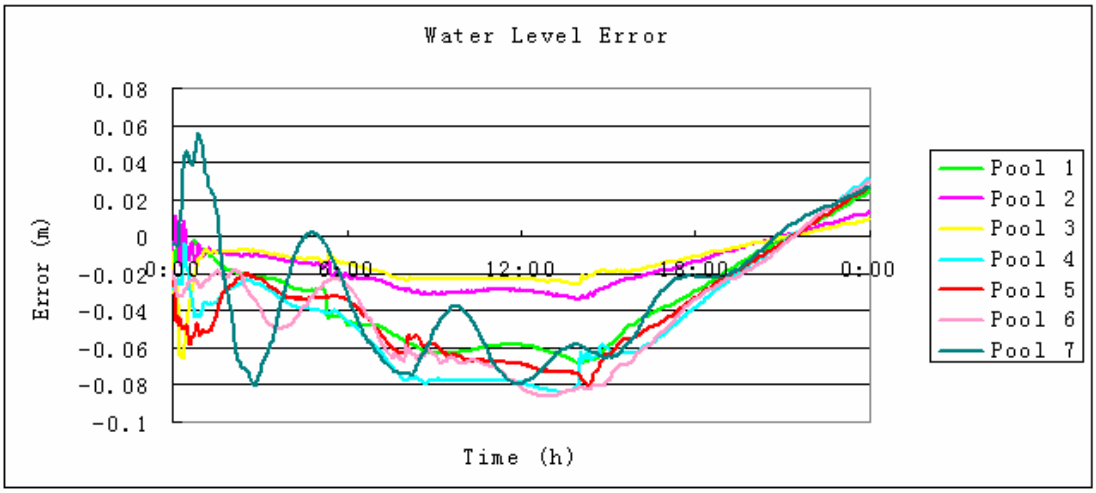

Figure V10, Water level deviations

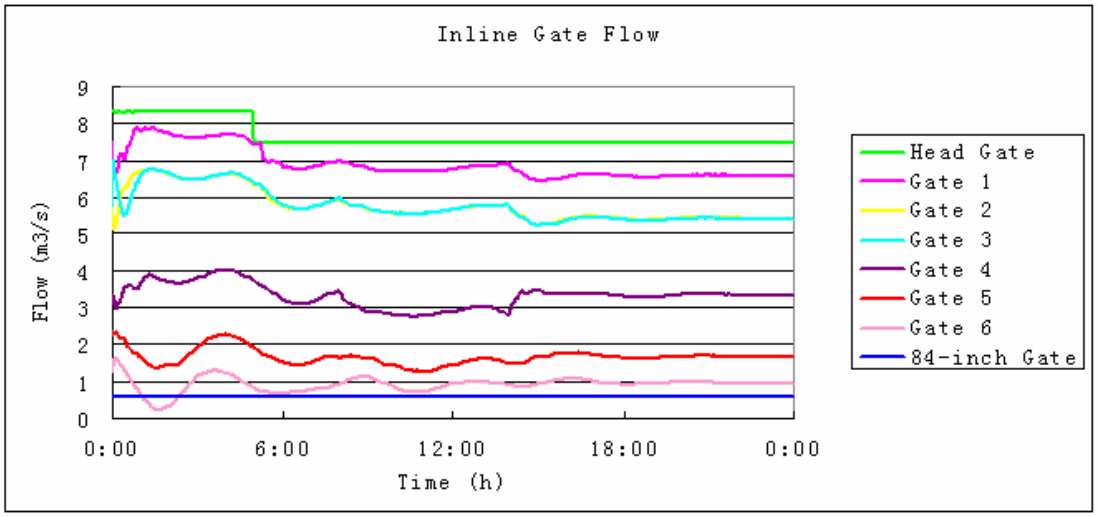

Figure V11, Control flows through inline gates

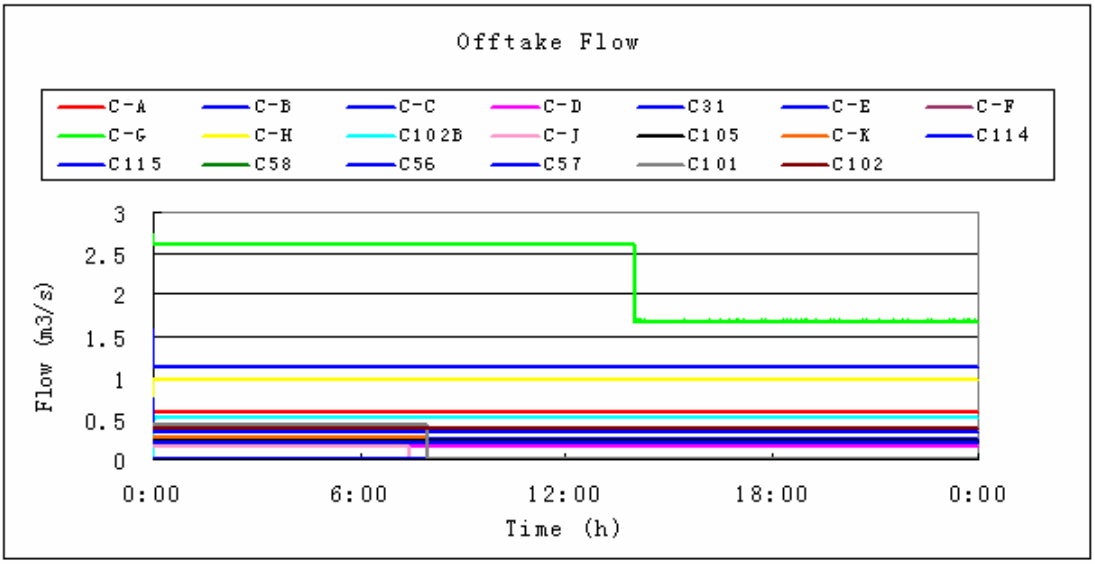

Figure V12, Offtake flows

08-13-2006

Table V5, Flow mismatches (13 August, 2006)

Flow(m3/s)	0:00-6:00	6:00-10:00	10:00-14:00	14:00-17:00	17:00-18:00	18:00-24:00
Mismatch	1.52	1.00	1.00	1.00	0.38	1.03

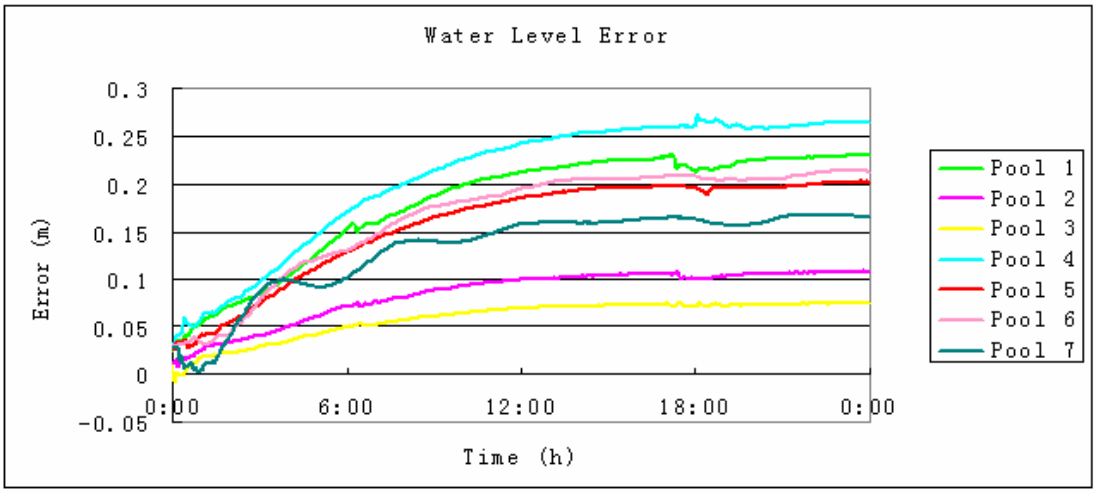

Figure V13, Water level deviations

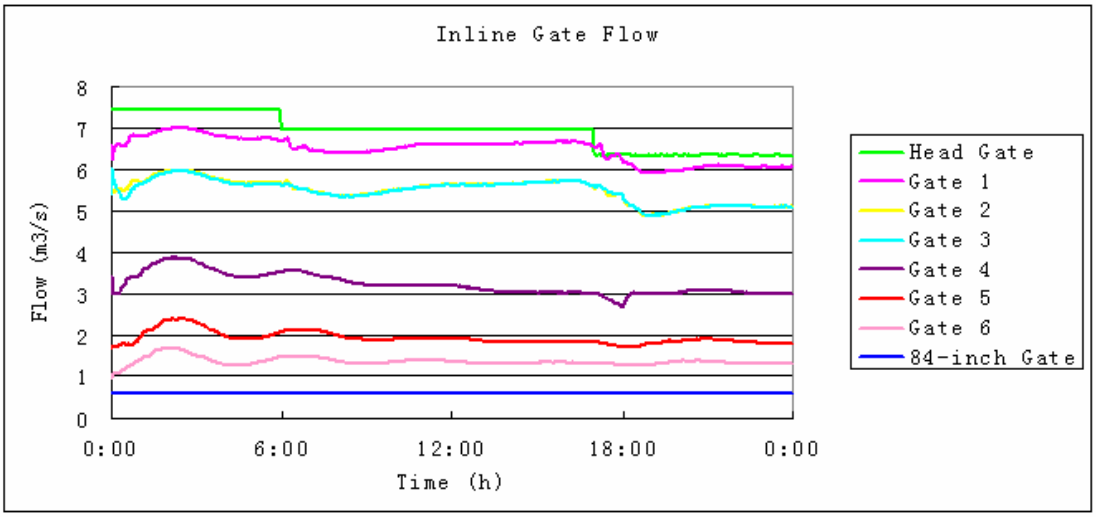

Figure V14, Control flows through inline gates

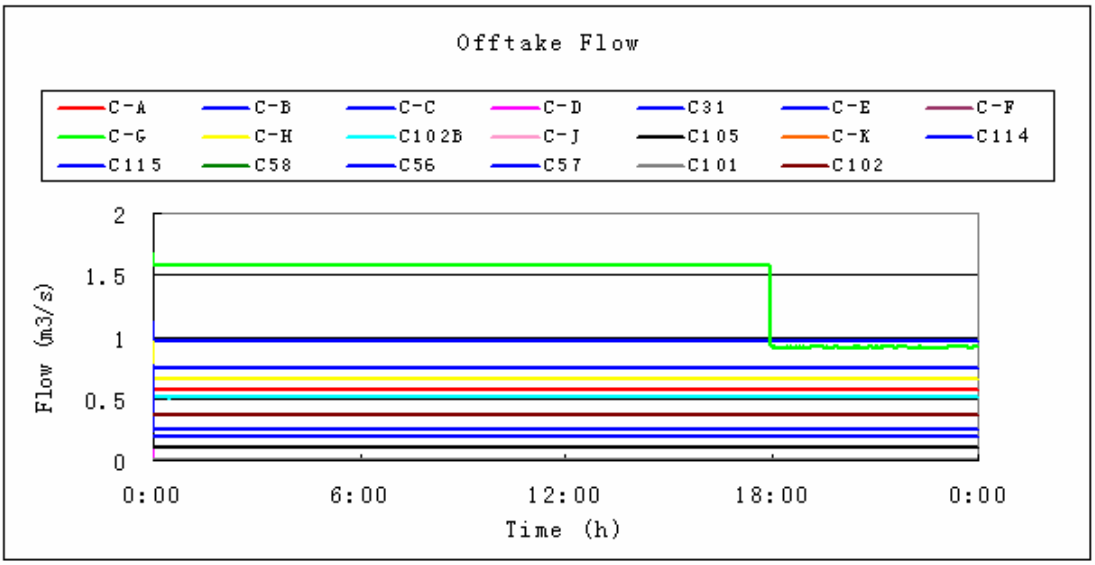

Figure V15, Offtake flows

08-14-2006

Table V6, Flow mismatches (14 August, 2006)

Flow(m3/s)	0:00-5:00	5:00-10:00	10:00-14:00	14:00-16:00	16:00-18:00	18:00-24:00
Mismatch	0.69	0.98	0.98	1.40	0.97	0.97

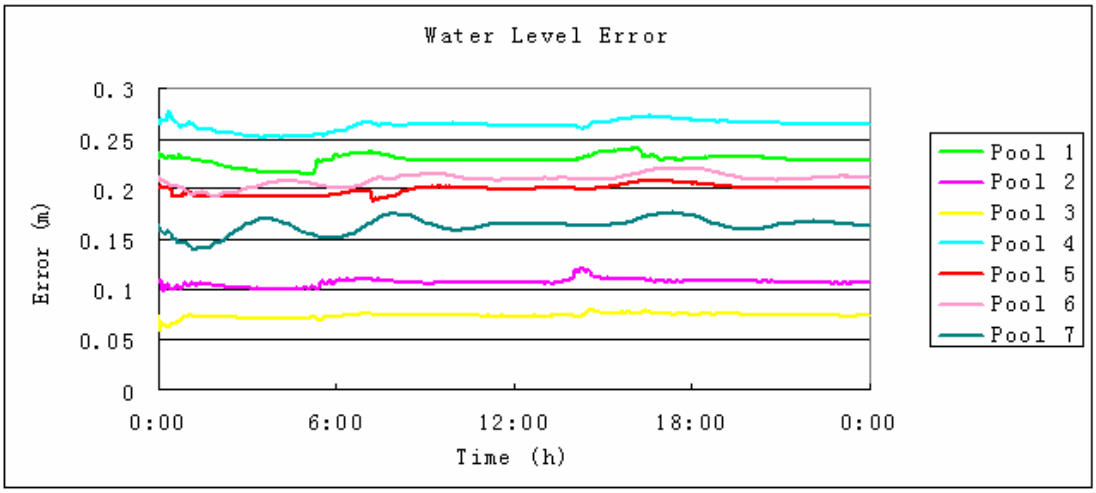

Figure V16, Water level deviations

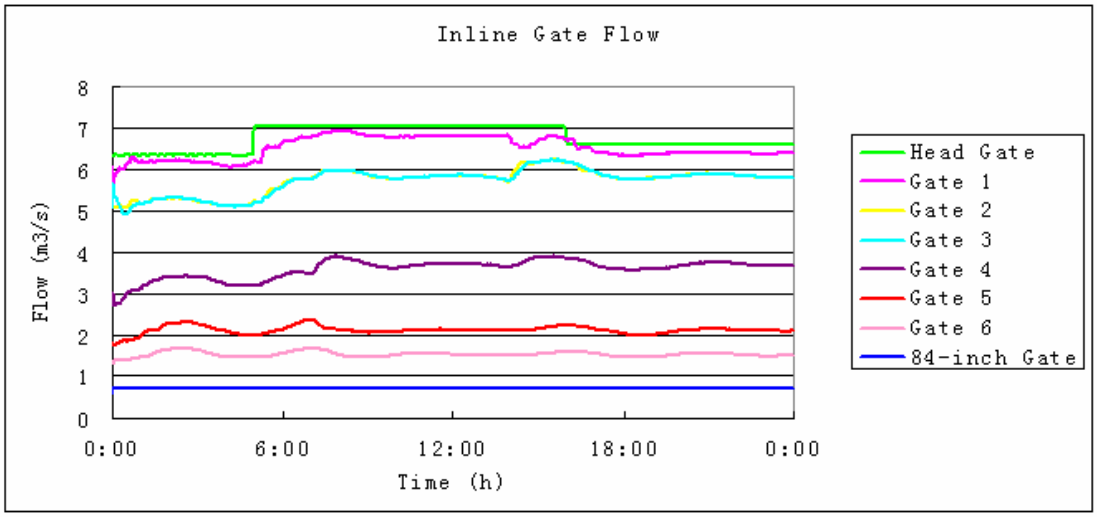

Figure V17, Control flows through inline gates

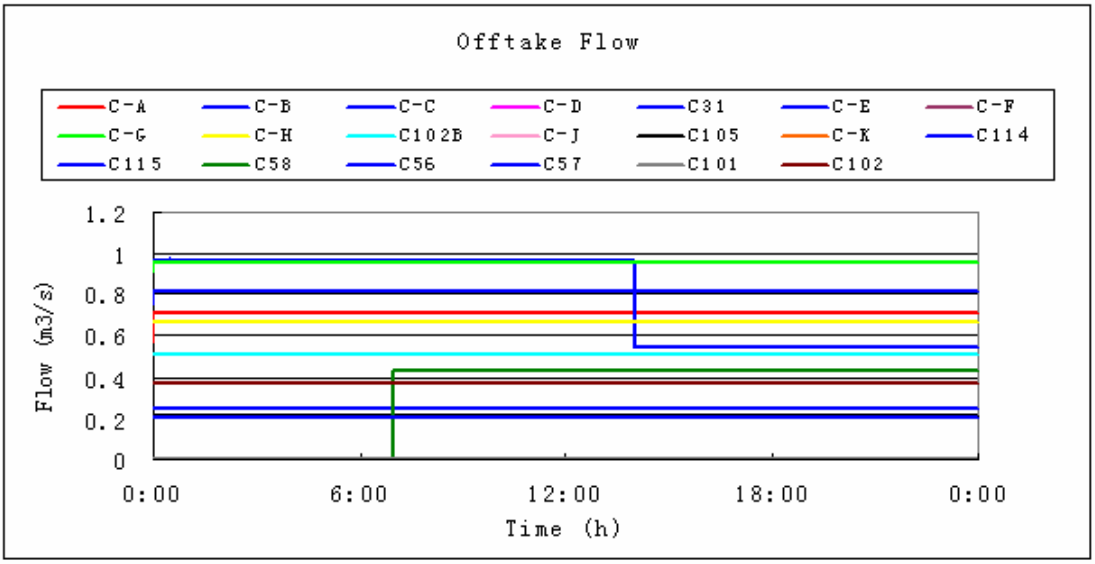

Figure V18, Offtake flows